Ann. Inst. H. Poincaré D
Comb. Phys. Interact. (Online first)
DOI 10.4171/AIHPD/171

A vertex model for supersymmetric LLT polynomials

Andrew Gitlin and David Keating

Abstract. We describe a Yang–Baxter integrable vertex model, which can be realized as a degeneration of a vertex model introduced by Aggarwal, Borodin, and Wheeler (2021). From this vertex model, we construct a certain class of partition functions that we show are essentially equal to the super ribbon functions of Lam. Using the vertex model formalism, we give proofs of many properties of these polynomials, namely a Cauchy identity and generalizations of known identities for supersymmetric Schur polynomials.

1. Introduction

LLT polynomials were originally introduced by Lascoux, Leclerc, and Thibon (for whom the polynomials are eponymously named) in [22]. They are a class of symmetric polynomials and can be seen as a t-deformation of products of (skew) Schur functions. The original motivation for LLT polynomials was to study certain plethysm coefficients, and they were defined via a relationship with the Fock space representation of a quantum affine Lie algebra. The original definition expresses the LLT polynomials as a sum over semistandard k-ribbon tableaux, weighted with a spin statistic which arises naturally in this representation [19,22]. Bylund and Haiman discovered an alternative way to model LLT polynomials. They constructed a family of symmetric polynomials indexed by k-tuples of skew Young diagrams, weighted with an inversion statistic (Remark B.1). The Bylund–Haiman model is described in more detail in [18]. The relationship between the two definitions uses the Littlewood quotient map (sometimes called the Stanton–White correspondence) [28], which sends semistandard k-ribbon tableaux to k-tuples of semistandard Young tableaux.

Supersymmetric LLT polynomials $\mathcal{G}^{(k)}_{\lambda/\mu}(X_n; Y_m; t)$ were introduced in [21] (in which they are called super ribbon functions). As the name suggests, these polynomials are supersymmetric in the X and Y variables (see Definition 4.6) and specialize to LLT polynomials when $m = 0$ (see Remark B.3). They also specialize to the LLT

2020 Mathematics Subject Classification. Primary 05E05; Secondary 05E10, 81R12.
Keywords. Algebraic combinatorics, LLT polynomials, supersymmetric LLT polynomials, super ribbon functions, vertex models, Yang–Baxter equation.

polynomials (on the conjugate shape) when $n = 0$ (see Theorem 4.3). The supersymmetric LLT polynomials have several other interesting specializations, including the metaplectic symmetric functions introduced in [9] and the supersymmetric Schur polynomials, which can be realized as characters of certain simple modules of the Lie superalgebra $\mathfrak{gl}(n|m)$ [5].

The goal of the present work is to study supersymmetric LLT polynomials from the perspective of integrable vertex models. While the study of integrable systems is a classical subject (see [3,27], for example), they have recently enjoyed an advent into the world of (non)symmetric polynomials [7,11,29,30]. Also known as vertex models, ice models, or multiline queues, these models have been generalized to colored vertex models [6, 8, 10, 12, 14, 16] and polyqueue tableaux [2, 14].

It has recently been shown [1, 13, 15] that the LLT polynomials can be realized as a certain class of partition functions constructed from an integrable vertex model. In [9], the authors constructed a vertex model whose partition functions are the metaplectic symmetric functions, a certain specialization of the supersymmetric LLT polynomials. In this paper, we generalize these results by showing that there is an integrable vertex model whose partition functions are the supersymmetric LLT polynomials. Our vertex model is adapted from the work of [13] and can also be realized as a degeneration of a colored vertex model introduced in [1].

The layout of our paper is as follows. In Section 2, we discuss relevant background. We define coinversion LLT polynomials and spin LLT polynomials. We describe how to relate the tuples of semistandard Young tableaux to semistandard ribbon tableaux through the Littlewood quotient map, and we extend this map to the case of super tableaux.

In Section 3, we introduce the vertex models we will use throughout the paper. We show that they are integrable in the sense that they satisfy a Yang–Baxter equation (YBE), and we define the relevant partition functions that give rise to the supersymmetric LLT polynomials $\mathcal{L}^S_{\boldsymbol{\lambda}/\boldsymbol{\mu}}$.

In Section 4, we prove a variety of properties of the $\mathcal{L}^S_{\boldsymbol{\lambda}/\boldsymbol{\mu}}$. The main result is the following theorem.

Theorem 1.1. *The polynomials $\mathcal{L}^S_{\boldsymbol{\lambda}/\boldsymbol{\mu}}(X_n; Y_m; t)$ satisfy the following properties:*

(1) (Symmetry, Lemma 4.4) *The polynomials $\mathcal{L}^S_{\boldsymbol{\lambda}/\boldsymbol{\mu}}(X_n; Y_m; t)$ are symmetric in the X and Y variables.*

(2) (Cancellation, Lemma 4.5)

$$\mathcal{L}^S_{\boldsymbol{\lambda}/\boldsymbol{\mu}}(X_{n-1}, r; Y_{m-1}, -r; t) = \mathcal{L}^S_{\boldsymbol{\lambda}/\boldsymbol{\mu}}(X_{n-1}; Y_{m-1}; t).$$

(3) (Homogeneity, Lemma 4.9) *The polynomials $\mathcal{L}^S_{\boldsymbol{\lambda}/\boldsymbol{\mu}}(X_n; Y_m; t)$ are homogeneous in the X and Y variables of degree $|\boldsymbol{\lambda}/\boldsymbol{\mu}| = |\boldsymbol{\lambda}| - |\boldsymbol{\mu}|$.*

(4) (Restriction, Lemma 4.8)

$$\mathcal{L}^S_{\boldsymbol{\lambda}/\boldsymbol{\mu}}(X_{n-1}, 0; Y_m; t) = \mathcal{L}^S_{\boldsymbol{\lambda}/\boldsymbol{\mu}}(X_{n-1}; Y_m; t),$$
$$\mathcal{L}^S_{\boldsymbol{\lambda}/\boldsymbol{\mu}}(X_n; Y_{m-1}, 0; t) = \mathcal{L}^S_{\boldsymbol{\lambda}/\boldsymbol{\mu}}(X_n; Y_{m-1}; t).$$

(5) (Factorization, Lemma 4.10) *If there exist* $\boldsymbol{\tau}$ *and* $\boldsymbol{\eta}$ *such that*

$$\lambda^{(i)} = (m + \tau_1^{(i)}, \ldots, m + \tau_n^{(i)}, \eta_1^{(i)}, \ldots, \eta_s^{(i)})$$

for all i*, then*

$$\mathcal{L}^S_{\boldsymbol{\lambda}}(X_n; Y_m; t) = \mathcal{L}_{\boldsymbol{\tau}}(X_n; t) \cdot t^{g(\boldsymbol{\eta})} \mathcal{L}_{\boldsymbol{\eta}'}(Y_m; t^{-1}) \cdot \prod_{l=0}^{k-1} \prod_{i=1}^{n} \prod_{j=1}^{m} (t^l x_i + y_j).$$

Note the first two properties together imply that the polynomials $\mathcal{L}^S_{\boldsymbol{\lambda}/\boldsymbol{\mu}}(X_n; Y_m; t)$ are supersymmetric. In the case where $\boldsymbol{\lambda} = (\lambda)$ is a 1-tuple of partitions, one can show that the supersymmetric LLT polynomial $\mathcal{L}^S_{\boldsymbol{\lambda}}(X_n; Y_m; t)$ is exactly the supersymmetric Schur polynomial $s_\lambda(X_n; Y_m)$. In fact, taking $\boldsymbol{\mu} = \mathbf{0}$ and $k = 1$ in Theorem 1.1, these properties uniquely characterize the supersymmetric Schur polynomials (see [25, Section 2.1.2] and [24, Example I.3.23]). However, we suspect (but do not prove) that the properties in Theorem 1.1 do not uniquely characterize the supersymmetric LLT polynomials, even in the case $\boldsymbol{\mu} = \mathbf{0}$.

In Section 5, we relate the coinversion supersymmetric LLT polynomials to the ribbon supersymmetric LLT polynomials of Lam. The main result is the following theorem.

Theorem 1.2 (Propositions 3.3 and 5.9). *Suppose the* k*-tuple of skew shapes* $\boldsymbol{\lambda}/\boldsymbol{\mu}$ *is the* k*-quotient of the skew shape* λ/μ*. Then there is a Yang–Baxter integrable vertex model whose partition function* $\mathcal{L}^S_{\boldsymbol{\lambda}/\boldsymbol{\mu}}(X_n; Y_m; t)$ *is equal to*

$$\mathcal{L}^S_{\boldsymbol{\lambda}/\boldsymbol{\mu}}(X_n; Y_m; t) = t^{\square} \mathcal{G}^{(k)}_{\lambda/\mu}(X_n; Y_m; t^{1/2})$$

for some half-integer $\square \in \frac{1}{2}\mathbb{Z}$*, where* $\mathcal{G}^{(k)}_{\lambda/\mu}(X_n; Y_m; t)$ *is the super ribbon LLT polynomial.*

Finally, in Section 6, we show that the supersymmetric LLT polynomials satisfy a Cauchy identity. The main result is the next assertion.

Theorem 1.3. *Let* $\boldsymbol{\mu}$ *and* $\boldsymbol{\nu}$ *be tuples of partitions, each with infinitely many parts only finitely many of which are non-zero. Fix positive integers* n, m, p, q*. Then*

$$\sum_{\boldsymbol{\lambda}} t^{d(\boldsymbol{\mu},\boldsymbol{\lambda})} \mathcal{L}^S_{\boldsymbol{\nu}/\boldsymbol{\lambda}}(X_n, Y_m; t) \mathcal{L}^S_{\boldsymbol{\mu}/\boldsymbol{\lambda}}(W_p, Z_q; t)$$
$$= \Omega(X_n, Y_m, W_p, Z_q; t) \sum_{\boldsymbol{\lambda}} t^{d(\boldsymbol{\lambda},\boldsymbol{\nu})} \mathcal{L}^S_{\boldsymbol{\lambda}/\boldsymbol{\mu}}(X_n, Y_m; t) \mathcal{L}^S_{\boldsymbol{\lambda}/\boldsymbol{\nu}}(W_p, Z_q; t),$$

where

$$\Omega(X_n, Y_m, W_p, Z_q; t) = \prod_{l=0}^{k-1} \prod_{i,i'=1}^{n} \prod_{j,j'=1}^{m} \prod_{\alpha,\alpha'=1}^{p} \prod_{\beta,\beta'=1}^{q} \frac{(1 - x_i w_\alpha t^l)(1 - y_{j'} z_{\beta'} t^l)}{(1 + y_j w_{\alpha'} t^l)(1 + x_{i'} z_\beta t^l)}.$$

2. LLT polynomials, super ribbon functions, and the Littlewood quotient map

This section provides necessary background information and establishes some notation for the rest of this paper. First we venture into the world of tableaux on tuples of skew shapes and define coinversion LLT polynomials. Then we venture into the world of ribbon tableaux and define super ribbon function. Finally, we connect these two worlds via the Littlewood quotient map.

2.1. Tuples of skew shapes and coinversion LLT polynomials

We begin by discussing semistandard Young tableaux on tuples of skew shapes, which we use to give one formulation of LLT polynomials.

Fix a non-negative integer p. A *partition* with p parts is a weakly decreasing sequence $\lambda = (\lambda_1 \geq \cdots \geq \lambda_p \geq 0)$ of p non-negative integers. Note that here we consider our partitions to have a fixed number of parts but allow for the possibility of parts equalling zero; later we will also consider partitions with an infinite number of parts, only finitely many of which are non-zero. We let the length $\ell(\lambda)$ be the number of non-zero parts of λ, and we let the size $|\lambda|$ be the sum $\lambda_1 + \cdots + \lambda_p$ of its parts. We associate to λ its Young (or Ferrers) diagram $D(\lambda) \subseteq \mathbb{Z} \times \mathbb{Z}$ given as

$$D(\lambda) = \{(i, j) \mid 1 \leq i \leq \ell(\lambda),\ 1 \leq j \leq \lambda_i\}.$$

We refer to the elements of $D(\lambda)$ as cells. We draw our diagrams in French notation in the first quadrant, with the first row on the bottom and the first column on the left, such as

$$\lambda = (4, 2, 1), \quad D(\lambda) =$$

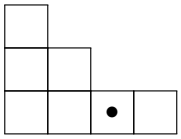

The cell labeled above has coordinates (1,3). The *content* of a cell $u = (i, j)$ in row i and column j of any Young diagram is $c(u) = j - i$. In what follows, we will use λ and $D(\lambda)$ interchangeably, when it will not cause confusion.

If λ and μ are partitions such that $D(\lambda) \supseteq D(\mu)$, then the *skew shape* λ/μ is the set of cells in $D(\lambda)$ that are not in $D(\mu)$. We draw the diagram of λ/μ by coloring

the cells in $D(\mu)$ gray, such as

$$\lambda = (4,2,1), \quad \mu = (2,1), \quad D(\lambda/\mu) =$$

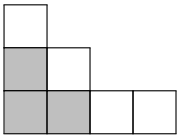

The size $|\lambda/\mu|$ of λ/μ is $|\lambda| - |\mu|$.

A *semistandard Young tableau* of shape λ/μ is a filling of each cell of $D(\lambda/\mu)$ with a positive integer such that the rows are weakly increasing and the columns are strictly increasing. We call the set of all such fillings $\mathrm{SSYT}(\lambda/\mu)$. Let

$$\boldsymbol{\lambda/\mu} = (\lambda^{(1)}/\mu^{(1)}, \ldots, \lambda^{(k)}/\mu^{(k)})$$

be a tuple of skew partitions. We define its size to be

$$|\boldsymbol{\lambda/\mu}| = |\lambda^{(1)}/\mu^{(1)}| + \cdots + |\lambda^{(k)}/\mu^{(k)}|,$$

and we define a semistandard Young tableau of shape $\boldsymbol{\lambda/\mu}$ to be a semistandard Young tableau on each $\lambda^{(j)}/\mu^{(j)}$, that is,

$$\mathrm{SSYT}(\boldsymbol{\lambda/\mu}) = \mathrm{SSYT}(\lambda^{(1)}/\mu^{(1)}) \times \cdots \times \mathrm{SSYT}(\lambda^{(k)}/\mu^{(k)}).$$

We can picture this as placing the Young diagrams diagonally "on content lines" with the first shape in the south-west direction and the last shape in the north-east direction.

Example 2.1. Let $\boldsymbol{\lambda/\mu} = ((3,1),(2,2,2)/(1,1,1),(1),(2,1)/(2))$. The top row labels the contents of each line,

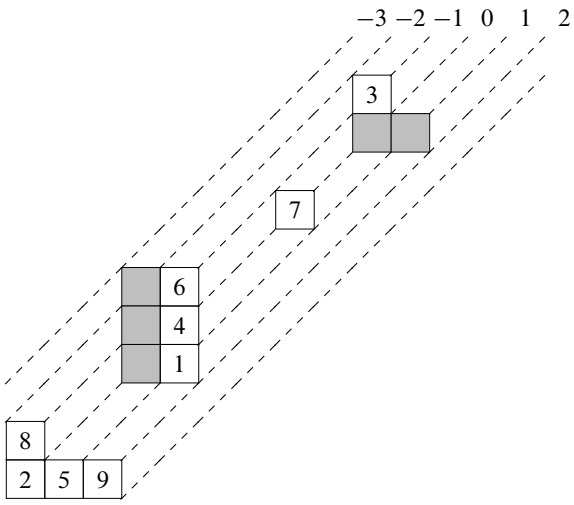

We will use tuples of skew partitions to index our formulation of LLT polynomials. Given a tuple $\boldsymbol{\lambda}/\boldsymbol{\mu}$ of skew partitions, we say three cells $u, v, w \in \mathbb{Z} \times \mathbb{Z}$ form a *triple* if

(1) $v \in \boldsymbol{\lambda}/\boldsymbol{\mu}$;

(2) they are situated with v and w on the same content line and w in a later shape, and u on a content line one smaller, in the same row as w:

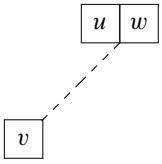

(3) if u and w are in row r of $\lambda^{(j)}/\mu^{(j)}$, then u and w must be between the cells $(r, \mu_r^{(j)})$ and $(r, \lambda_r^{(j)} + 1)$, inclusive.

It is important to note that while v must be a cell in $\boldsymbol{\lambda}/\boldsymbol{\mu}$, this is not true of u and w. If not in $\boldsymbol{\lambda}/\boldsymbol{\mu}$, then u must be at the end of some row in $\boldsymbol{\mu}$, and w must be the cell directly to the right of the end of some row in $\boldsymbol{\lambda}$.

Definition 2.2. Let $\boldsymbol{\lambda}/\boldsymbol{\mu}$ be a tuple of skew partitions and let $T \in \mathrm{SSYT}(\boldsymbol{\lambda}/\boldsymbol{\mu})$. Let a, b, c be the entries in the cells of a triple u, v, w, where we set $a = 0$ and $c = \infty$ if the respective cell is not in $\boldsymbol{\lambda}/\boldsymbol{\mu}$. Given the triple of entries

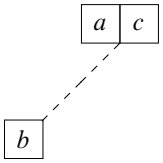

we say this is a *coinversion (inversion) triple* if $a \leq b \leq c$ ($b < a \leq c$ or $a \leq c < b$).

There are 7 coinversion triples in Example 2.1 above: (0, 2, 4), (0, 2, 7), (3,4,∞), (0,4,7), (4,5,∞), (1,9,∞), and (0,9,∞).

With these definitions in place, we are finally able to define the coinversion LLT polynomials.

Definition 2.3. The *coinversion LLT polynomial* associated to a tuple $\boldsymbol{\lambda}/\boldsymbol{\mu}$ of skew partitions is the generating function

$$\mathcal{L}_{\boldsymbol{\lambda}/\boldsymbol{\mu}}(X; t) = \sum_{T \in \mathrm{SSYT}(\boldsymbol{\lambda}/\boldsymbol{\mu})} t^{\mathrm{coinv}(T)} x^T,$$

where $\mathrm{coinv}(T)$ is the number of coinversion triples in T and $x^T = \prod_{\text{entries } e \text{ in } T} x_e$.

See Appendix B for other formulations of LLT polynomials that appear in the literature.

2.2. Ribbon tableaux and the Littlewood quotient map

Next we discuss semistandard ribbon tableaux. We define a bijection, called the Littlewood quotient map, relating them and tuples of semistandard Young tableaux.

Fix a positive integer k. A *k-ribbon* is a skew shape of size k that is connected and does not contain any 2×2 square. The head (tail) of a k-ribbon is the most south-east (most north-west) cell in its Young diagram. A *horizontal (vertical) k-ribbon strip* of shape λ/μ is a tiling of λ/μ by k-ribbons such that the head (tail) of each ribbon is adjacent to the southern (western) boundary of the shape. We let $\mathrm{HRS}_k(\lambda/\mu)$ ($\mathrm{VRS}_k(\lambda/\mu)$) denote the set of horizontal (vertical) k-ribbon strips of shape λ/μ.

Throughout this paper, we will omit k when it is clear from context. For example, we will use "ribbon" and "k-ribbon" interchangeably.

Definition 2.4. A *semistandard k-ribbon tableau* of shape λ/μ is a tiling of λ/μ by k-ribbons and a labeling of the k-ribbons by positive integers such that for all i,

(1) removing all ribbons labeled j for $j > i$ gives a valid skew shape $\lambda_{\leq i}/\mu$,
(2) the subtableau of ribbons labeled i form a horizontal k-ribbon strip of shape $\lambda_{\leq i}/\lambda_{\leq i-1}$.

We let $\mathrm{SSRT}_k(\lambda/\mu)$ denote the set of semistandard k-ribbon tableau of shape λ/μ.

Following the exposition of [26, Section 3], we now define the Littlewood k-quotient map. This map was introduced in [23]; another (perhaps clearer) formulation, as well as a proof that the map is a bijection, is given in [28].

We first define the *k-quotient map*, which is a function

$$\{\text{skew partitions } \lambda/\mu\} \to \left\{k\text{-tuples } \boldsymbol{\lambda}/\boldsymbol{\mu} = (\lambda^{(0)}/\mu^{(0)}, \ldots, \lambda^{(k-1)}/\mu^{(k-1)}) \text{ of skew partitions}\right\}.$$

This function can be defined graphically as follows. Given a partition λ, we associate a finite sequence $(a_0, \ldots, a_{r-1})$ of east $= \circ$ and south $= \bullet$ steps, called the *Maya diagram* of λ, by following the north-east boundary of λ from north-west to south-east.

Example 2.5. The Maya diagram of (4,3,2,2,1) is $\circ \bullet \circ \bullet \bullet \circ \bullet \circ \bullet$,

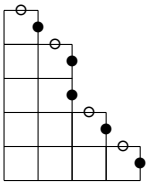

Remark 2.6. Observe that postpending finitely many $\circ$'s to a Maya diagram does not change the corresponding partition. Thus we can take the length r of the Maya diagram $(a_0, \ldots, a_{r-1})$ to be a multiple of k.

Let λ be a partition with Maya diagram $(a_0, \ldots, a_{r-1})$. By the preceding remark, we may assume $s = r/k$ is an integer. We define the *k-quotient* of λ to be the k-tuple of partitions

$$\boldsymbol{\lambda} = (\lambda^{(0)}, \ldots, \lambda^{(k-1)}),$$

where, for each i, $\lambda^{(i)}$ is the partition corresponding to the Maya diagram

$$(a_i, a_{k+i}, \ldots, a_{(s-1)k+i}).$$

We define the k-quotient of a skew partition λ/μ to be the k-tuple $\boldsymbol{\lambda}/\boldsymbol{\mu}$ of skew partitions, where $\boldsymbol{\lambda}$ and $\boldsymbol{\mu}$ are the k-quotients of λ and μ, respectively. Here we require λ and μ to have the same number of parts, padding μ with zeroes if necessary.

Example 2.7. The 3-quotient of (4,3,2,2,1) is ((1,1),(0,0),(2)),

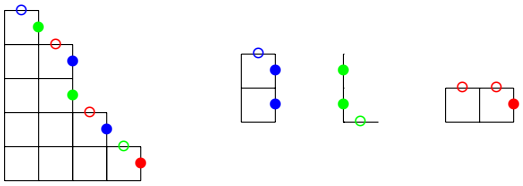

We are now ready to define the Littlewood k-quotient map.

Definition 2.8. Let $\boldsymbol{\lambda}/\boldsymbol{\mu}$ be the k-quotient of λ/μ. The *Littlewood k-quotient map* is a bijection

$$\mathrm{SSRT}_k(\lambda/\mu) \to \mathrm{SSYT}(\boldsymbol{\lambda}/\boldsymbol{\mu})$$

defined as follows. Fix $T \in \mathrm{SSRT}_k(\lambda/\mu)$. For each i, we put an i into each cell of the k-quotient of $\lambda_{\leq i}/\lambda_{\leq i-1}$ (which lies inside $\boldsymbol{\lambda}/\boldsymbol{\mu}$). In this fashion, we place positive integers into the cells of $\boldsymbol{\lambda}/\boldsymbol{\mu}$, resulting in

$$\boldsymbol{T} = (T^{(0)}, \ldots, T^{(k-1)}) \in \mathrm{SSYT}(\boldsymbol{\lambda}/\boldsymbol{\mu}).$$

Example 2.9. In Example 2.7, we found that the 3-quotient of $\lambda = (4,3,2,2,1)$ is $\boldsymbol{\lambda} = ((1,1),(0,0),(2))$. One can compute that

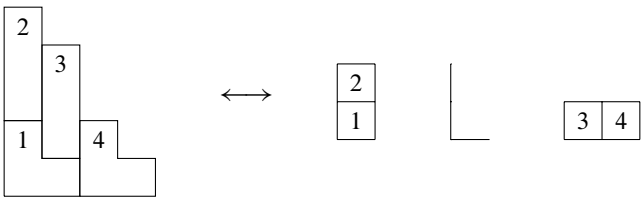

via the Littlewood 3-quotient map. For example, when $i = 3$, one can compute the k-quotient of $\lambda_{\leq i}/\lambda_{\leq i-1}$ as follows:

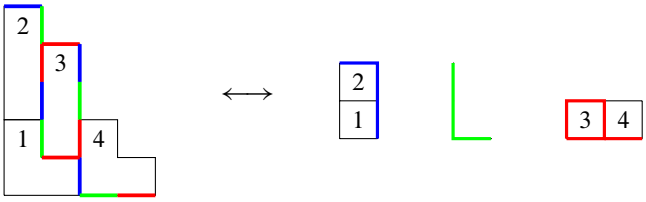

Here we have drawn the Maya diagrams of both $\lambda_{\leq 3}$ and $\lambda_{\leq 2}$. From this, we see that a box at coordinates $(1, 1)$ is added in $T^{(2)}$, and we fill it with 3.

2.3. Extending the Littlewood quotient map to super tableaux

Finally, we extend the Littlewood quotient map to a bijection between super ribbon tableaux (Definition 2.10) and semistandard super Young tableaux (Definition 2.13). This bijection plays a pivotal role in the rest of the paper because it allows us to relate our partition functions (Definition 3.8) to the super ribbon functions (Definition 2.11) in Proposition 5.9.

Throughout this subsection, let $\mathcal{A} = \{1 < 2 < \cdots\}$ and $\mathcal{A}' = \{1' < 2' < \cdots\}$. Also fix a total order on $\mathcal{A} \cup \mathcal{A}'$ that is compatible with the natural orders on $\mathcal{A}$ and $\mathcal{A}'$.

Definition 2.10. A *super k-ribbon tableau* of shape λ/μ is a tiling of λ/μ by k-ribbons and a labeling of the k-ribbons by the alphabet $\mathcal{A} \cup \mathcal{A}'$ such that

(1) for $i \in \mathcal{A} \cup \mathcal{A}'$, removing all ribbons labeled j for $j > i$ gives a valid skew shape $\lambda_{\leq i}/\mu$;

(2) for $i \in \mathcal{A}$, the subtableau of ribbons labeled i forms a horizontal k-ribbon strip;

(3) for $i' \in \mathcal{A}'$, the subtableau of ribbons labeled i' forms a vertical k-ribbon strip.

We let $\mathrm{SRT}_k(\lambda/\mu)$ denote the set of super k-ribbon tableau of shape λ/μ.

Note that a SRT in the alphabet $\mathcal{A}$ of shape λ/μ is the same as a SSRT of shape λ/μ. Moreover, there is a bijection between SRT in the alphabet $\mathcal{A}'$ of shape λ/μ and SSRT of shape λ'/μ', given by conjugation (and unpriming the labels).

The height $h(R)$ of a ribbon R is the number of rows it contains. The *spin* of a super ribbon tableau T is

$$\mathrm{spin}(T) = \sum_R (h(R) - 1),$$

where the sum is taken over all ribbons R in T.

Definition 2.11 ([21, Definition 44]). The *super k-ribbon function* associated to a skew partition λ/μ is the generating function

$$\mathcal{G}^{(k)}_{\lambda/\mu}(X;Y;t) = \sum_{T \in \mathrm{SRT}_k(\lambda/\mu)} t^{\mathrm{spin}(T)} x^{\mathrm{weight}(T)} y^{\mathrm{weight}'(T)}.$$

Example 2.12. We use the ordering $1 < 2 < \cdots < 1' < 2' < \cdots$ on $\mathcal{A} \cup \mathcal{A}'$. Let $k = 3$ and $\lambda/\mu = (8,7,6,6,6,4,1)/(2)$. The super ribbon tableau

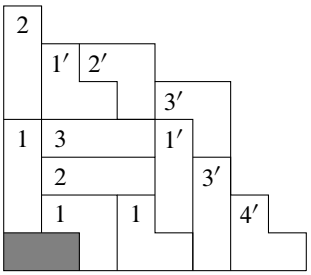

has spin 14 and contributes

$$t^{14} x_1^3 x_2^2 x_3^1 y_1^2 y_2^1 y_3^2 y_4^1$$

to $\mathcal{G}^{(k)}_{\lambda/\mu}(X;Y;t)$.

Definition 2.13. A *semistandard super Young tableau* of shape λ/μ is a filling of each cell of $D(\lambda)$ with an element of $\mathcal{A} \cup \mathcal{A}'$ such that

(1) the rows and the columns are weakly increasing,

(2) the entries in $\mathcal{A}$ are strictly increasing along columns,

(3) the entries in $\mathcal{A}'$ are strictly increasing along rows.

We let $\mathrm{SSSYT}(\lambda/\mu)$ denote the set of semistandard super Young tableaux of shape λ/μ. Given a tuple $\boldsymbol{\lambda}/\boldsymbol{\mu} = (\lambda^{(1)}/\mu^{(1)}, \ldots, \lambda^{(k)}/\mu^{(k)})$ of skew partitions, a semistandard super Young tableau of shape $\boldsymbol{\lambda}/\boldsymbol{\mu}$ is a semistandard super Young tableau on each $\lambda^{(j)}/\mu^{(j)}$, that is,

$$\mathrm{SSSYT}(\boldsymbol{\lambda}/\boldsymbol{\mu}) = \mathrm{SSSYT}(\lambda^{(1)}/\mu^{(1)}) \times \cdots \times \mathrm{SSSYT}(\lambda^{(k)}/\mu^{(k)}).$$

Note that a SSSYT in the alphabet $\mathcal{A}$ of shape λ/μ is the same as a SSYT of shape λ/μ. Moreover, there is a bijection between SSSYT in the alphabet $\mathcal{A}'$ of shape λ/μ and SSYT of shape λ'/μ', given by conjugation (and unpriming the labels).

We are now ready to extend the Littlewood k-quotient map.

Definition 2.14. The *(extended) Littlewood k-quotient map* is a bijection

$$\mathrm{SRT}_k(\lambda/\mu) \to \mathrm{SSSYT}(\boldsymbol{\lambda}/\boldsymbol{\mu}),$$

where $\boldsymbol{\lambda}/\boldsymbol{\mu}$ is the k-quotient of λ/μ. We simply take Definition 2.8 and extend the set of labels: for each $i \in \mathcal{A} \cup \mathcal{A}'$, we put an i into each cell of the k-quotient of $\lambda_{\leq i}/\lambda_{\leq i-1}$.

Example 2.15.

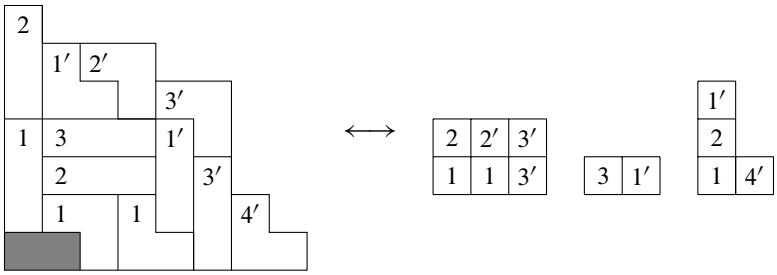

The following facts can be useful in computing the Littlewood k-quotient map in examples.

Lemma 2.16. *Suppose $T \leftrightarrow \boldsymbol{T}$ via the Littlewood k-quotient map.*

(1) *A ribbon in T labeled i corresponds to a cell labeled i in $\boldsymbol{T}$, so the number of ribbons in T labeled i equals the number of cells labeled i in $\boldsymbol{T}$.*

(2) *Two ribbons R, R' in T whose tails u, u' have the same content modulo k correspond to two cells v, v' in the same shape in $\boldsymbol{T}$. Moreover, in this case,*

$$\frac{c(u) - c(u')}{k} = c(v) - c(v').$$

Both the non-extended and the extended Littlewood k-quotient maps have these properties. The proof for the non-extended map follows from the proof for the extended map, which is given in Appendix A.

3. Vertex models, Yang–Baxter equations, and partition functions

In this section, we introduce several types of vertex models. We show that these models are integrable in the sense that they satisfy several Yang–Baxter equations. Then we use these vertex models to construct certain families of partition functions. Studying these families of partition functions, in particular the family in Definition 3.8, will be the main focus of the rest of the paper.

We begin with some notation. For a vector $\boldsymbol{I} = (I_1, \ldots, I_k) \in \mathbb{R}^k$, we define

$$|\boldsymbol{I}| = \sum_{m=1}^{k} I_i.$$

For vectors $\boldsymbol{I} = (I_1, \ldots, I_k), \boldsymbol{J} = (J_1, \ldots, J_k) \in \mathbb{R}^k$, we define

$$\varphi(\boldsymbol{I}, \boldsymbol{J}) = \sum_{1 \le i < j \le k} I_i J_j.$$

For variables x and t and an integer $n \ge 0$, we define the t-Pochhammer symbol

$$(x;t)_n = \prod_{m=0}^{n-1} (1 - xt^m).$$

We are now ready to define our vertices algebraically. We will define five vertices: the L-matrix, the L'-matrix, the R-matrix, the R'-matrix, and the R''-matrix. The L- and L'-matrices are families of functions $(\{0,1\}^k)^4 \to \mathbb{C}[x,t]$, one for each integer $k \ge 0$; the R-, R'-, and R''-matrices are families of functions $(\{0,1\}^k)^4 \to \mathbb{C}(x,y,t)$, one for each integer $k \ge 0$. In other words, each vertex associates a *weight* (either a polynomial in x, t or a rational function in x, y, t) to every 4-tuple of vectors in $\{0,1\}^k$ for each integer $k \ge 0$. Table 1 gives the algebraic definitions of these vertices.

Type of vertex	**Algebraic definition**
L	$L_x^{(k)}(\boldsymbol{I},\boldsymbol{J},\boldsymbol{K},\boldsymbol{L}) = \mathbf{1}_{\boldsymbol{I}+\boldsymbol{J}=\boldsymbol{K}+\boldsymbol{L}} \prod_{i=1}^k \mathbf{1}_{I_i+J_i \ne 2} \cdot x^{\lvert\boldsymbol{L}\rvert} t^{\varphi(\boldsymbol{L},\boldsymbol{I}+\boldsymbol{J})}$
L'	$L'^{(k)}_x(\boldsymbol{I},\boldsymbol{J},\boldsymbol{K},\boldsymbol{L}) = \mathbf{1}_{\boldsymbol{I}+\boldsymbol{J}=\boldsymbol{K}+\boldsymbol{L}} \prod_{i=1}^k \mathbf{1}_{K_i \ge J_i} \cdot x^{\lvert\boldsymbol{L}\rvert} t^{\varphi(\boldsymbol{L},\boldsymbol{K}-\boldsymbol{J})}$
R	$R^{(k)}_{y/x}(\boldsymbol{I},\boldsymbol{J},\boldsymbol{K},\boldsymbol{L}) = \mathbf{1}_{\boldsymbol{I}+\boldsymbol{J}=\boldsymbol{K}+\boldsymbol{L}} \prod_{i=1}^k \mathbf{1}_{J_i \ge K_i} \cdot (-1)^{\lvert\boldsymbol{J}\rvert-\lvert\boldsymbol{K}\rvert} (y/x)^{\lvert\boldsymbol{J}\rvert} \times (x/y;t)_{\lvert\boldsymbol{J}\rvert-\lvert\boldsymbol{K}\rvert} t^{\varphi(\boldsymbol{J},\boldsymbol{K}-\boldsymbol{J})}$
R'	$R'^{(k)}_{y/x}(\boldsymbol{I},\boldsymbol{J},\boldsymbol{K},\boldsymbol{L}) = \mathbf{1}_{\boldsymbol{I}+\boldsymbol{J}=\boldsymbol{K}+\boldsymbol{L}} \prod_{i=1}^k \mathbf{1}_{I_i+J_i \ne 2} \cdot (x/y)^{\lvert\boldsymbol{L}\rvert} \times (-x/y;t)^{-1}_{\lvert\boldsymbol{K}\rvert+\lvert\boldsymbol{L}\rvert} t^{\varphi(\boldsymbol{L},\boldsymbol{K}+\boldsymbol{L})}$
R''	$R''^{(k)}_{x/y}(\boldsymbol{I},\boldsymbol{J},\boldsymbol{K},\boldsymbol{L}) = \mathbf{1}_{\boldsymbol{I}+\boldsymbol{J}=\boldsymbol{K}+\boldsymbol{L}} \prod_{i=1}^k \mathbf{1}_{K_i \ge J_i} \cdot (x/y)^{\lvert\boldsymbol{L}\rvert} \times (x/y;t)_{\lvert\boldsymbol{K}\rvert-\lvert\boldsymbol{J}\rvert} t^{\varphi(\boldsymbol{L},\boldsymbol{K}-\boldsymbol{J})}$

Table 1. Algebraic definitions of the L-, L'-, R-, R'-, and R''-matrices.

However, it is often useful to think of a vertex graphically. We can draw a vertex as a face with four incident edges, each labeled by an element of $\{0,1\}^k$. The face takes one of two forms,

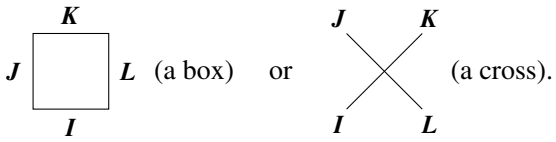

The edge labels describe colored paths moving through the face south-west-to-north-east (for a box) or left-to-right (for a cross). If an edge has the label $\boldsymbol{I} = (I_1, \ldots, I_k) \in \{0,1\}^k$, then for each $i \in [k]$, a path of color i is incident at the edge if and only if

$I_i = 1$. For example, with $k = 2$ (letting blue be color 1 and red be color 2), the path configuration associated to the edge labels $\boldsymbol{I} = (0,1)$, $\boldsymbol{J} = (1,0)$, $\boldsymbol{K} = (0,1)$, $\boldsymbol{L} = (1,0)$ is

 (for a box) or  (for a cross).

The factor of $\mathbf{1}_{\boldsymbol{I}+\boldsymbol{J}=\boldsymbol{K}+\boldsymbol{L}}$ that appears in the algebraic definitions of all five vertices imposes a *path conservation* restriction: in order for a vertex to have a non-zero weight, the paths entering the vertex and the paths exiting the vertex must be the same. To define the vertex weights graphically, we start by defining the weights in the case $k = 1$ in Table 2.

Type of vertex	**One-color definition**					
L	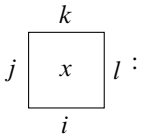					
	$L_x^{(1)}(i,j,k,l)$:	1	x	x	1	1
L'	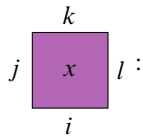					
	$L'^{(1)}_x(i,j,k,l)$:	1	1	x	1	x
R	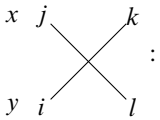					
	$R^{(1)}_{y/x}(i,j,k,l)$:	$1-y/x$	y/x	1	y/x	1
R'	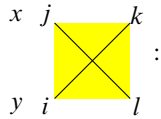					
	$R'^{(1)}_{y/x}(i,j,k,l)$:	$\frac{1}{1+y/x}$	$\frac{y/x}{1+y/x}$	$\frac{1}{1+y/x}$	$\frac{y/x}{1+y/x}$	1
R''	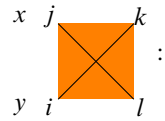					
	$R''^{(1)}_{x/y}(i,j,k,l)$:	$1-x/y$	1	x/y	x/y	1

Table 2. Graphical definitions of the L-, L'-, R-, R'-, and R''-matrices in the case $k = 1$.

The k-color weights are then defined in terms of the one-color weights in Table 3.

Type of vertex	***k*-color definition**
L	$L^{(k)}_x(\boldsymbol{I},\boldsymbol{J},\boldsymbol{K},\boldsymbol{L}) = \prod_{i=1}^k L^{(1)}_{xt^{\delta_i}}(I_i,J_i,K_i,L_i)$, where δ_i = # colors greater than i that are present
L'	$L'^{(k)}_x(\boldsymbol{I},\boldsymbol{J},\boldsymbol{K},\boldsymbol{L}) = \prod_{i=1}^k L'^{(1)}_{xt^{\delta'_i}}(I_i,J_i,K_i,L_i)$, where δ'_i = # colors greater than i of the form 
R	$R^{(k)}_{y/x}(\boldsymbol{I},\boldsymbol{J},\boldsymbol{K},\boldsymbol{L}) = \prod_{i=1}^k R^{(1)}_{y/(xt^{\varepsilon_i})}(I_i,J_i,K_i,L_i)$, where ε_i = # colors greater than i of the form 
R'	$R'^{(k)}_{y/x}(\boldsymbol{I},\boldsymbol{J},\boldsymbol{K},\boldsymbol{L}) = \prod_{i=1}^k R'^{(1)}_{y/(xt^{\varepsilon'_i})}(I_i,J_i,K_i,L_i)$, where ε'_i = # colors greater than i that are present
R''	$R''^{(k)}_{x/y}(\boldsymbol{I},\boldsymbol{J},\boldsymbol{K},\boldsymbol{L}) = \prod_{i=1}^k R''^{(1)}_{t^{\varepsilon''_i}x/y}(I_i,J_i,K_i,L_i)$, where ε''_i = # colors greater than i of the form 

Table 3. Graphical definitions of the L-, L'-, R-, R'-, and R''-matrices for general k.

We leave it as an exercise for the reader to check that the algebraic and graphical definitions are equivalent.

We remark that the L-matrix and the R-matrix appeared in [13]. Moreover, by the following lemma, the weights of all five vertices can be realized as degenerations of the vertex weights $W_z(\mathbf{A},\mathbf{B};\mathbf{C},\mathbf{D} \mid r,s)$ from [1, Definition 5.1.1].

Lemma 3.1. *We adopt the notation of* [1]*, except we use t in place of q. In particular, we let $W_z(\mathbf{A},\mathbf{B};\mathbf{C},\mathbf{D} \mid r,s)$ be the vertex weights from* [1, Definition 5.1.1] *with t in place of q. Then*

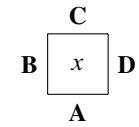

$$= \lim_{\alpha\to 0}(-\alpha)^d \lim_{\beta\to 0}\beta^{-2d} W_{x/\alpha}(\mathbf{A},\mathbf{B};\mathbf{C},\mathbf{D} \mid (x/\alpha)^{1/2},\beta),$$

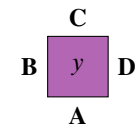

$$= \lim_{Y\to 0} Y^{-d} \lim_{S\to 0} W_1(\mathbf{A},\mathbf{B};\mathbf{C},\mathbf{D} \mid Sy^{-1/2}, SY^{1/2}),$$

$$= \lim_{\alpha\to 0} W_{x/y}(\mathbf{A},\mathbf{B};\mathbf{C},\mathbf{D} \mid (x/\alpha)^{1/2},(y/\alpha)^{1/2}),$$

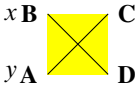

$$= \lim_{\alpha\to 0} W_{x/\alpha}(\mathbf{A},\mathbf{B};\mathbf{C},\mathbf{D} \mid (x/\alpha)^{1/2},(-y/\alpha)^{-1/2}),$$

$$= \lim_{S\to 0} W_1(\mathbf{A},\mathbf{B};\mathbf{C},\mathbf{D} \mid Sx^{-1/2}, Sy^{-1/2}).$$

Proof. This follows from various corollaries in [1, Section 8.3] along with the algebraic definitions of the matrices L (white box), L' (purple box), R (white cross), R' (yellow cross), and R'' (orange cross),

- [1, Corollary 8.3.6] for the L-matrix,
- [1, Corollary 8.3.4] for the L'-matrix,
- [1, Corollary 8.3.1] (substituting $s = (y/\alpha)^{1/2}$) for the R-matrix,
- [1, Corollary 8.3.8] (substituting $s = (-y/\alpha)^{-1/2}$) for the R'-matrix,
- [1, Corollary 8.3.3] for the R''-matrix. ∎

It turns out that these vertices satisfy three Yang–Baxter equations. All three follow from [1, Proposition 5.1.4] and Lemma 3.1; for interested readers, we give a detailed derivation of Propositions 3.3 and 3.4 in Appendix C. Proposition 3.2 is proven in a different way in [13, Theorem 4.1].

Proposition 3.2. *The L- and R-matrices satisfy the Yang–Baxter equation*

$$\sum_{\text{interior paths}} w\left(\begin{array}{ccc} & \boldsymbol{K}_3 & \\ \boldsymbol{J}_1 & y \quad \boldsymbol{I}_3 & \\ \boldsymbol{I}_1 & x \quad \boldsymbol{J}_3 & \\ & \boldsymbol{K}_1 & \end{array}\right) = \sum_{\text{interior paths}} w\left(\begin{array}{ccc} & \boldsymbol{K}_3 & \\ \boldsymbol{J}_1 & x \quad \boldsymbol{I}_3 & \\ \boldsymbol{I}_1 & y \quad \boldsymbol{J}_3 & \\ & \boldsymbol{K}_1 & \end{array}\right)$$

for any choice of boundary conditions $\boldsymbol{I}_1, \boldsymbol{J}_1, \boldsymbol{K}_1, \boldsymbol{I}_3, \boldsymbol{J}_3, \boldsymbol{K}_3$.

Proposition 3.3. *The L-, L'-, and R'-matrices satisfy the Yang–Baxter equation*

$$\sum_{\text{interior paths}} w\left(\begin{array}{ccc} & \boldsymbol{K}_3 & \\ \boldsymbol{J}_1 & y \quad \boldsymbol{I}_3 & \\ \boldsymbol{I}_1 & x \quad \boldsymbol{J}_3 & \\ & \boldsymbol{K}_1 & \end{array}\right) = \sum_{\text{interior paths}} w\left(\begin{array}{ccc} & \boldsymbol{K}_3 & \\ \boldsymbol{J}_1 & x \quad \boldsymbol{I}_3 & \\ \boldsymbol{I}_1 & y \quad \boldsymbol{J}_3 & \\ & \boldsymbol{K}_1 & \end{array}\right)$$

for any choice of boundary conditions $\boldsymbol{I}_1, \boldsymbol{J}_1, \boldsymbol{K}_1, \boldsymbol{I}_3, \boldsymbol{J}_3, \boldsymbol{K}_3$.

Proposition 3.4. *The L'- and R''-matrices satisfy the Yang–Baxter equation*

$$\sum_{\text{interior paths}} w\left(\begin{array}{ccc} & \boldsymbol{K}_3 & \\ \boldsymbol{J}_1 & y \quad \boldsymbol{I}_3 & \\ \boldsymbol{I}_1 & x \quad \boldsymbol{J}_3 & \\ & \boldsymbol{K}_1 & \end{array}\right) = \sum_{\text{interior paths}} w\left(\begin{array}{ccc} & \boldsymbol{K}_3 & \\ \boldsymbol{J}_1 & x \quad \boldsymbol{I}_3 & \\ \boldsymbol{I}_1 & y \quad \boldsymbol{J}_3 & \\ & \boldsymbol{K}_1 & \end{array}\right)$$

for any choice of boundary conditions $\boldsymbol{I}_1, \boldsymbol{J}_1, \boldsymbol{K}_1, \boldsymbol{I}_3, \boldsymbol{J}_3, \boldsymbol{K}_3$.

Remark 3.5. Let us say a few words about where the weights W_z [1, Definition 5.1.1] and the YBE [1, Proposition 5.1.4] come from. Bazhanov and Shadrikov [4] constructed the fundamental R-matrix for the quantum affine superalgebra $U_q(\widehat{\mathfrak{sl}}(m|n))$, and showed that it satisfied the Yang–Baxter equation. (Although this was not the method used in [4, Section 3], the fact that this matrix satisfies the Yang–Baxter equation can be verified via a direct computation using the explicit formulae for its entries.) Aggarwal, Borodin, and Wheeler [1] constructed the weights W_z by applying the fusion procedure originating in [20] to the fundamental R-matrix, specializing to $m = 1$, and applying analytic continuation. The Yang–Baxter equation for the weights W_z falls out from the Yang–Baxter equation for the fundamental R-matrix.

We use these vertices to construct three classes of partition functions, the first of which was studied in [13]. Given a lattice L, the associated *partition function* is

$$\sum_{C \in LC(L)} \text{weight}(C),$$

where $LC(L)$ is the set of valid configurations on the lattice L. In what follows, let

$$\boldsymbol{\lambda}/\boldsymbol{\mu} = (\lambda^{(1)}/\mu^{(1)}, \ldots, \lambda^{(k)}/\mu^{(k)})$$

be a k-tuple of skew partitions, each having p parts.

Theorem 3.6 ([13, Theorem 3.4]). *The coinversion LLT polynomial $\mathcal{L}_{\boldsymbol{\lambda}/\boldsymbol{\mu}}(X_n; t)$ is the partition function associated to the lattice*

$W_n(\boldsymbol{\lambda}/\boldsymbol{\mu}) :=$

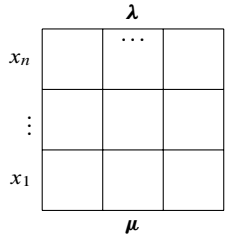

Definition 3.7. We define $\mathcal{L}^{P}_{\boldsymbol{\lambda}/\boldsymbol{\mu}}(X_n; t)$ to be the partition function associated to the lattice

$P_n(\boldsymbol{\lambda}/\boldsymbol{\mu}) :=$

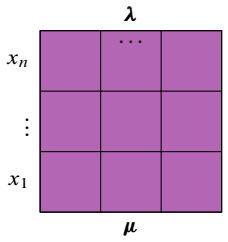

Definition 3.8. We define $\mathcal{L}^{S}_{\boldsymbol{\lambda}/\boldsymbol{\mu}}(X_n; Y_m; t)$ to be the partition function associated to the lattice

$S_{n,m}(\boldsymbol{\lambda}/\boldsymbol{\mu}) :=$ 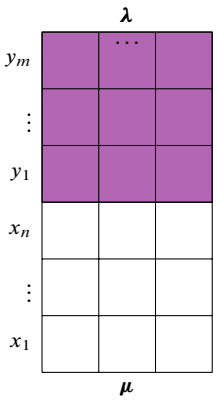

Often, when it is clear from context, we will abuse notation and let the drawing of the lattice be equal to the partition function of the vertex model on the lattice.

4. Identities of supersymmetric LLT polynomials

The main goal of this section is to establish various properties of the partition functions $\mathcal{L}^{S}_{\boldsymbol{\lambda}/\boldsymbol{\mu}}$ from Definition 3.8. These include four properties (summarized in Theorem 1.1) which generalize four properties that uniquely characterize the supersymmetric Schur polynomials.

Let $P_p^{(k)}$ be the set of k-tuples of partitions, each having p parts. Given $\boldsymbol{\lambda}, \boldsymbol{\mu} \in P_p^{(k)}$ and a non-negative integer n, there is a bijection

$$\psi\colon LC(W_n(\boldsymbol{\lambda}/\boldsymbol{\mu})) \to LC(P_n(\boldsymbol{\lambda}'/\boldsymbol{\mu}')),$$

where $W_n(\boldsymbol{\lambda}/\boldsymbol{\mu})$ is defined in Theorem 3.6 and $P_n(\boldsymbol{\lambda}'/\boldsymbol{\mu}')$ is defined in Definition 3.7. Explicitly, $\psi(C)$ is obtained from C by inverting the vertical parts of the paths, reflecting the lattice over its left edge, changing each color i to color $k-i$, and making the vertices purple. For example,

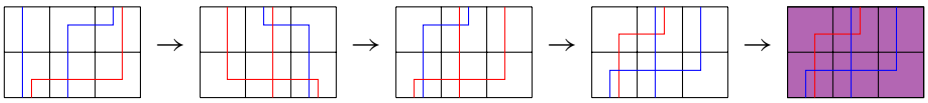

where we have done each step in order (and where blue is color 1 and red is color 2).

Fix $\boldsymbol{\lambda}, \boldsymbol{\mu} \in P_p^{(k)}$. Also fix a sufficiently large number of columns; specifically, the number of columns must be larger than each $p + \lambda_1^{(i)}$ and $p + \mu_1^{(i)}$. If $\boldsymbol{\lambda}/\boldsymbol{\mu}$ is a horizontal strip, then there is a unique configuration $C_{\boldsymbol{\lambda}/\boldsymbol{\mu}}$ on a single white row with top boundary $\boldsymbol{\lambda}$, bottom boundary $\boldsymbol{\mu}$, and empty left/right boundaries. Similarly,

if $\boldsymbol{\lambda}/\boldsymbol{\mu}$ is a vertical strip, then there is a unique configuration on a single purple row with top boundary $\boldsymbol{\lambda}$, bottom boundary $\boldsymbol{\mu}$, and empty left/right boundaries.

Lemma 4.1. *There exists a function* $g\colon P_p^{(k)} \to \mathbb{Z}_{\geq 0}$ *such that*

$$\mathcal{L}_{\boldsymbol{\lambda}/\boldsymbol{\mu}}(x;t) = t^{g(\boldsymbol{\lambda})-g(\boldsymbol{\mu})}\mathcal{L}^P_{\boldsymbol{\lambda}'/\boldsymbol{\mu}'}(x;t^{-1})$$

for all $\boldsymbol{\lambda}, \boldsymbol{\mu} \in P_p^{(k)}$ *such that* $\boldsymbol{\lambda}/\boldsymbol{\mu}$ *is a horizontal strip.*

Proof. Fix $\boldsymbol{\lambda}, \boldsymbol{\mu} \in P_p^{(k)}$ such that $\boldsymbol{\lambda}/\boldsymbol{\mu}$ is a horizontal strip. Let $C = C_{\boldsymbol{\lambda}/\boldsymbol{\mu}}$. Note that C is the unique configuration on a single white row with top boundary $\boldsymbol{\lambda}$, bottom boundary $\boldsymbol{\mu}$, and empty left/right boundaries. Moreover, $\psi(C)$ is the unique configuration on a single purple row with top boundary $\boldsymbol{\lambda}'$, bottom boundary $\boldsymbol{\mu}'$, and empty left/right boundaries. Thus

$$\begin{aligned}\mathcal{L}_{\boldsymbol{\lambda}/\boldsymbol{\mu}}(x;t) &= \text{weight}(C) = x^\alpha t^\beta,\\ \mathcal{L}^P_{\boldsymbol{\lambda}/\boldsymbol{\mu}}(x;t) &= \text{weight}(\psi(C)) = x^\gamma t^\delta\end{aligned}$$

for some non-negative integers $\alpha, \beta, \gamma, \delta$. Note

$$\begin{aligned}\alpha &= \#\{(i,j) \mid \text{the } i\text{-th smallest color exits right in the } b\text{-th leftmost box in } C\}\\ &= \#\{(i,j) \mid \text{the } i\text{-th largest color exits right in the } b\text{-th rightmost box}\\ &\qquad\qquad \text{in } \psi(C)\} = \gamma.\end{aligned}$$

Therefore,

$$\mathcal{L}_{\boldsymbol{\lambda}/\boldsymbol{\mu}}(x;t) = x^\alpha t^\beta = t^{\beta+\delta}x^\gamma t^{-\delta} = t^{\beta+\delta}\mathcal{L}^P_{\boldsymbol{\lambda}/\boldsymbol{\mu}}(x;t^{-1}).$$

Note that

$$\begin{aligned}\beta+\delta &= \#\{(i,j,b) \mid i<j, \text{ in box } b \text{ of } C \text{ color } i \text{ exits right and color } j \text{ is present}\}\\ &\quad + \#\{(i',j',b') \mid i'>j', \text{ in box } b' \text{ of } \psi(C) \text{ color } i' \text{ is vertical and color } j'\\ &\qquad\qquad \text{exits right}\}\\ &= \#\{(i,j,b) \mid i<j, \text{ in box } b \text{ of } C \text{ color } i \text{ exits right and color } j \text{ is present}\}\\ &\quad + \#\{(i,j,b) \mid i<j, \text{ in box } b \text{ of } C \text{ color } i \text{ is absent and color } j \text{ enters}\\ &\qquad\qquad \text{from the left}\} = \sum_b \sum_{i<j} \mathbf{1}_{b \text{ is ``good'' for } i \text{ and } j},\end{aligned}$$

where we say a box b is "good" for the colors $i<j$ if either color i exits right and color j is present, or color i is absent and color j enters from the left. Therefore,

$$\mathcal{L}_{\boldsymbol{\lambda}/\boldsymbol{\mu}}(x;t) = t^{\widetilde{g}(\boldsymbol{\lambda}/\boldsymbol{\mu})}\mathcal{L}^P_{\boldsymbol{\lambda}'/\boldsymbol{\mu}'}(x;t^{-1}),$$

where we have defined

$$\widetilde{g}(\boldsymbol{\lambda}/\boldsymbol{\mu}) := \sum_{\substack{\text{boxes } b \\ \text{of } C_{\boldsymbol{\lambda}/\boldsymbol{\mu}}}} \sum_{\substack{\text{colors} \\ i<j}} \mathbf{1}_{b \text{ is ``good'' for } i \text{ and } j}.$$

We can recursively define the desired function g by the rule

$$g(\boldsymbol{\lambda}) = \begin{cases} g(\boldsymbol{\mu}) + \widetilde{g}(\boldsymbol{\lambda}/\boldsymbol{\mu}) & \text{if there exists } \boldsymbol{\mu} \in P_p^{(k)} - \{\boldsymbol{\lambda}\} \text{ such that } \boldsymbol{\lambda}/\boldsymbol{\mu} \text{ is} \\ & \text{a horizontal strip,} \\ 0 & \text{otherwise (i.e., if } \boldsymbol{\lambda} = \mathbf{0}). \end{cases}$$

Provided that $g(\boldsymbol{\lambda})$ is well defined (i.e., $g(\boldsymbol{\mu}) + \widetilde{g}(\boldsymbol{\lambda}/\boldsymbol{\mu})$ is independent of $\boldsymbol{\mu}$) for all $\boldsymbol{\lambda} \in P_p^{(k)}$,

$$\mathcal{L}_{\boldsymbol{\lambda}/\boldsymbol{\mu}}(x;t) = t^{\widetilde{g}(\boldsymbol{\lambda}/\boldsymbol{\mu})} \mathcal{L}^P_{\boldsymbol{\lambda}'/\boldsymbol{\mu}'}(x;t^{-1}) = t^{g(\boldsymbol{\lambda})-g(\boldsymbol{\mu})} \mathcal{L}^P_{\boldsymbol{\lambda}'/\boldsymbol{\mu}'}(x;t^{-1})$$

for all $\boldsymbol{\lambda}, \boldsymbol{\mu} \in P_p^{(k)}$ such that $\boldsymbol{\lambda}/\boldsymbol{\mu}$ is a horizontal strip. To show g is well defined, we proceed by induction on the number of cells in $\boldsymbol{\lambda}$. Clearly, $g(\mathbf{0}) = 0$ is well defined. Fix $\boldsymbol{\lambda} \in P_p^{(k)} - \{\mathbf{0}\}$ and assume g is well defined on elements of $P_p^{(k)}$ with strictly fewer boxes than $\boldsymbol{\lambda}$. Fix $\boldsymbol{\alpha}, \boldsymbol{\mu} \in P_p^{(k)} - \{\boldsymbol{\lambda}\}$ such that $\boldsymbol{\lambda}/\boldsymbol{\alpha}$ and $\boldsymbol{\lambda}/\boldsymbol{\mu}$ are horizontal strips. There exist (not necessarily distinct)

$$\begin{aligned} \boldsymbol{\beta}^0 &= \mathbf{0}, \quad \ldots, \quad \boldsymbol{\beta}^{r-1} = \boldsymbol{\alpha}, \quad \boldsymbol{\beta}^r = \boldsymbol{\lambda} \in P_p^{(k)}, \\ \boldsymbol{\nu}^0 &= \mathbf{0}, \quad \ldots, \quad \boldsymbol{\nu}^{r-1} = \boldsymbol{\mu}, \quad \boldsymbol{\nu}^r = \boldsymbol{\lambda} \in P_p^{(k)} \end{aligned}$$

such that $\boldsymbol{\beta}^i/\boldsymbol{\beta}^{i-1}$ and $\boldsymbol{\nu}^i/\boldsymbol{\nu}^{i-1}$ are horizontal strips for all i. Note that each sequence completely determines a configuration of paths on an $r \times M$ lattice with top boundary $\boldsymbol{\lambda}$ and bottom boundary $\mathbf{0}$, since they determine the state of the paths at every row.

Since the two configurations have the same top and bottom boundaries, it is possible to get from one configuration to the other via corner flips

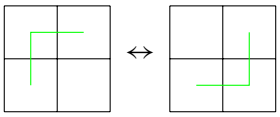

Some straightforward computations (which we verified with a computer) show that for any configuration on a 2×2 white lattice and for any colors $h < i < j$ such that color i has the form

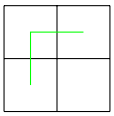

in the configuration, flipping color i changes neither the number of boxes that are "good" for h and i, nor the number of boxes that are "good" for i and j. Using the flipping argument repeatedly, we see that the quantity

$$\sum_b \sum_{i<j} \mathbf{1}_{b \text{ is "good" for } i \text{ and } j}$$

is the same for both configurations. Therefore,

$$\begin{aligned}\widetilde{g}(\boldsymbol{\beta}^r/\boldsymbol{\beta}^{r-1}) + \widetilde{g}(\boldsymbol{\beta}^{r-1}/\boldsymbol{\beta}^{r-2}) + \cdots + \widetilde{g}(\boldsymbol{\beta}^1/\boldsymbol{\beta}^0) \\ = \widetilde{g}(\boldsymbol{\nu}^r/\boldsymbol{\nu}^{r-1}) + \widetilde{g}(\boldsymbol{\nu}^{r-1}/\boldsymbol{\nu}^{r-2}) + \cdots + \widetilde{g}(\boldsymbol{\nu}^1/\boldsymbol{\nu}^0).\end{aligned}$$

Applying the inductive hypothesis, we have

$$\begin{aligned}\widetilde{g}(\boldsymbol{\beta}^r/\boldsymbol{\beta}^{r-1}) + g(\boldsymbol{\beta}^{r-1}) - g(\boldsymbol{\beta}^{r-2}) + \cdots + g(\boldsymbol{\beta}^1) - g(\boldsymbol{\beta}^0) \\ = \widetilde{g}(\boldsymbol{\nu}^r/\boldsymbol{\nu}^{r-1}) + g(\boldsymbol{\nu}^{r-1}) - g(\boldsymbol{\nu}^{r-2}) + \cdots + g(\boldsymbol{\nu}^1) - g(\boldsymbol{\nu}^0).\end{aligned}$$

The sums telescope to give

$$\widetilde{g}(\boldsymbol{\beta}^r/\boldsymbol{\beta}^{r-1}) + g(\boldsymbol{\beta}^{r-1}) - g(\boldsymbol{\beta}^0) = \widetilde{g}(\boldsymbol{\nu}^r/\boldsymbol{\nu}^{r-1}) + g(\boldsymbol{\nu}^{r-1}) - g(\boldsymbol{\nu}^0),$$

which we can rewrite as

$$\widetilde{g}(\boldsymbol{\lambda}/\boldsymbol{\alpha}) + g(\boldsymbol{\alpha}) - g(\mathbf{0}) = \widetilde{g}(\boldsymbol{\lambda}/\boldsymbol{\mu}) + g(\boldsymbol{\mu}) - g(\mathbf{0}).$$

Therefore, $g(\boldsymbol{\alpha}) + \widetilde{g}(\boldsymbol{\lambda}/\boldsymbol{\alpha}) = g(\boldsymbol{\mu}) + \widetilde{g}(\boldsymbol{\lambda}/\boldsymbol{\mu})$. ∎

Corollary 4.2. *For any* $\boldsymbol{\lambda} \in P_p^{(k)}$, $g(\boldsymbol{\lambda}) = g(\boldsymbol{\lambda}')$.

Proof. We proceed by induction on the number of cells in $\boldsymbol{\lambda}$. Note that $g(\mathbf{0}) = 0 = g(\mathbf{0}')$. Fix $\boldsymbol{\lambda} \in P_p^{(k)} - \{\mathbf{0}\}$ and assume $g(\boldsymbol{\mu}) = g(\boldsymbol{\mu}')$ for all $\boldsymbol{\mu} \in P_p^{(k)}$ with strictly fewer cells than $\boldsymbol{\lambda}$. Since $\boldsymbol{\lambda} \neq \mathbf{0}$, there exists $\boldsymbol{\mu} \in P_p^{(k)}$ that can be obtained by removing a single cell u from $\boldsymbol{\lambda}$. We want to show $g(\boldsymbol{\lambda}) = g(\boldsymbol{\lambda}')$. It is enough to show $\widetilde{g}(\boldsymbol{\lambda}/\boldsymbol{\mu}) = \widetilde{g}(\boldsymbol{\lambda}'/\boldsymbol{\mu}')$, since then

$$g(\boldsymbol{\lambda}) = g(\boldsymbol{\mu}) + \widetilde{g}(\boldsymbol{\lambda}/\boldsymbol{\mu}) = g(\boldsymbol{\mu}') + \widetilde{g}(\boldsymbol{\lambda}'/\boldsymbol{\mu}') = g(\boldsymbol{\lambda}').$$

Let $\lambda^{(i)}$ be the partition to which u belongs. Since $\boldsymbol{\lambda}/\boldsymbol{\mu}$ consists of the single cell u in $\lambda^{(i)}/\mu^{(i)}$, every color in every box in $C_{\boldsymbol{\lambda}/\boldsymbol{\mu}}$ is either vertical or absent, with the exception of the color i in two adjacent boxes, which has the form

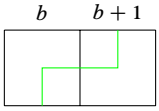

Note that $C_{\boldsymbol{\lambda}'/\boldsymbol{\mu}'}$ is exactly the configuration of $\psi(C_{\boldsymbol{\lambda}/\boldsymbol{\mu}})$ with white in place of purple. Therefore, every color in every box in $C_{\boldsymbol{\lambda}'/\boldsymbol{\mu}'}$ is either vertical or absent, with the exception of the color $i' = k - i$ in two adjacent boxes, which has the form

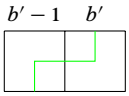

We have

$$\begin{aligned}\widetilde{g}(\boldsymbol{\lambda}/\boldsymbol{\mu}) &= \#\{j > i \mid j \text{ is vertical in box } b \text{ of } C_{\boldsymbol{\lambda}/\boldsymbol{\mu}}\} \\ &\quad + \#\{h < i \mid h \text{ is absent in box } b+1 \text{ of } C_{\boldsymbol{\lambda}/\boldsymbol{\mu}}\} \\ &= \#\{j' < i' \mid j' \text{ is absent in box } b' \text{ of } C_{\boldsymbol{\lambda}'/\boldsymbol{\mu}'}\} \\ &\quad + \#\{h' > i' \mid h' \text{ is vertical in box } b'-1 \text{ of } C_{\boldsymbol{\lambda}'/\boldsymbol{\mu}'}\} = \widetilde{g}(\boldsymbol{\lambda}'/\boldsymbol{\mu}'). \quad \blacksquare\end{aligned}$$

Equipped with Lemma 4.1 and Corollary 4.2, we can now prove the following identity relating $\mathcal{L}^S_{\boldsymbol{\lambda}/\boldsymbol{\mu}}$ and $\mathcal{L}^S_{\boldsymbol{\lambda}'/\boldsymbol{\mu}'}$. This is equivalent to [15, Proposition 2.2].

Theorem 4.3. *For any* $\boldsymbol{\lambda}, \boldsymbol{\mu} \in P_p^{(k)}$,

$$\mathcal{L}^S_{\boldsymbol{\lambda}/\boldsymbol{\mu}}(X_n; Y_m; t) = t^{g(\boldsymbol{\lambda})-g(\boldsymbol{\mu})}\mathcal{L}^S_{\boldsymbol{\lambda}'/\boldsymbol{\mu}'}(Y_m; X_n; t^{-1}).$$

Proof. If $\boldsymbol{\lambda}/\boldsymbol{\mu}$ is a horizontal strip, then by Lemma 4.1, we have

$$\mathcal{L}_{\boldsymbol{\lambda}/\boldsymbol{\mu}}(x; t) = t^{g(\boldsymbol{\lambda})-g(\boldsymbol{\mu})}\mathcal{L}^P_{\boldsymbol{\lambda}'/\boldsymbol{\mu}'}(x; t^{-1}).$$

If $\boldsymbol{\lambda}/\boldsymbol{\mu}$ is a vertical strip, then by Lemma 4.1 (with t^{-1} in place of t and $\boldsymbol{\lambda}'/\boldsymbol{\mu}'$ in place of $\boldsymbol{\lambda}/\boldsymbol{\mu}$) and Corollary 4.2, we have

$$\mathcal{L}^P_{\boldsymbol{\lambda}/\boldsymbol{\mu}}(x; t) = t^{g(\boldsymbol{\lambda})-g(\boldsymbol{\mu})}\mathcal{L}_{\boldsymbol{\lambda}'/\boldsymbol{\mu}'}(x; t^{-1}).$$

Using these lemmas at each row of our lattice, we have

$\mathcal{L}^S_{\boldsymbol{\lambda}/\boldsymbol{\mu}}(X_n; Y_m; t) =$

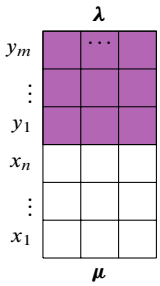

$$\begin{aligned}&= \sum \mathcal{L}^P_{\boldsymbol{\lambda}/\boldsymbol{\alpha}^{m+n-1}}(y_m; t)\cdots\mathcal{L}^P_{\boldsymbol{\alpha}^{n+1}/\boldsymbol{\alpha}^n}(y_1; t)\mathcal{L}_{\boldsymbol{\alpha}^n/\boldsymbol{\alpha}^{n-1}}(x_n; t)\cdots\mathcal{L}_{\boldsymbol{\alpha}^1/\boldsymbol{\mu}}(x_1; t) \\ &= \sum t^{g(\boldsymbol{\lambda})-g(\boldsymbol{\mu})}\mathcal{L}_{\boldsymbol{\lambda}'/\boldsymbol{\alpha}^{m+n-1'}}(y_m; t^{-1})\cdots\mathcal{L}_{\boldsymbol{\alpha}^{n+1'}/\boldsymbol{\alpha}^{n'}}(y_1; t^{-1}) \\ &\qquad \times \mathcal{L}^P_{\boldsymbol{\alpha}^{n'}/\boldsymbol{\alpha}^{n-1'}}(x_n; t^{-1})\cdots\mathcal{L}^P_{\boldsymbol{\alpha}^{1'}/\boldsymbol{\mu}'}(x_1; t^{-1})\end{aligned}$$

$$= t^{g(\boldsymbol{\lambda})-g(\boldsymbol{\mu})} \sum \mathcal{L}_{\boldsymbol{\lambda}'/\boldsymbol{\beta}^{m+n-1}}(y_m;t^{-1}) \cdots \mathcal{L}_{\boldsymbol{\beta}^{n+1}/\boldsymbol{\beta}^{n}}(y_1;t^{-1})$$
$$\times \mathcal{L}^{P}_{\boldsymbol{\beta}^{n}/\boldsymbol{\beta}^{n-1}}(x_n;t^{-1}) \cdots \mathcal{L}^{P}_{\boldsymbol{\beta}^{1}/\boldsymbol{\mu}'}(x_1;t^{-1})$$

$= t^{g(\boldsymbol{\lambda})-g(\boldsymbol{\mu})}$ 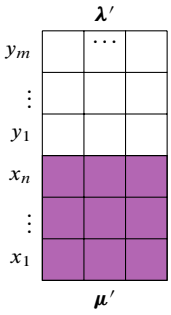

$= t^{g(\boldsymbol{\lambda})-g(\boldsymbol{\mu})}$ 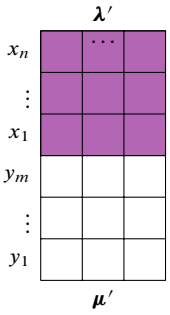

$$= \mathcal{L}^{S}_{\boldsymbol{\lambda}'/\boldsymbol{\mu}'}(Y_m;X_n;t^{-1}),$$

where

- the sums in the second and third lines are over all $\boldsymbol{\alpha}^0 = \boldsymbol{\mu}, \ldots, \boldsymbol{\alpha}^{m+n} = \boldsymbol{\lambda}$ such that $\boldsymbol{\alpha}^i/\boldsymbol{\alpha}^{i-1}$ is a horizontal strip for all $i \leq n$ and a vertical strip for all $i > n$,
- the sum in the fourth line is over all $\boldsymbol{\beta}^0 = \boldsymbol{\mu}', \ldots, \boldsymbol{\beta}^{m+n} = \boldsymbol{\lambda}'$ such that $\boldsymbol{\beta}^i/\boldsymbol{\beta}^{i-1}$ is a vertical strip for all $i \leq n$ and a horizontal strip for all $i > n$,
- the second-to-last equality uses repeated applications of Proposition 3.3, as illustrated below:

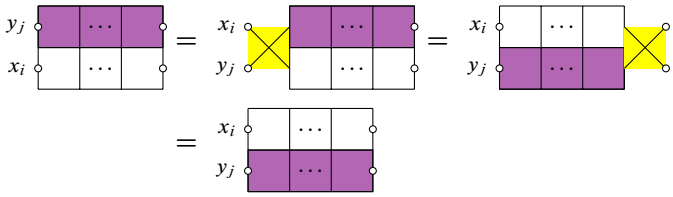

■

The technique used to swap a white row and a purple row at the end of the previous proof is sometimes called the "train argument." This technique is used again to prove the following lemma.

Lemma 4.4. *The partition function associated to any lattice that can be obtained from the lattice $S_{n,m}$ (Definition 3.8) by permuting the rows equals $\mathcal{L}^{S}_{\boldsymbol{\lambda}/\boldsymbol{\mu}}(X_n;Y_m;t)$. In particular, $\mathcal{L}^{S}_{\boldsymbol{\lambda}/\boldsymbol{\mu}}(X_n;Y_m;t)$ is symmetric in the X and Y variables separately.*

Proof. Two rows can be swapped using the train argument along with Proposition 3.2 (to swap two white rows), Proposition 3.3 (to swap a white row and a purple row), or Proposition 3.4 (to swap two purple rows). ■

Lemma 4.5. *Suppose $n, m \geq 1$. Then*

$$\mathcal{L}^{S}_{\boldsymbol{\lambda}/\boldsymbol{\mu}}(X_{n-1}, r; Y_{m-1}, -r; t) = \mathcal{L}^{S}_{\boldsymbol{\lambda}/\boldsymbol{\mu}}(X_{n-1}; Y_{m-1}; t).$$

Proof. Using Lemma 4.4, we can write

$$\mathcal{L}^S_{\boldsymbol{\lambda}/\boldsymbol{\mu}}(X_{n-1}, r; Y_{m-1}, -r; t) =$$

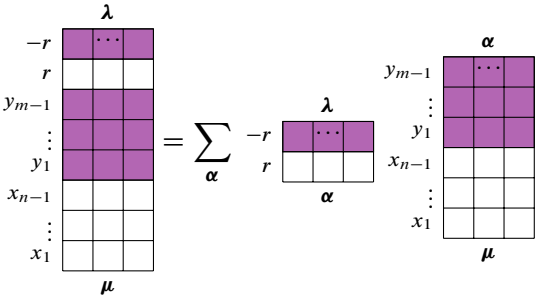

We will show that, for all $\boldsymbol{\alpha} \neq \boldsymbol{\lambda}$, there is an involution $\varphi_{\boldsymbol{\alpha}}$ on the set of configurations of the lattice

$$L_{\boldsymbol{\lambda}/\boldsymbol{\alpha}} =$$

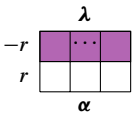

such that $\text{weight}(\varphi_{\boldsymbol{\alpha}}(C)) = -\text{weight}(C)$ for all C. Therefore,

$$\mathcal{L}^S_{\boldsymbol{\lambda}/\boldsymbol{\mu}}(X_{n-1}, r; Y_{m-1}, -r; t) =$$

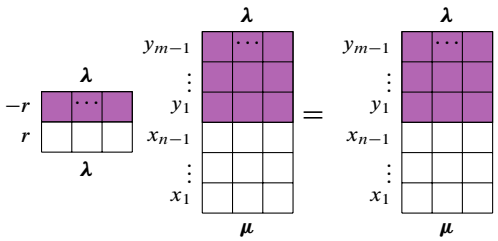

$$= \mathcal{L}^S_{\boldsymbol{\lambda}/\boldsymbol{\mu}}(X_{n-1}; Y_{m-1}; t).$$

Fix $\boldsymbol{\alpha} \neq \boldsymbol{\lambda}$ and fix a configuration C on the lattice $L_{\boldsymbol{\lambda}/\boldsymbol{\alpha}}$. Since $\boldsymbol{\alpha} \neq \boldsymbol{\lambda}$, there exist two consecutive columns c and $c+1$ of C and a color i such that, in columns c and $c+1$ of C, color i has the form

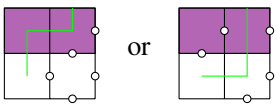

Let c be the rightmost column for which there exists a color of this form in columns c and $c+1$, and let i be the largest color of this form in columns c and $c+1$. We define $\varphi_{\boldsymbol{\alpha}}(C)$ to be the result of flipping color i in columns c and $c+1$

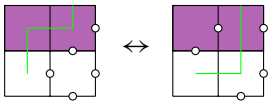

Clearly, $\varphi_{\boldsymbol{\alpha}}$ is an involution. To show

$$\mathrm{weight}(\varphi_{\boldsymbol{\alpha}}(C)) = -\,\mathrm{weight}(C),$$

we need to show

weight (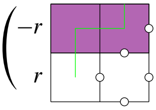) = − weight (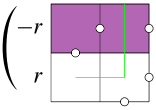)   (4.1)

regardless of the paths taken by the other colors. However, by the maximality of c and i, we know that every color not equal to i must have the form

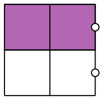

and every color greater than i must not have the form

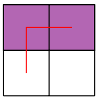

or

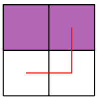

With these constraints, some straightforward computations (which we verified with a computer) show that equation (4.1) holds. ∎

Combining Lemmas 4.4 and 4.5, we can now conclude that the polynomials $\mathcal{L}^S_{\boldsymbol{\lambda}/\boldsymbol{\mu}}(X;Y;t)$ are supersymmetric in the X and Y variables.

Definition 4.6. A family of polynomials $\{p(X_n;Y_m;t) \mid n,m \in \mathbb{Z}_{\geq 0}\}$ is *supersymmetric* if

- $p(\sigma(X_n);Y_m;t) = p(X_n;Y_m;t)$ for any permutation $\sigma \in S_n$ (i.e., $p(X_n;Y_m;t)$ is symmetric in the X variables),
- $p(X_n;\tau(Y_m);t) = p(X_n;Y_m;t)$ for any permutation $\tau \in S_m$ (i.e., $p(X_n;Y_m;t)$ is symmetric in the Y variables),
- $p(X_{n-1},r;Y_{m-1},-r;t) = p(X_{n-1};Y_{m-1};t)$ when $n,m \geq 1$.

Theorem 4.7. *The polynomials $\mathcal{L}^S_{\boldsymbol{\lambda}/\boldsymbol{\mu}}(X_n;Y_m;t)$ are supersymmetric in the X and Y variables.*

Now we proceed by proving a certain restriction property for the polynomials $\mathcal{L}^S_{\boldsymbol{\lambda}/\boldsymbol{\mu}}(X_n;Y_m;t)$.

Lemma 4.8 (Restriction). *We have*

$$\mathcal{L}^S_{\boldsymbol{\lambda}/\boldsymbol{\mu}}(X_{n-1},0;Y_m;t) = \mathcal{L}^S_{\boldsymbol{\lambda}/\boldsymbol{\mu}}(X_{n-1};Y_m;t),$$
$$\mathcal{L}^S_{\boldsymbol{\lambda}/\boldsymbol{\mu}}(X_n;Y_{m-1},0;t) = \mathcal{L}^S_{\boldsymbol{\lambda}/\boldsymbol{\mu}}(X_n;Y_{m-1};t).$$

Proof. Using Lemma 4.4, we can write

$$\mathcal{L}^S_{\boldsymbol{\lambda}/\boldsymbol{\mu}}(X_{n-1},0;Y_m;t) =$$

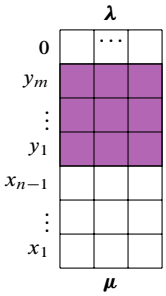

$$= \sum_{\boldsymbol{\alpha}}$$

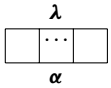

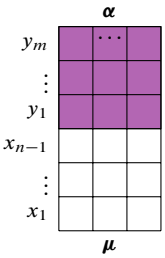

It is easy to see that

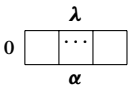

$$= 1_{\boldsymbol{\lambda}=\boldsymbol{\alpha}}.$$

Therefore,

$$\mathcal{L}^S_{\boldsymbol{\lambda}/\boldsymbol{\mu}}(X_{n-1},0;Y_m;t) =$$

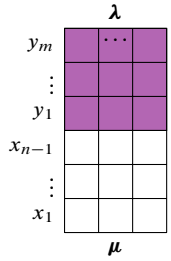

$$= \mathcal{L}^S_{\boldsymbol{\lambda}/\boldsymbol{\mu}}(X_{n-1};Y_m;t). \tag{4.2}$$

A similar argument shows that

$$\mathcal{L}^S_{\boldsymbol{\lambda}/\boldsymbol{\mu}}(X_n;Y_{m-1},0;t) = \mathcal{L}^S_{\boldsymbol{\lambda}/\boldsymbol{\mu}}(X_n;Y_{m-1};t).$$

Alternatively, we can deduce

$$\begin{aligned}
\mathcal{L}^S_{\boldsymbol{\lambda}/\boldsymbol{\mu}}(X_n;Y_{m-1},0;t) &\overset{\text{Theorem 4.3}}{=} t^{g(\boldsymbol{\lambda})-g(\boldsymbol{\mu})}\mathcal{L}^S_{\boldsymbol{\lambda}'/\boldsymbol{\mu}'}(Y_{m-1},0;X_n;t^{-1}) \\
&\overset{(4.2)}{=} t^{g(\boldsymbol{\lambda})-g(\boldsymbol{\mu})}\mathcal{L}^S_{\boldsymbol{\lambda}'/\boldsymbol{\mu}'}(Y_{m-1};X_n;t^{-1}) \\
&\overset{\text{Theorem 4.3}}{=} t^{g(\boldsymbol{\lambda})-g(\boldsymbol{\mu})}(t^{-1})^{g(\boldsymbol{\lambda}')-g(\boldsymbol{\mu}')}\mathcal{L}^S_{\boldsymbol{\lambda}/\boldsymbol{\mu}}(X_n;Y_{m-1};t) \\
&\overset{\text{Corollary 4.2}}{=} \mathcal{L}^S_{\boldsymbol{\lambda}/\boldsymbol{\mu}}(X_n;Y_{m-1};t).
\end{aligned}$$

■

Lemma 4.9. *The polynomial $\mathcal{L}^S_{\boldsymbol{\lambda}/\boldsymbol{\mu}}(X_n;Y_m;t)$ is homogeneous in the X and Y variables of degree*

$$|\boldsymbol{\lambda}/\boldsymbol{\mu}| = |\boldsymbol{\lambda}| - |\boldsymbol{\mu}|,$$

that is,

$$\mathcal{L}^S_{\boldsymbol{\lambda}/\boldsymbol{\mu}}(rX_n;rY_m;t) = r^{|\boldsymbol{\lambda}/\boldsymbol{\mu}|}\mathcal{L}^S_{\boldsymbol{\lambda}/\boldsymbol{\mu}}(X_n;Y_m;t).$$

Proof. This follows from the fact that in any configuration of the lattice

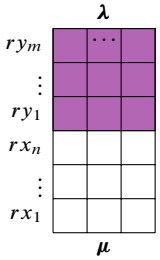

the total number of right steps taken by the paths is $|\boldsymbol{\lambda}/\boldsymbol{\mu}|$. ∎

4.1. The factorization property

The goal of this subsection is to prove the following lemma.

Lemma 4.10 (Factorization). *Fix $\boldsymbol{\lambda} \in P_p^{(k)}$. Suppose there exist $\boldsymbol{\tau}$ and $\boldsymbol{\eta}$ such that for all i,*

$$\lambda^{(i)} = (m + \tau_1^{(i)}, \ldots, m + \tau_n^{(i)}, \eta_1^{(i)}, \ldots, \eta_s^{(i)}),$$

where $s = p - n$. Then

$$\mathcal{L}_{\boldsymbol{\lambda}}^S(X_n; Y_m; t) = \mathcal{L}_{\boldsymbol{\tau}}(X_n; t) \cdot t^{g(\boldsymbol{\eta})} \mathcal{L}_{\boldsymbol{\eta}'}(Y_m; t^{-1}) \cdot \prod_{l=0}^{k-1} \prod_{i=1}^{n} \prod_{j=1}^{m} (t^l x_i + y_j).$$

Throughout this subsection, let $\boldsymbol{\lambda}$, $\boldsymbol{\tau}$, and $\boldsymbol{\eta}$ be as in the above lemma. Moreover, it is easy to see that the above lemma holds if $n = 0$ or $m = 0$, so we will assume $n, m \geq 1$ throughout the rest of this subsection. To prove the above lemma, we need two smaller lemmas.

Lemma 4.11. *Let $\boldsymbol{\lambda}$, $\boldsymbol{\tau}$, and $\boldsymbol{\eta}$ be as in Lemma 4.10. The polynomial*

$$t^{g(\boldsymbol{\eta})} \mathcal{L}_{\boldsymbol{\eta}'}(Y_m; t^{-1}) = \mathcal{L}_{\boldsymbol{\eta}}^P(Y_m; t)$$

is a factor of the polynomial $\mathcal{L}_{\boldsymbol{\lambda}}^S(X_n; Y_m; t)$. In fact,

$$\mathcal{L}_{\boldsymbol{\lambda}}^S(X_n; Y_m; t) = \mathcal{L}_{\boldsymbol{\eta}}^P(Y_m; t) \cdot \mathcal{L}_{m+\boldsymbol{\tau}}^S(X_n; Y_m; t),$$

where $(m + \boldsymbol{\tau})_j^{(i)} = m + \boldsymbol{\tau}_j^{(i)}$ for all i and j.

Lemma 4.12. *Let $\boldsymbol{\lambda}$, $\boldsymbol{\tau}$, and $\boldsymbol{\eta}$ be as in Lemma 4.10. Then*

$$\mathcal{L}_{\boldsymbol{\lambda}}^S(X_{n-1}, r; Y_{m-1}, -t^l r; t) = 0$$

for all $l \in \{0, \ldots, k-1\}$.

Given these two lemmas, let us prove Lemma 4.10.

Proof of Lemma 4.10. Fix $l \in \{0, \dots, k-1\}$. Since

$$\mathcal{L}^S_{\boldsymbol{\lambda}}(X_{n-1}, r; Y_{m-1}, -t^l r; t) = 0,$$

by Lemma 4.12, we know that $t^l x_n + y_m$ is a factor of $\mathcal{L}^S_{\boldsymbol{\lambda}}(X_n; Y_m; t)$. Thus, since $\mathcal{L}^S_{\boldsymbol{\lambda}}(X_n; Y_m; t)$ is symmetric in the X and Y variables separately by Lemma 4.4, we know that

$$\prod_{i=1}^{n}\prod_{j=1}^{m}(t^l x_i + y_j)$$

is a factor of $\mathcal{L}^S_{\boldsymbol{\lambda}}(X_n; Y_m; t)$. Since this holds for all $l \in \{0, \dots, k-1\}$, we know that

$$\prod_{l=0}^{k-1}\prod_{i=1}^{n}\prod_{j=1}^{m}(t^l x_i + y_j)$$

is a factor of $\mathcal{L}^S_{\boldsymbol{\lambda}}(X_n; Y_m; t)$. Moreover, since the polynomial $t^{g(\boldsymbol{\eta})}\mathcal{L}_{\boldsymbol{\eta}'}(Y_m; t^{-1})$ is a factor of $\mathcal{L}^S_{\boldsymbol{\lambda}}(X_n; Y_m; t)$ by Lemma 4.11, we know that

$$t^{g(\boldsymbol{\eta})}\mathcal{L}_{\boldsymbol{\eta}'}(Y_m; t^{-1}) \cdot \prod_{l=0}^{k-1}\prod_{i=1}^{n}\prod_{j=1}^{m}(t^l x_i + y_j)$$

is a factor of $\mathcal{L}^S_{\boldsymbol{\lambda}}(X_n; Y_m; t)$. Thus there is a polynomial $f(X_n; Y_m; t)$ such that

$$\mathcal{L}^S_{\boldsymbol{\lambda}}(X_n; Y_m; t) = f(X_n; Y_m; t) \cdot t^{g(\boldsymbol{\eta})}\mathcal{L}_{\boldsymbol{\eta}'}(Y_m; t^{-1}) \cdot \prod_{l=0}^{k-1}\prod_{i=1}^{n}\prod_{j=1}^{m}(t^l x_i + y_j). \quad (4.3)$$

It remains to show $f(X_n; Y_m; t) = \mathcal{L}_{\boldsymbol{\tau}}(X_n; t)$.

Combining equation (4.3) with Lemma 4.11, we get

$$\mathcal{L}^S_{m+\boldsymbol{\tau}}(X_n; Y_m; t) = f(X_n; Y_m; t) \cdot \prod_{l=0}^{k-1}\prod_{i=1}^{n}\prod_{j=1}^{m}(t^l x_i + y_j). \quad (4.4)$$

Given a polynomial $p(X_n; Y_m; t)$, let $\deg_Y(p(X_n; Y_m; t))$ be the total degree of $p(X_n; Y_m; t)$ in the Y variables. Recall $\mathcal{L}^S_{m+\boldsymbol{\tau}}(X_n; Y_m; t)$ is the partition function associated to the lattice $S_{n,m}(m + \boldsymbol{\tau})$ from Definition 3.8.

In any configuration of this lattice, a given path can take at most one step to the right in a purple row. Thus, since there are m purple rows and since there are n paths of each of the k colors, we have

$$\deg_Y(\mathcal{L}^S_{m+\boldsymbol{\tau}}(X_n; Y_m; t)) \leq mnk = \deg_Y\left(\prod_{l=0}^{k-1}\prod_{i=1}^{n}\prod_{j=1}^{m}(t^l x_i + y_j)\right).$$

This inequality along with equation (4.4) implies $f(X_n; Y_m; t) = h(X_n; t)$ for some polynomial $h(X_n; t)$. It remains to show $h(X_n; t) = \mathcal{L}_{\boldsymbol{\tau}}(X_n; t)$.

We can rewrite equation (4.4) as

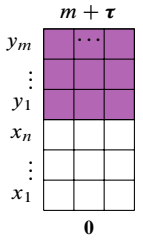

$$= h(X_n;t)\cdot\prod_{l=0}^{k-1}\prod_{i=1}^{n}\prod_{j=1}^{m}(t^l x_i + y_j).$$

We interpret both sides of this equation as polynomials in the Y variables. On the right-hand side, the coefficient of $y_1^{nk}\cdots y_m^{nk}$ is $h(X_n;t)$. For the lattice on the left-hand side, a configuration has a weight of the form $p(X_n;t)\cdot y_1^{nk}\cdots y_m^{nk}$ for some polynomial $p(X_n;t)$ if and only if each path of each color takes one step to the right in each purple row. Thus the $y_1^{nk}\cdots y_m^{nk}$ term on the left-hand side is exactly

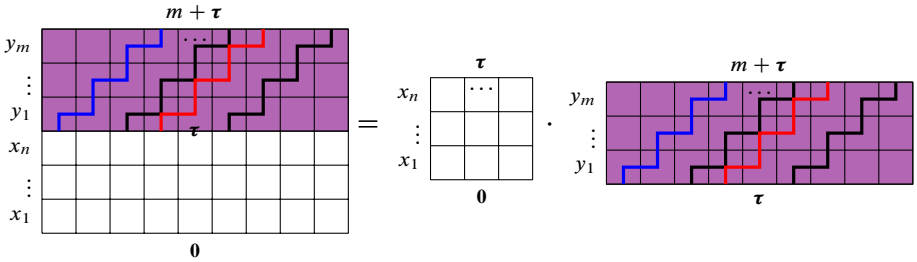

$$= \mathcal{L}_{\tau}(X_n;t)\cdot y_1^{nk}\cdots y_m^{nk}.$$

(Here, each path takes one step to the right in each purple row.) Thus

$$h(X_n;t) = \mathcal{L}_{\tau}(X_n;t).$$ ∎

We are left to prove Lemmas 4.11 and 4.12.

Proof of Lemma 4.11. Using Theorem 4.3 and the fact that $g(\mathbf{0}) = 0$, we have

$$\mathcal{L}^P_{\eta}(Y_m;t) = \mathcal{L}^S_{\eta}(\cdot;Y_m;t) = t^{g(\eta)}\mathcal{L}^S_{\eta'}(Y_m;\cdot;t^{-1}) = t^{g(\eta)}\mathcal{L}_{\eta'}(Y_m;t^{-1}).$$

Recall $\mathcal{L}^S_{\lambda}(X_n;Y_m;t)$ is the partition function associated to the lattice

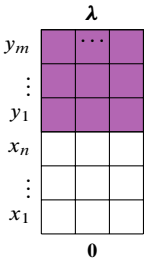

Any configuration of this lattice must have the form

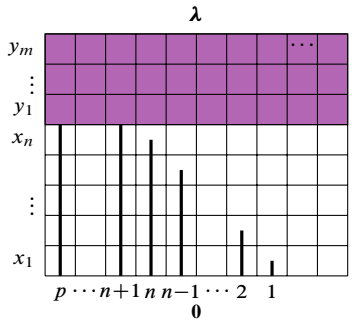

where we have labeled the columns for convenience. Fix $j \in \{1, \ldots, m\}$. Note that a path can take at most one step to the right in a given purple row. Since

$$\lambda_n^{(i)} = m + \tau_n^{(i)} \geq m$$

for all i, the paths starting in column n must exit the m-th purple row weakly right of column $n - m$, so the paths starting in column n must exit the j-th purple row weakly right of column $n - j$. Since the paths starting in column $n + 1$ enter the first purple row in column $n + 1$, they must exit the j-th purple row weakly to the left of column $n + 1 - j$. This argument shows that the remainder of the paths starting in columns $n + 1, \ldots, p$ and the remainder of the paths starting in columns $1, \ldots, n$ can be chosen independently of each other, and that the weight of the overall configuration is the weight of the configuration consisting of the paths starting in columns $n + 1, \ldots, p$ times the weight of the configuration consisting of the paths starting in columns $1, \ldots, n$.

It follows that

$$\mathcal{L}_{\boldsymbol{\lambda}}^{S}(X_n; Y_m; t) =$$

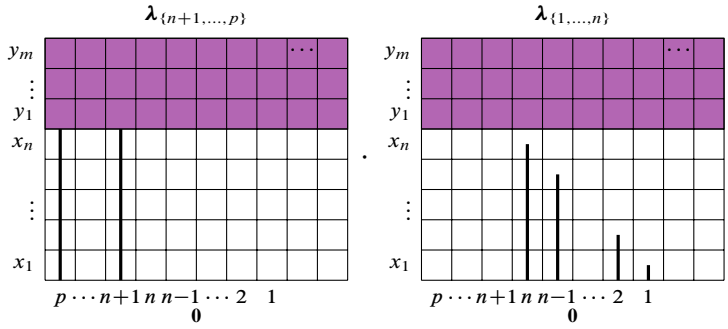

where for a set $S = \{s_1 < \cdots < s_j\} \subseteq \{1, \ldots, p\}$, we define

$$\boldsymbol{\lambda}_S = (\lambda_S^{(1)}, \ldots, \lambda_S^{(k)}) \quad \text{with } \lambda_S^{(i)} = (\lambda_{s_1}^{(k)}, \ldots, \lambda_{s_j}^{(k)}).$$

Since $\boldsymbol{\lambda}_{\{n+1,\ldots,p\}} = \boldsymbol{\eta}$, the first factor is exactly

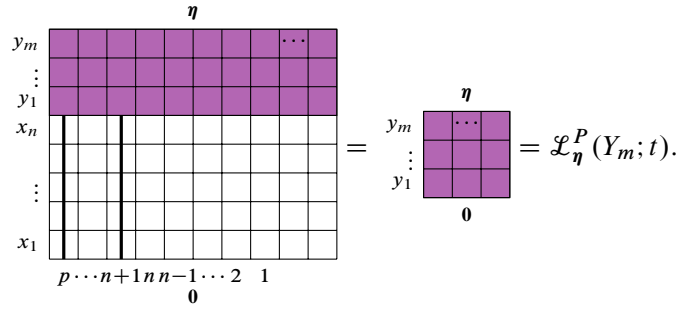

$$= \mathcal{L}^P_{\boldsymbol{\eta}}(Y_m; t).$$

Since $\boldsymbol{\lambda}_{\{1,\ldots,n\}} = m + \boldsymbol{\tau}$, the second factor is exactly

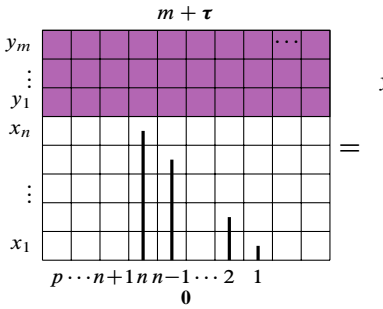

$$= \mathcal{L}^S_{m+\boldsymbol{\tau}}(X_n; Y_m; t).$$ ∎

Proof of Lemma 4.12. By Lemma 4.4, $\mathcal{L}^S_{\boldsymbol{\lambda}}(X_{n-1}, r; Y_{m-1}, -t^l r; t)$ is the partition function associated to the lattice

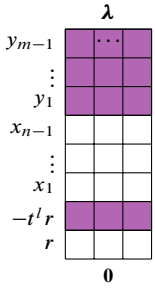

Any configuration of this lattice must have the form

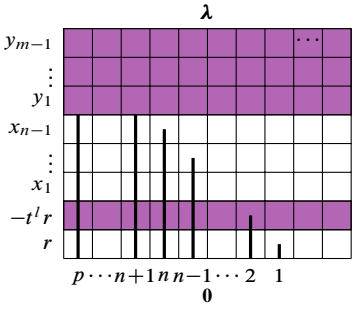

where we have labeled the columns for convenience. In a configuration, if there exists a color i such that the path of color i starting in column 1 goes vertically in the bottom two rows, then color i must have the form

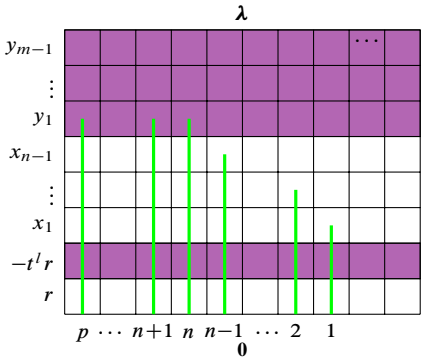

A path can take at most one step to the right in a given purple row, so the path of color i starting in column n can make at most $m-1$ total steps to the right in the lattice. However, since

$$\lambda_n^{(i)} = m + \tau_n^{(i)} \geq m,$$

the path of color i starting in column n must make at least m total steps to the right in the lattice. This is a contradiction, which means that in any configuration, every path starting in column 1 must make at least one step to the right somewhere in the bottom two rows. Therefore,

$$\mathcal{L}^S_{\boldsymbol{\lambda}/\boldsymbol{\mu}}(X_{n-1}, r; Y_{m-1}, -t^l r; t)$$

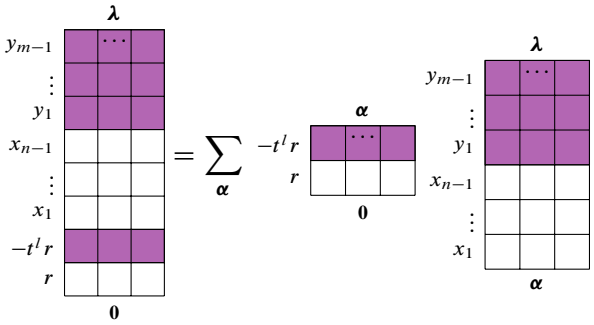

where the sum is over all $\boldsymbol{\alpha}$ such that $\alpha_1^{(i)} > 0$ for all i. We will show that for all such $\boldsymbol{\alpha}$, there is an involution $\varphi_{\boldsymbol{\alpha}}$ on the set of configurations of the lattice

$L_{\boldsymbol{\alpha}} =$

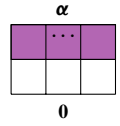

such that $\text{weight}(\varphi_{\boldsymbol{\alpha}}(C)) = -\text{weight}(C)$ for all C. Therefore,

$$\mathcal{L}^S_{\boldsymbol{\lambda}/\boldsymbol{\mu}}(X_{n-1}, r; Y_{m-1}, -r; t) = 0.$$

Fix $\boldsymbol{\alpha}$ with $\alpha_1^{(i)} > 0$ for all i and fix a configuration C on the lattice $L_{\boldsymbol{\alpha}}$. We label the columns for convenience as follows:

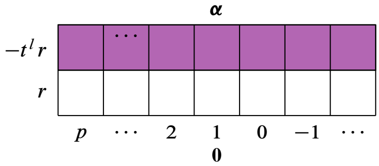

Given a color i, let c_i be the column in which the path of color i starting in column 1 exits the lattice through the top. Since every path starting in column 1 must make at least one step to the right, we have $c_i \le 0$ for all i. We define an ordering $\prec$ on the colors by

$$i \prec j \Leftrightarrow c_i > c_j \quad \text{or} \quad c_i = c_j \quad \text{and} \quad i < j.$$

Let i be the $(l+1)$-th largest color in this ordering (so that $l = \#\{j \mid i \prec j\}$). In columns $c_i + 1$ and c_i of C, color i has the form

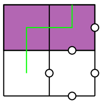 or 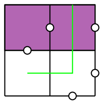

We define $\varphi_{\boldsymbol{\alpha}}(C)$ to be the result of flipping color i in columns $c_i + 1$ and c_i

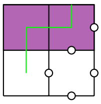 $\leftrightarrow$ 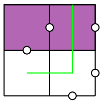

Clearly, $\varphi_{\boldsymbol{\alpha}}$ is an involution. To show $\text{weight}(\varphi_{\boldsymbol{\alpha}}(C)) = -\,\text{weight}(C)$, we need to show

weight $\Bigg($ $-t^l r$, r 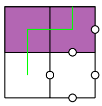 $\Bigg)$ $= -\,$weight $\Bigg($ $-t^l r$, r 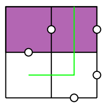 $\Bigg)$ (4.5)

regardless of the paths taken by the other colors. We label the boxes for convenience as follows:

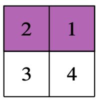

Compared to the configuration with color i absent, the presence of color i in the form

$-t^l r$, r 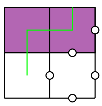

contributes $-t^l r \cdot t^a$ to the overall weight, where

$$a = \#\{j > i \mid j \text{ is vertical in box } 2\} + \#\{j < i \mid j \text{ exits right in box } 3\}.$$

Compared to the configuration with color i absent, the presence of color i in the form

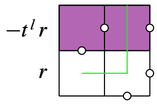

contributes $r \cdot t^b$ to the overall weight, where

$$\begin{aligned} b = {} & \#\{j > i \mid j \text{ appears in box 3}\} + \#\{j < i \mid j \text{ exits right in box 1}\} \\ & + \#\{j < i \mid j \text{ exits right in box 3}\} \\ & + \#\{j < i \mid j \text{ exits right in box 4}\}. \end{aligned}$$

It is easy to see that

$$\begin{aligned} b - a = {} & \#\{j > i \mid j \text{ appears in box 3}\} - \#\{j > i \mid j \text{ is vertical in box 2}\} \\ & + \#\{j < i \mid j \text{ exits right in box 1}\} \\ & + \#\{j < i \mid j \text{ exits right in box 4}\} \\ = {} & \#\{j > i \mid c_i \geq c_j\} + \#\{j < i \mid c_i > c_j\} = \#\{j \mid j \succ i\} = l. \end{aligned}$$

Therefore,

weight (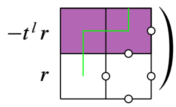

)

divided by

weight (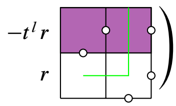

)

$$= \frac{-t^l r \cdot t^a}{r \cdot t^b} = -t^{l+a-b} = -1.$$

Thus equation (4.5) holds. ■

4.2. Swapping single rows

In this subsection, we prove an identity of the supersymmetric LLT polynomials in the case $p = 1$ and $\boldsymbol{\mu} = \mathbf{0}$. Since $p = 1$, $\boldsymbol{\lambda}$ can be written as $((\lambda_1), \ldots, (\lambda_k))$. Moreover, in any configuration of the lattice $S_{n,m}(\boldsymbol{\lambda})$, there is exactly one path of each of the k colors, and these paths enter the lattice through the bottom in the same column. Given non-negative integers $\nu_1, \ldots, \nu_k$, we define

$$\mathrm{Inv}((\nu_1), \ldots, (\nu_k)) = \#\{a < b \mid \nu_a > \nu_b\}.$$

Given $\boldsymbol{\lambda} \in P_1^{(k)}$, we say that $\boldsymbol{\nu} \in P_1^{(k)}$ is a rearrangement of $\boldsymbol{\lambda}$ if there exists a permutation $\sigma \in S_k$ such that $\nu_i = \lambda_{\sigma(i)}$ for all $i \in \{1, \ldots, k\}$.

Proposition 4.13. *Let $\boldsymbol{\lambda} \in P_1^{(k)}$. If $\boldsymbol{\nu} \in P_1^{(k)}$ is a rearrangement of $\boldsymbol{\lambda}$, then*

$$\mathcal{L}^S_{\boldsymbol{\lambda}}(X_n; Y_m; t) = t^{\mathrm{Inv}(\boldsymbol{\lambda}) - \mathrm{Inv}(\boldsymbol{\nu})} \mathcal{L}^S_{\boldsymbol{\nu}}(X_n; Y_m; t).$$

Proof. We start with some simple reductions. It is enough to consider the case where $\lambda_1 \geq \cdots \geq \lambda_k$. Thus it is enough to show that, given $i \in \{1, \ldots, k-1\}$,

$$\mathcal{L}^S_{\boldsymbol{\lambda}}(X_n; Y_m; t) = t \cdot \mathcal{L}^S_{\boldsymbol{\nu}}(X_n; Y_m; t),$$

where $\lambda_1 \geq \cdots \geq \lambda_i > \lambda_{i+1} \geq \cdots \geq \lambda_k$ and

$$\nu_j = \begin{cases} \lambda_j, & j \neq i, i+1, \\ \lambda_{i+1}, & j = i, \\ \lambda_i, & j = i+1. \end{cases}$$

We will let blue be color i and red be color $i+1$.

We will now define a bijection

$$\rho\colon LC(S_{n,m}(\boldsymbol{\lambda})) \to LC(S_{n,m}(\boldsymbol{\nu})).$$

Fix a configuration $C \in S_{n,m}(\boldsymbol{\lambda})$. Since $\lambda_i \geq \lambda_{i+1}$, the column in which color i exits the lattice is strictly to the right of the column in which color $i+1$ exits the lattice. Therefore, since color i and color $i+1$ enter the lattice in the same column, C must have a row in which color i enters weakly from the left and exits strictly to the right of color $i+1$. Thus C must have a vertex of the form

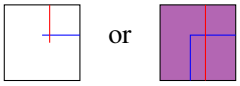

Consider the north-eastern-most vertex V of this form. Swap color i and color $i+1$ in every vertex north-east of V. For example,

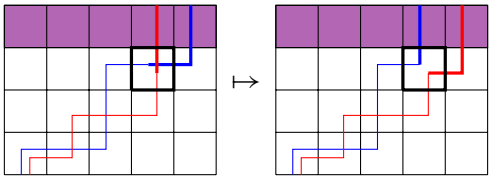

and

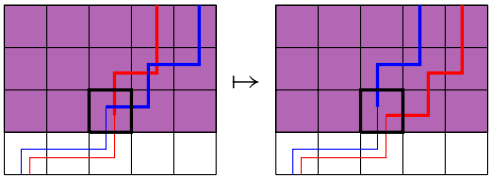

The result is a configuration $\rho(C) \in LC(S_{n,m}(\boldsymbol{\nu}))$. It is clear that ρ is a bijection. We will now compare weight(C) with weight$(\rho(C))$. There are four types of vertices to consider.

(1) For the vertex V itself, the effect of applying ρ is

In either case, it is easy to see that the weight before applying ρ is t times the weight after applying ρ.

(2) For any vertex that is not north-east of V, ρ does not change the configuration, so the weight is not changed.

(3) For any vertex that is north-east of V such that either color i or color $i+1$ is absent in this vertex, ρ swaps color i or color $i+1$, but the weight is not changed.

(4) For any vertex that is north-east of V such that both color i and color $i+1$ are present in this vertex, this vertex must have the form

Applying ρ swaps color i and color $i+1$, resulting in

It is easy to see that the weight is not changed.

Therefore,

$$\text{weight}(C) = t \cdot \text{weight}(\rho(C))$$

and the proposition follows. ∎

Remark 4.14. The above proposition extends [13, Proposition 5.5], and in fact these two propositions are proven in nearly identical ways.

5. Relating $\mathscr{L}^S$ to $\mathscr{G}$

The goal of this section is to relate the partition function $\mathscr{L}^S_{\boldsymbol{\lambda}/\boldsymbol{\mu}}$ from Definition 3.8 to the super ribbon function $\mathscr{G}^{(k)}_{\lambda/\mu}$ from Definition 2.11. In [15], the authors construct a lattice model whose partition function is equal to the spin LLT polynomials. Lemma 5.6 below, which relates our vertex model to the spin LLT polynomials, can

also be interpreted as a mapping between our vertex model and the one in [15] (see Remark 5.7). We will adopt the following conventions. Fix a positive integer k. Let $\boldsymbol{\lambda}/\boldsymbol{\mu}$ be the k-quotient of λ/μ. Let $\mathcal{A} = \{1 < 2 < \cdots < n\}$ and $\mathcal{A}' = \{1' < 2' < \cdots < m'\}$. We use the ordering $1 < 2 < \cdots < n < 1' < 2' < \cdots < m'$ on $\mathcal{A} \cup \mathcal{A}'$.

We begin by constructing a bijection

$$\mathrm{SSSYT}(\boldsymbol{\lambda}/\boldsymbol{\mu}) \to LC(S_{n,m}(\boldsymbol{\lambda}/\boldsymbol{\mu})),$$

where $LC(S_{n,m}(\boldsymbol{\lambda}/\boldsymbol{\mu}))$ is the set of configurations on the lattice $S_{n,m}(\boldsymbol{\lambda}/\boldsymbol{\mu})$ from Definition 3.8. We do this in the usual way in which each row of i-th tableaux maps to a path of color i. Precisely, given $\boldsymbol{T} = (T^{(1)}, \ldots, T^{(k)}) \in \mathrm{SSSYT}(\boldsymbol{\lambda}/\boldsymbol{\mu})$, the corresponding $C \in LC(S_{n,m}(\boldsymbol{\lambda}/\boldsymbol{\mu}))$ is constructed as follows. Fix $i \in [k]$ and fix a row

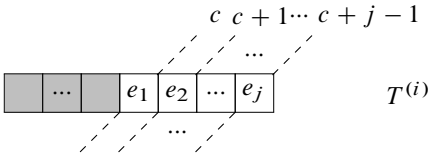

in $T^{(i)}$. (Here we have labeled the diagonal content lines going through the row.) The corresponding path in C has color i, enters the lattice via the bottom of column c, exits the lattice via the top of column $c + j$, and crosses from column $c + l - 1$ to column $c + l$ at

$$\begin{cases} \text{the } a\text{-th white row} & \text{if } e_l = a \in \mathcal{A}, \\ \text{the } a\text{-th purple row} & \text{if } e_l = a' \in \mathcal{A}' \end{cases}$$

for each index $l \in [j]$. Recall that the Littlewood k-quotient map is a bijection

$$\mathrm{SRT}_k(\lambda/\mu) \to \mathrm{SSSYT}(\boldsymbol{\lambda}/\boldsymbol{\mu}).$$

The composition of these two bijections gives a bijection

$$\theta\colon \mathrm{SRT}_k(\lambda/\mu) \to LC(S_{n,m}(\boldsymbol{\lambda}/\boldsymbol{\mu})).$$

Example 5.1. Let $n = 3$, $m = 4$, and $k = 3$. Recall Example 2.15.

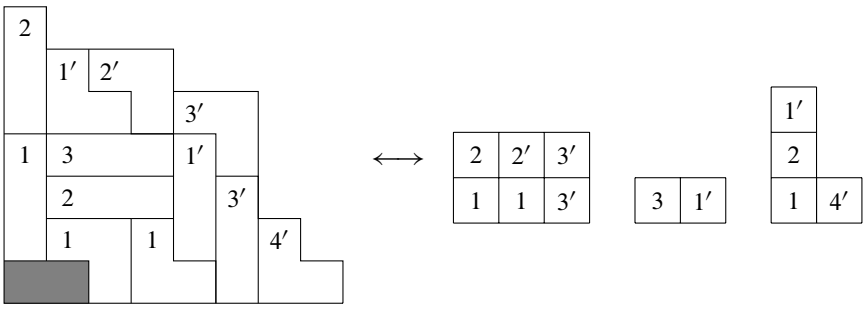

The corresponding configuration is

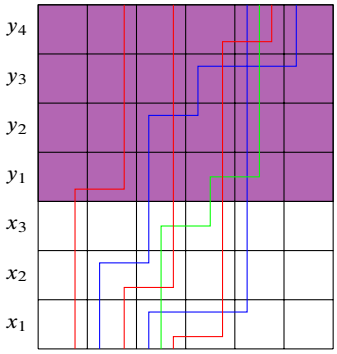

where blue is color 1, green is color 2, and red is color 3.

Remark 5.2. When $m = 0$, the bijection $\mathrm{SSSYT}(\boldsymbol{\lambda}/\boldsymbol{\mu}) \to LC(S_{n,m}(\boldsymbol{\lambda}/\boldsymbol{\mu}))$ becomes a bijection

$$\mathrm{SSYT}(\boldsymbol{\lambda}/\boldsymbol{\mu}) \to LC(W_n(\boldsymbol{\lambda}/\boldsymbol{\mu})).$$

This bijection was used in [13] to prove Theorem 3.6.

Remark 5.3. The bijection θ restricts to bijections

$$\mathrm{HRS}_k(\lambda/\mu) \to LC(W_1(\boldsymbol{\lambda}/\boldsymbol{\mu})), \quad \mathrm{VRS}_k(\lambda/\mu) \to LC(P_1(\boldsymbol{\lambda}/\boldsymbol{\mu}))$$

by artificially labeling each ribbon in a horizontal (vertical) k-ribbon strip with a 1 ($1'$).

For the rest of this section, we will switch to drawing our Young diagrams in Russian convention, so that rows are oriented south-west-to-north-east and columns are oriented south-east-to-north-west. The reason for this switch is to allow for an elegant graphical interpretation of θ. Let $T \in \mathrm{SRT}_k(\lambda/\mu)$ and $C = \theta(T) \in LC(S_{n,m}(\boldsymbol{\lambda}/\boldsymbol{\mu}))$. By the construction of θ, we note that

(1) for each $i \in \mathcal{A}$, the horizontal ribbon strip $\lambda_{\leq i}/\lambda_{\leq i-1}$ of ribbons labeled i in T corresponds to the i-th white row in C;

(2) for each $i' \in \mathcal{A}'$, the vertical ribbon strip $\lambda_{\leq i}/\lambda_{\leq i-1}$ of ribbons labeled i' in T corresponds to the i-th purple row in C.

Given a horizontal (vertical) ribbon strip inside T, we "drop down" the Maya diagrams of the top and bottom boundaries to obtain the top and bottom boundaries of the corresponding white (purple) row in C. Moreover, the top and bottom boundaries of the row uniquely determine the path configuration of the row.

Example 5.4. Take $k = 3$. Let blue be color 1, green color 2, and red color 3. Consider the following horizontal 3-ribbon strip of shape $(6, 6, 3, 0, 0, 0)/(0, 0, 0, 0, 0, 0)$:

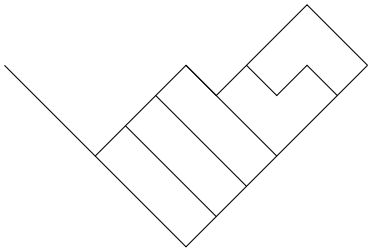

We now color the steps on the top and bottom boundaries from left to right. A south-east step in position $i \mod k$ gets color i. North-east steps are not colored,

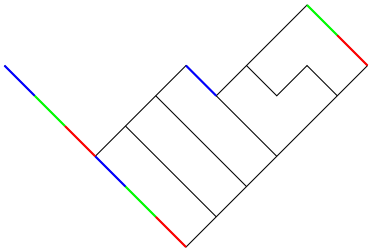

We now "drop down" the steps on the top and bottom boundaries of the horizontal 3-ribbon strip to obtain the top and bottom boundaries of the corresponding white row. The steps in positions $(j-1)k+1,\ldots,(j-1)k+k$ correspond to the j-th leftmost vertex. A step of color i corresponds to a particle of color i, indicating that a path of color i is incident at the edge,

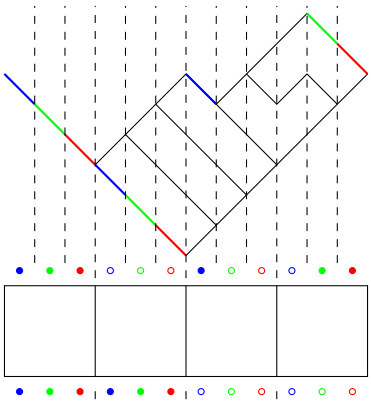

With these top and bottom boundary conditions (and requiring that no paths be incident at the left and right edges of the row), there is a unique path configuration,

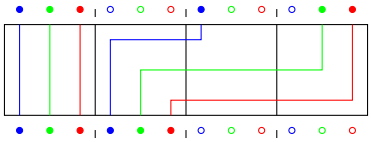

Remark 5.5. We leave it as an exercise for the reader to verify that our graphical interpretation of θ is correct (see Lemma 2.16). We also leave it as an exercise for the reader to check that the diagram

$$\begin{array}{ccc} \mathrm{HRS}_k(\lambda/\mu) & \xrightarrow{\text{conjugate}} & \mathrm{VRS}_k(\lambda'/\mu') \\ \downarrow\theta & & \downarrow\theta \\ LC(W_1(\boldsymbol{\lambda}/\boldsymbol{\mu})) & \xrightarrow{\psi} & LC(P_1(\boldsymbol{\lambda}'/\boldsymbol{\mu}')) \end{array}$$

commutes. Here ψ is the bijection defined at the beginning of Section 4. (This result is not needed in the rest of this paper.)

In order to relate $\mathcal{L}^S_{\boldsymbol{\lambda}/\boldsymbol{\mu}}$ to $\mathcal{G}^{(k)}_{\lambda/\mu}$, we must consider how the spin

$$\mathrm{spin}(T) = \sum_{\text{ribbons } \boldsymbol{R} \text{ in } \boldsymbol{T}} (h(R) - 1)$$

of a horizontal (vertical) ribbon strip T appears in the corresponding path configuration $\theta(T)$ of a single white (purple) row. Clearly, $\mathrm{spin}(T)$ equals the number of positions that the tile

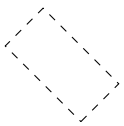

(two cells in the same column and ribbon) can be placed in T. For example, if T is

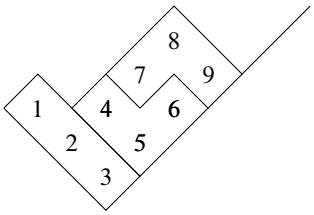

there are 4 such positions—cells 1 and 2, cells 2 and 3, cells 4 and 5, and cells 8 and 9—and indeed the spin is 4. We can count these positions according to the "slice" containing the middle of each tile. In our example, the slices are given by

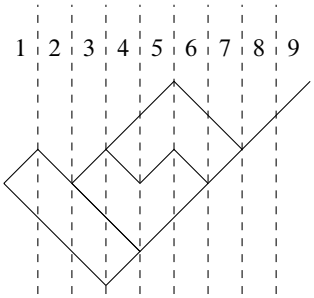

so slices 2, 3, 4, and 6 each contribute 1 to the spin, and the other slices do not contribute to the spin. In each slice, there are only four shapes that can appear:

(1) a column parallelogram (two adjacent halves of cells in the same column and ribbon),

(2) a row parallelogram (two adjacent halves of cells in the same row and ribbon),

(3) a head triangle (half of the head of a ribbon),

(4) a tail triangle (half of the tail of a ribbon),

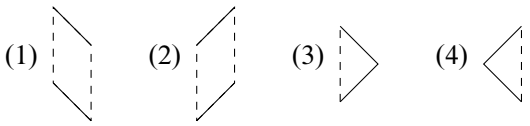

(Of course, a slice could also consist of a single south-east step or a single north-east step.) Any other shapes cannot appear in a slice because otherwise the ribbon containing the shape would either contain a 2×2 square or not be a valid skew shape. It is clear that the contribution of a slice to the spin equals the number of column parallelograms in the slice.

In the following two lemmas, we use the above discussion to characterize the spin in terms of $\theta(T)$, when T is a horizontal/vertical ribbon strip.

Lemma 5.6. *Let T be a horizontal k-ribbon strip. In the corresponding white row $\theta(T)$,*

$$\mathrm{spin}(T) = \sum_{a<b} \Big(\#\,\square_{a,b} + \#\,\square_{a,b} + \#\,\square_{a,b} + \#\,\square_{a,b} \Big),$$

where blue is color a and red is color b.

Proof. The fact that T is a horizontal ribbon strip restricts the possible forms of the slices:

(1) If a head triangle appears, it must be at the bottom of the slice. This is because the head of a ribbon must touch the south-east boundary.

(2) If a tail triangle appears, it must be at the top of the slice. Suppose the tail triangle of ribbon R appears below a shape in ribbon S in slice i. Then, in all slices in which both R and S appear, S is above R. Note that R appears in slices $i, \ldots, i+k$ as every ribbon has length k. Similarly, S appears in slices $i-j, \ldots, i-j+k$ for some $j \in \{0, \ldots, k\}$. In particular, in slice $i-j+k$, the head triangle of S appears above R, which contradicts the first restriction.

With these restrictions in mind, one can show that each slice must have one of the following five forms:

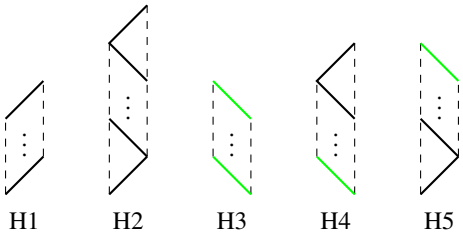

Here $\vdots$ indicates arbitrarily many (possibly 0) copies of the shape, and south-east steps on the top/bottom boundaries are colored as in our graphical interpretation of θ (see Example 5.4).

Remark 5.7. The five types of slices we draw here are in bijection with the five types of allowed vertices given in [15, Figure 14]. To see this, suppose we are looking at a slice whose top and bottom boundaries correspond to color a. Then we can map it to a vertex of the form given in [15] by assigning arrows to the edges of the vertex according to the rules:

(1) If the top boundary of the slice is a north-east (south-east) step, then the top edge of the vertex gets a down (up) arrow. Similarly for the bottom boundary of the slice.

(2) If the slice contains a head triangle, assign a left arrow to the k-th eastern horizontal edge. If the slice contains a tail triangle, assign a left arrow to the 1-st western horizontal edge.

(3) If a ribbon whose head is in a slice of color b passes through the slice, then assign left arrows to the $(b + k - a \bmod k)$-th eastern horizontal edge and the $((b + k - a \bmod k) + 1)$-st western horizontal edge.

(4) Otherwise, assign right arrows to the horizontal edges.

Assigning each slice a weight of x if there is a head triangle, and $t^{\#\text{column parallelogram}}$, makes this a weight-preserving bijection. Through the bijection θ defined above, the rest of this lemma can be seen as giving a weight-preserving bijection between our vertex model and that of [15].

We claim that there is a one-to-one correspondence between the five possible forms of a slice in T and the five possible path configurations of the corresponding color in the corresponding white vertex in $\theta(T)$,

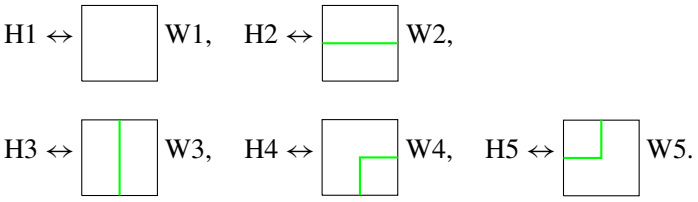

The correspondence is obvious for H3, H4, and H5 from the top/bottom boundary conditions. Moreover, from the top/bottom boundary conditions, slices of the form H1 or H2 correspond to path configurations of the form W1 or W2. To show the correspondence for H1 and H2, we will show that a slice of the form H2 always gives a configuration of the form W2 and vice versa.

- Suppose slice i has the form H2. It contains the head triangle of a ribbon, so slice $i-k$ will contain the tail triangle of this ribbon. This slice then must have the form H2 or H4. If slice $i-k$ has the form H2, then we can repeat this argument to show that slice $i-2k$ has the form H2 or H4. Since there are finitely many ribbons, eventually we find that slice $i-jk$ has the form H4, for some positive integer j, and slices $i-(j-1)k,\ldots,i-k,i$ have the form H2. Since slice $i-jk$ has the form H4, the corresponding path configuration has the form W4, in which the path exits right. Thus the path configuration corresponding to slice $i-(j-1)k$ must have the path entering from the left, so it must have the form W2, in which the path exits right. Repeating, we conclude that the path configuration corresponding to slice i has the form W2.
- Suppose slice i corresponds to a path configuration of the form W2. We know a path enters the slice from the left, so slice $i-k$ must correspond to a path configuration in which the path exits right. This path configuration must have the form W2 or W4. If slice $i-k$ corresponds to a path configuration of the form W2, then we can repeat this argument to show that slice $i-2k$ corresponds to a path configuration of the form W2 or W4. Since there are finitely many vertices, eventually we find that slice $i-jk$ corresponds to a path configuration of the form W4 and slices $i-(j-1)k,\ldots,i-k,i$ correspond to path configurations of the form W2, for some positive integer j. Since slice $i-jk$ corresponds to a path configuration of the form W4, it must have the form H4, so it contains the tail triangle of a ribbon. We see that slice $i-(j-1)k$ contains the head triangle of this ribbon, so this slice has the form H2. It follows that slice $i-(j-1)k$ also contains the tail triangle of a ribbon. Repeating, we conclude that slice i has the form H2.

Recall that slice $i=(j-1)k+a$ in T corresponds to color a in the j-th leftmost vertex V in $\theta(T)$. The contribution of this slice to $\mathrm{spin}(T)$ equals the number of column parallelograms in the slice. Looking at the five possible forms of a slice, we see that this equals zero if slice i has the form H1, which is equivalent to color a being absent in V. Otherwise, it equals the number of ribbons R that appear in slice i but whose head/tail triangles do not.

Let R be such a ribbon, and let slice s be the slice that contains the tail triangle of R. Since slice a contains a column parallelogram of R but not the head/tail triangle of R, we have $s<i<s+k$. Let $b\in\{1,\ldots,k\}$ be such that $b\equiv s \bmod k$, and note

that $b \neq a$. If $b < a$, then the tail triangle of R appears in slice $(j-1)k+b$, so slice $(j-1)\times k+b$ has the form H2 or H4, so the path configuration of color b in V has the form W2 or W4, so color b exits V to the right. If $b > a$, then the head triangle of R appears in slice $(j-1)k+b$, so slice $(j-1)k+b$ has the form H2 or H5, so the path configuration of color b in V has the form W2 or W5, so color b enters V from the right.

We can now conclude that

$$\begin{aligned}\operatorname{spin}(T) &= \sum_V \sum_a \mathbf{1}_{a \text{ appears in } V} \cdot \left(\sum_{b<a} \mathbf{1}_{b \text{ exits } V \text{ to the right}} + \sum_{b>a} \mathbf{1}_{b \text{ enters } V \text{ from the left}} \right) \\ &= \sum_{a<b} \Big(\#\, \square_{a,b} + \#\, \square_{a,b} \Big) + \sum_{a<b} \Big(\#\, \square_{a,b} + \#\, \square_{a,b} \Big) \\ &= \sum_{a<b} \Big(\#\, \square_{a,b} + \#\, \square_{a,b} + \#\, \square_{a,b} + \#\, \square_{a,b} \Big),\end{aligned}$$

where V varies over the vertices in $\theta(T)$, and a and b vary over the colors. ∎

Lemma 5.8. *Let T be a vertical k-ribbon strip. In the corresponding purple row $\theta(T)$,*

$$\operatorname{spin}(T) = \sum_{a<b} \Big(\#\, \square_{a,b} + \#\, \square_{a,b} + \#\, \square_{a,b} + \#\, \square_{a,b} \Big),$$

where blue is color a and red is color b.

Proof. We follow the same ideas as in the proof of the previous lemma. The fact that T is a vertical ribbon strip restricts the possible forms of the slices:

(1) If a tail triangle appears, it must be at the bottom of the slice.

(2) If a head triangle appears, it must be at the top of the slice.

With these restrictions in mind, we see that each slice must have one of the following five forms:

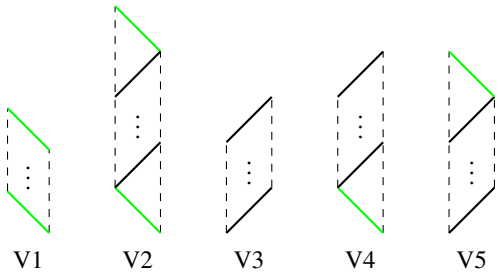

Arguing similarly to Lemma 5.6, one can show that there is a one-to-one correspondence between the five possible forms of a slice in T and the five possible path configurations of the corresponding color in the corresponding purple vertex of $\theta(T)$,

V1 $\leftrightarrow$  P1, V2 $\leftrightarrow$  P2,

V3 $\leftrightarrow$  P3, V4 $\leftrightarrow$  P4, V5 $\leftrightarrow$  P5.

Recall that slice $i = (j-1)k + a$ in T corresponds to color a in the j-th leftmost vertex V in $\theta(T)$. The contribution of this slice to $\mathrm{spin}(T)$ equals the number of column parallelograms in the slice. Looking at the five possible forms of a slice, we see that this equals zero unless slice i has the form V1, which is equivalent to the path configuration of color a having form P1 in V, that is, color a being vertical in V. In that case, the contribution to the spin equals the number of ribbons R that appear in slice i but whose head/tail triangles do not. One can show that this equals the number of smaller colors $b < a$ that exits V to the right plus the number of larger colors $b > a$ that enter V from the left.

From this we conclude

$$\mathrm{spin}(T) = \sum_V \sum_a \mathbf{1}_{a \text{ is vertical in } V} \cdot \Big(\sum_{b<a} \mathbf{1}_{b \text{ exits } V \text{ to the right}} + \sum_{b>a} \mathbf{1}_{b \text{ enters } V \text{ from the left}} \Big)$$

$$= \sum_{a<b} \Big(\#\,\text{  } + \#\,\text{  } \Big) + \sum_{a<b} \Big(\#\,\text{  } + \#\,\text{ 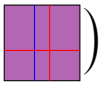 } \Big)$$

$$= \sum_{a<b} \Big(\#\,\text{  } + \#\,\text{  } + \#\,\text{  } + \#\,\text{  } \Big),$$

where V varies over the vertices in $\theta(T)$ and a and b vary over the colors. ∎

We are now ready to relate $\mathcal{L}^S_{\boldsymbol{\lambda}/\boldsymbol{\mu}}$ to $\mathcal{G}^{(k)}_{\lambda/\mu}$.

Proposition 5.9. *Let $\boldsymbol{\lambda}/\boldsymbol{\mu}$ be the k-quotient of λ/μ. Then*

$$\mathcal{L}^S_{\boldsymbol{\lambda}/\boldsymbol{\mu}}(X_n; Y_m; t) = t^{\square} \mathcal{G}^{(k)}_{\lambda/\mu}(X_n; Y_m; t^{1/2})$$

for some half-integer $\square \in \frac{1}{2}\mathbb{Z}$. In fact, in any configuration of the lattice $S_{n,m}(\boldsymbol{\lambda}/\boldsymbol{\mu})$,

$$\square = \frac{1}{2} \sum_{a<b} \Big(\#\,\text{  } + \#\,\text{  } - \#\,\text{  } - \#\,\text{ 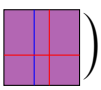 } \Big)$$

$$+ \frac{1}{2} \sum_{a<b} \Big(\#\,\text{  } - \#\,\text{  } \Big).$$

Proof. Recall the bijection $\theta\colon \mathrm{SRT}_k(\lambda/\mu) \to LC(S_{n,m}(\boldsymbol{\lambda}/\boldsymbol{\mu}))$. It is enough to show that $\mathrm{weight}(\theta(T)) = t^{\square} t^{\mathrm{spin}(T)} x^{\mathrm{weight}(T)} y^{\mathrm{weight}'(T)}$ for all $T \in \mathrm{SRT}_k(\lambda/\mu)$, for some half-integer $\square$ that does not depend on T. Fix a super ribbon tableaux $T \in \mathrm{SRT}_k(\lambda/\mu)$ and let $C = \theta(T) \in LC(S_{n,m}(\boldsymbol{\lambda}/\boldsymbol{\mu}))$ be the corresponding path configuration. It is clear that the x weights (y weights) match, since each ribbon labeled $a \in \mathcal{A}$ ($a' \in \mathcal{A}'$) in T corresponds to a path taking a step to the right in the a-th white (purple) row of C. We are left to consider the powers of t. From the previous lemmas, we see that

$$\mathrm{spin}(T) = \sum_{a<b} \Big(\#$$

$$+ \#$$

$$+ \#$$

$$+ \#$$

$$\Big) + \sum_{a<b} \Big(\#$$

$$+ \#$$

$$+ \#$$

$$+ \#$$

$$\Big)$$

$$= \sum_{a<b} \Big(2 \cdot \#$$

$$+ \#$$

$$+ \#$$

$$\Big) + \sum_{a<b} \Big(\#$$

$$+ \#$$

$$+ \#$$

$$+ \#$$

$$\Big)$$

$$= 2\,\mathrm{coinv}(C) - \sum_{a<b} \Big(\#$$

$$- \#$$

$$\Big)$$

$$+ 2\,\mathrm{coinv}'(C) - \sum_{a<b} \Big(\#$$

$$+ \#$$

$$- \#$$

$$- \#$$
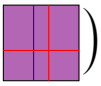
$$\Big),$$

where

$$\mathrm{coinv}(C) = \sum_{a<b} \Big(\#$$

$$+ \#$$

$$\Big)$$

is the power of t coming from the white boxes in C and

$$\mathrm{coinv}'(C) = \sum_{a<b} \Big(\#$$

$$+ \#$$

$$\Big)$$

is the power of t coming from the purple boxes in C. Thus

$$\frac{1}{2}\,\mathrm{spin}(T) + \square = \mathrm{coinv}(C) + \mathrm{coinv}'(C),$$

where

$$\square = \frac{1}{2} \sum_{a<b} \Big(\#$$

$$+ \#$$

$$- \#$$

$$- \#$$

$$\Big)$$

$$+ \frac{1}{2} \sum_{a<b} \Big(\#$$

$$- \#$$

$$\Big).$$

If we can show that $\square$ is independent of the configuration C, then the result follows. It is enough to check this for two colors. This can be shown with a standard corner flipping argument, which we verified with a computer. ∎

6. Cauchy identity

Recall from [1, 13, 21] that the LLT polynomials satisfy a Cauchy identity. We would like to prove a similar theorem for the supersymmetric LLT polynomials. We will do so in the style of [13, 30].

We will need the following change of variables for the L and L' weights, which we represent as a gray face and a pink face, respectively:

$$\begin{array}{ccc} & \boldsymbol{K} & \\ \boldsymbol{J} & \overline{x} & \boldsymbol{L} \\ & \boldsymbol{I} & \end{array} := x^k t^{\binom{k}{2}} L^{(k)}_{\overline{x}}(\boldsymbol{I}, \boldsymbol{J}; \boldsymbol{K}, \boldsymbol{L}),$$

$$\begin{array}{ccc} & \boldsymbol{K} & \\ \boldsymbol{J} & \overline{x} & \boldsymbol{L} \\ & \boldsymbol{I} & \end{array} := x^k L'^{(k)}_{1/x}(\boldsymbol{I}, \boldsymbol{J}; \boldsymbol{K}, \boldsymbol{L}).$$

Here

$$\overline{x} = \frac{1}{xt^{k-1}}.$$

This change of variable is chosen in part so that the gray face, in which every color appears as a horizontal path, and the pink face, in which every color appears as a cross, have weight one,

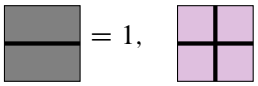 $= 1,$ $= 1.$

It will also be useful to define $P^{(k)}_{l_1,l_2}$, for $0 \le l_1, l_2 \le \infty$, to be the set of k-tuples of partitions with l_1 parts whose largest part is less than or equal to l_2.

6.1. Single rows

In order to construct our Cauchy identity, we will employ infinitely long rows of vertices. For the white and purple vertices, it is relatively easy to define a row of infinite length. We start by defining the following finite length rows, where the allowed states on the top and bottom boundaries are indexed by partitions $P^{(k)}_{l_1,l_2}$.

Pictorially these are given by

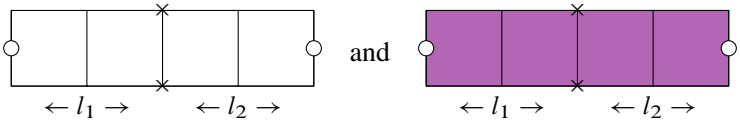

Each row has length $l_1 + l_2$, and we explicitly mark the zero content line. We can increase l_1 by extending the partitions indexing the boundary states with zero parts; similarly, we can increase l_2 by adding empty faces to the right. Note that increasing l_1 adds faces of the form

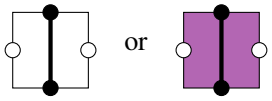

on the left, while increasing l_2 adds faces of the form

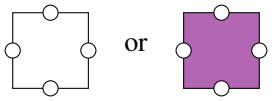

on the right; since these vertices have weight 1, increasing l_1 and l_2 does not change the weight of the row. In fact, we may take $l_1, l_2 \to \infty$ and allow the boundary states to be indexed by partitions with infinitely many parts as long as only finitely many parts are non-zero.

For the gray and pink vertices, we must be slightly more careful. Note that

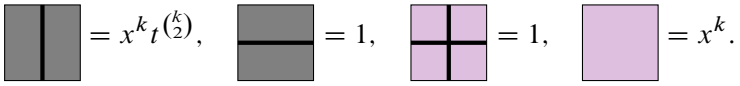

For the gray faces, we consider a row of finite length, such that the allowed states on the bottom are indexed by partitions in $P^{(k)}_{l_1,l_2}$, and the allowed states on the top are indexed by partitions in $P^{(k)}_{l_1-1,l_2}$. We draw this as

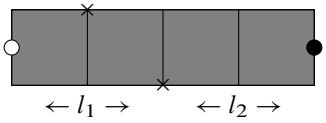

The boundary condition on the right allows us to increase l_2 by adding faces where every path is horizontal without changing the weight of the row. However, increasing l_1 by adding zero parts to the partitions does affect the weight since faces where all the paths are vertical have a non-trivial contribution due to the change of variable.

For the pink faces, we consider a row of finite length such that the allowed states on the bottom are indexed by partitions in $P^{(k)}_{l_1,l_2}$, and the allowed states on the top are indexed by partitions in $P^{(k)}_{l_1+1,l_2-1}$. We draw this as

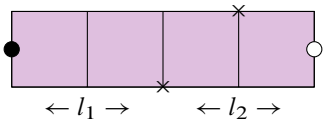

In this case, we can increase l_1 by adding zero parts to the partitions without changing the weight of the row, as this amounts to adding faces on the left, where every color is a cross. However, increasing l_2 by adding empty faces on the right does affect the weight. We will see later that the contribution to the weight coming from increasing l_1 in the case of the gray faces, and the contribution to the weight coming from increasing l_2 in the case of the pink faces, cancels out in the Cauchy identity, allowing us to circumvent this issue.

Remark 6.1. Suppose the bottom boundary of a row is indexed by $\boldsymbol{\mu}$ while the top boundary is indexed by $\boldsymbol{\lambda}$. Recall that, for the white faces, in order for the row to have a non-zero weight, $\boldsymbol{\lambda}$ must be obtained from $\boldsymbol{\mu}$ by adding a horizontal strip. Similarly, for the purple faces, $\boldsymbol{\lambda}$ must be obtained from $\boldsymbol{\mu}$ by adding a vertical strip. For the gray faces, $\boldsymbol{\lambda}$ must be obtained from $\boldsymbol{\mu}$ by removing a horizontal strip. For the pink faces, $\boldsymbol{\lambda}$ must be obtained from $\boldsymbol{\mu}$ by removing a vertical strip.

6.2. Some partition functions

Here we will construct certain lattice models using the single rows above, whose partition functions will be used in our Cauchy identities. In what follows, we will always consider our partitions $\boldsymbol{\lambda}$ and $\boldsymbol{\mu}$ to be k-tuples of partitions, each of which with a infinitely many parts, only finitely many of which are non-zero. We will truncate the partitions, removing only zero parts, to limit the number of parts as needed.

Given $\boldsymbol{\lambda}$ and $\boldsymbol{\mu}$, choose positive integers l_1, l_2 such that each partition has at most l_1 non-zero parts and largest part at most l_2. Truncate $\boldsymbol{\lambda}$ and $\boldsymbol{\mu}$ so that they are in $P^{(k)}_{l_1,l_2}$. Recall from Section 3 that for the white faces, we have

$$\mathcal{L}_{\boldsymbol{\lambda}/\boldsymbol{\mu}}(X_m;t) =$$

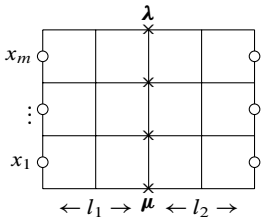

and for the purple faces, we have

$$\mathcal{L}^{P}_{\boldsymbol{\lambda}/\boldsymbol{\mu}}(X_m;t) =$$

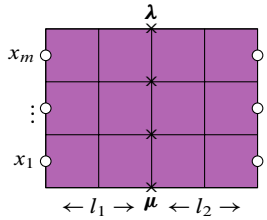

where both are independent of the choice of l_1 and l_2. In particular, the limit as $l_1, l_2 \to \infty$ of these partition functions is well defined.

For the gray faces, fix the number of variables m. This time, given $\boldsymbol{\lambda}$ and $\boldsymbol{\mu}$, choose positive integers l_1, l_2 such that each partition of $\boldsymbol{\lambda}$ has $\leq l_1$ non-zero parts, each partition of $\boldsymbol{\mu}$ has $\leq l_1 - m$ non-zero parts, and each partition of both tuples has largest part $\leq l_2$. Truncate the partitions so that $\boldsymbol{\lambda} \in P^{(k)}_{l_1,l_2}$ and $\boldsymbol{\mu} \in P^{(k)}_{l_1-m,l_2}$. Define

$$\mathcal{L}^{*}_{\boldsymbol{\lambda}/\boldsymbol{\mu}}(X_m;t) :=$$

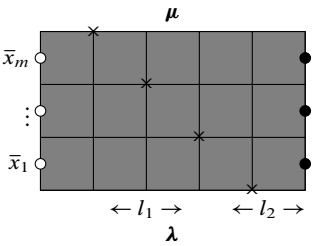

We have the following proposition.

Proposition 6.2. *We have*

$$\mathcal{L}^{*}_{\boldsymbol{\lambda}/\boldsymbol{\mu}}(X_m;t) = (x_1 \dots x_m)^{(l_1-m)k} (x^{\rho_m})^k t^{m(2l_1-m-1)\binom{k}{2}} t^{d(\boldsymbol{\lambda},\boldsymbol{\mu})} \mathcal{L}_{\boldsymbol{\lambda}/\boldsymbol{\mu}}(X_m;t),$$

where $d(\boldsymbol{\lambda},\boldsymbol{\mu})$ and $\mathcal{L}_{\boldsymbol{\lambda}/\boldsymbol{\mu}}$ are independent of l_1 and l_2. Furthermore, $d(\boldsymbol{\lambda},\boldsymbol{\mu})$ is given by

$$d(\boldsymbol{\lambda},\boldsymbol{\mu}) = \sum_{a<b} \#\{i,j \mid \mu^{(a)}_j - j > \mu^{(b)}_i - i\} - \sum_{a<b} \#\{i,j \mid \lambda^{(a)}_j - j > \lambda^{(b)}_i - i\}.$$

The proof is essentially identical to that of [13, Proposition 6.11], for which this is a slight generalization. (We can recover [13, Proposition 6.11] by taking $\boldsymbol{\mu} = \mathbf{0}$ and $l_1 = m = n$.) Note that $\mathcal{L}^*$ is independent of l_2, and we may take $l_2 \to \infty$.

For the pink faces, again fix the number of variables m. Given $\boldsymbol{\lambda}$ and $\boldsymbol{\mu}$, choose positive integers l_1, l_2 such that the number of non-zero parts of each partition of

both tuples is $\leq l_1$, the largest part of every partition in $\boldsymbol{\lambda}$ is $\leq l_2$, and the largest part of every partition in $\boldsymbol{\mu}$ is $\leq l_2 - m$. Truncate the partitions so that $\boldsymbol{\lambda} \in P^{(k)}_{l_1,l_2}$, and $\boldsymbol{\mu} \in P^{(k)}_{l_1+m,l_2-m}$. Define

$$(\mathcal{L}^P)^*_{\boldsymbol{\lambda}/\boldsymbol{\mu}}(X_m;t) :=$$

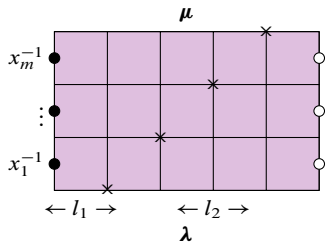

We would like to be able to write $(\mathcal{L}^P)^*$ in terms of $\mathcal{L}^P$. In order to do so, we will prove a series of lemmas.

Definition 6.3. Let N, n, k be non-negative integers. Given a partition λ with n non-negative parts, each of which is $\leq N$, we define its *complement* in an $n \times N$ box to be the partition

$$\lambda^c = (N - \lambda_n, \ldots, N - \lambda_1).$$

Given $\boldsymbol{\lambda} \in P^k_n$, we define its complement in an $N \times n$ box to be the k-tuple of partitions $\boldsymbol{\lambda}^c = ((\lambda^c)^{(1)}, \ldots, (\lambda^c)^{(k)})$, where

$$(\lambda^c)^{(i)} = (\lambda^{(k-i)})^c.$$

In other words, we complement each partition and reverse their order in the tuple.

Lemma 6.4. *Fix $\boldsymbol{\lambda} \in P^{(k)}_{l_1,l_2}$ and $\boldsymbol{\mu} \in P^{(k)}_{l_1,l_2-m}$. Let $\widetilde{\boldsymbol{\mu}} \in P^{(k)}_{l_1,l_2}$ be the tuple of partitions one gets by adding m to every part of every partition in $\boldsymbol{\mu}$. Then*

$$\mathcal{L}^P_{\widetilde{\boldsymbol{\mu}}/\boldsymbol{\lambda}}(X_m;t) = t^{d_P(\boldsymbol{\lambda},\boldsymbol{\mu})}\mathcal{L}^P_{\boldsymbol{\lambda}^c/\widetilde{\boldsymbol{\mu}}^c}(X_m;t),$$

where complements are taken in an $l_1 \times l_2$ box and $d_P(\boldsymbol{\lambda},\boldsymbol{\mu}) = d(\boldsymbol{\lambda},\boldsymbol{\mu})$ is independent of l_1, l_2.

Proof. There is a bijection between configurations with bottom boundary $\boldsymbol{\lambda}$ and top boundary $\widetilde{\boldsymbol{\mu}}$ and configurations with bottom boundary $\widetilde{\boldsymbol{\mu}}^c$ and top boundary $\boldsymbol{\lambda}^c$, given by rotating 180 degrees and reversing the order of the colors. For example, with

$$\boldsymbol{\lambda} = ((2,1,0),(1,1,1)), \quad \boldsymbol{\mu} = ((1,0,0),(1,1,0)), \quad l_1 = m = 3, \quad l_2 = 4,$$

we have

$$\boldsymbol{\lambda}^c = ((3,3,3),(4,3,2)), \quad \widetilde{\boldsymbol{\mu}} = ((4,3,3),(4,4,3)), \quad \widetilde{\boldsymbol{\mu}}^c = ((1,0,0),(1,1,0)).$$

For a particular configuration, we would map

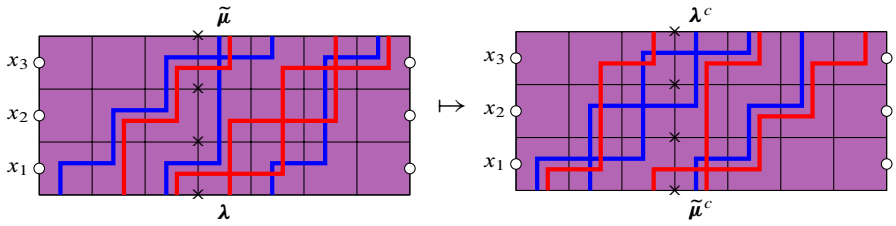

It is easy to show that under this bijection the x weight does not change, up to switching x_i and x_{m-i+1}, as horizontal steps in row i become horizontal steps in row $m-i+1$. A corner flipping argument shows that the difference in the power of t before and after the mapping does not depend on the configuration. This shows that

$$\mathcal{L}^P_{\tilde{\mu}/\lambda}(X_m;t) = t^{d_P(\lambda,\mu)}\mathcal{L}^P_{\lambda^c/\tilde{\mu}^c}(x_m,\ldots,x_1;t) = t^{d_P(\lambda,\mu)}\mathcal{L}^P_{\lambda^c/\tilde{\mu}^c}(X_m;t),$$

where the last equality uses the symmetry of $\mathcal{L}^P$. Note that increasing l_1 by adding zero parts to λ and parts of size m to $\tilde{\mu}$ does not change the power of t on either side of the bijection as this only adds paths that staircase (i.e., take one step to the right in each row). Similarly, increasing l_2 by adding empty columns does not affect the power of t on either side. Thus $d_P(\lambda,\mu)$ is independent of l_1 and l_2. As shown in the next lemma, $d_P(\lambda,\mu) = d(\lambda,\mu)$. ∎

Lemma 6.5. *Let λ, μ be as in the previous lemma. Then*

$$d_P(\lambda,\mu) = \sum_{a<b} \#\{i,j \mid \mu^{(a)}_j - j > \mu^{(b)}_i - i\} - \sum_{a<b} \#\{i,j \mid \lambda^{(a)}_j - j > \lambda^{(b)}_i - i\}.$$

Proof. First let us assume that $\mu = \mathbf{0}$ and $k = 2$. In this case, every part in $\tilde{\mu}$ equals m. We can calculate $d_P(\lambda,\mu)$ using any choice of configuration. We will pick the configuration T of $\tilde{\mu}/\lambda$ such all the paths are as low as possible. In this case, each path will begin as a staircase going right until it reaches the column in which it ends, and will then travel vertically to its endpoint. Consider a single path of the first color (blue) corresponding to the j-th row of the skew shape. For it to contribute a power of t, a path of the second color (red) must travel vertically in a face in which the blue path exits right. Suppose we have such a red path, corresponding to the i-th row. As a path travels vertically only in the column in which it ends, the blue path must end to the right of the red path, i.e., $j < i$. Further, in order for the red path to cross the blue path while traveling vertically its staircase must be weakly below the blue staircase, so the blue path must start weakly to the left of the red path, i.e., $\lambda^{(1)}_j - j \le \lambda^{(2)}_i - i$. We see that

$$\mathrm{coinv}'(T) = \#\{j < i \mid \lambda^{(1)}_j - j \le \lambda^{(2)}_i - i\},$$

where $\mathrm{coinv}'(T)$ is the power of t in the configuration T.

Using our mapping, the configuration T gets mapped to a configuration T' of $\boldsymbol{\lambda}^c/\widetilde{\boldsymbol{\mu}}^c$ in which all the paths are as high as possible. In this case, the paths all begin traveling vertically and then staircase to their endpoint. Similar reasoning shows that for the j-th blue path to exit right while the i-th red path is vertical, the blue path must begin weakly to the left of the red path, and the blue path must end to the right of the red path. This gives

$$\operatorname{coinv}'(T') = \#\{j \geq i \mid (\lambda^c)_j^{(1)} - j > (\lambda^c)_i^{(2)} - i\} = \#\{j \geq i \mid \lambda_j^{(1)} - j > \lambda_i^{(2)} - i\}.$$

From this we find

$$\begin{aligned} d_P(\boldsymbol{\lambda}, \mathbf{0}) &= \#\{j < i \mid \lambda_j^{(1)} - j \leq \lambda_i^{(2)} - i\} - \#\{j \geq i \mid \lambda_j^{(1)} - j > \lambda_i^{(2)} - i\} \\ &= \#\{j < i \mid \lambda_j^{(1)} - j \leq \lambda_i^{(2)} - i\} + \#\{j < i \mid \lambda_j^{(1)} - j > \lambda_i^{(2)} - i\} \\ &\quad - \#\{j < i \mid \lambda_j^{(1)} - j > \lambda_i^{(2)} - i\} - \#\{j \geq i \mid \lambda_j^{(1)} - j > \lambda_i^{(2)} - i\} \\ &= \#\{j < i\} - \#\{i, j \mid \lambda_j^{(1)} - j > \lambda_i^{(2)} - i\}. \end{aligned}$$

Noting that $\#\{i, j \mid \mu_j^{(1)} - j > \mu_i^{(2)} - i\} = \#\{j < i\}$ when $\boldsymbol{\mu} = \mathbf{0}$, we get the result in the case $\boldsymbol{\mu} = \mathbf{0}$ and $k = 2$. Summing over all pairs of colors $a < b$ gives the result in the case $\boldsymbol{\mu} = \mathbf{0}$ and k general.

To prove the general case, let $\boldsymbol{\lambda}$ and $\boldsymbol{\mu}$ be as in the statement of the lemma. Consider a lattice with $n + m$ rows. Let $\boldsymbol{\nu} = \mathbf{0}$, so that every part of $\widetilde{\boldsymbol{\nu}}$ equals $n + m$. From the above calculation, we know that

$$d_P(\boldsymbol{\lambda}, \mathbf{0}) = \sum_{a<b} \#\{j < i\} - \sum_{a<b} \#\{i, j \mid \lambda_j^{(a)} - j > \lambda_i^{(b)} - i\}.$$

This can be calculated using any configuration of $\boldsymbol{\lambda}/\widetilde{\boldsymbol{\nu}}$. Let us choose a configuration such that the top boundary of the m-th row is given by $\widetilde{\boldsymbol{\mu}}$. Then the contribution to the change in power of t from the rows above the m-th row is given by

$$d_P(\widetilde{\boldsymbol{\mu}}, \mathbf{0}) = \sum_{a<b} \#\{j < i\} - \sum_{a<b} \#\{i, j \mid \widetilde{\mu}_j^{(a)} - j > \widetilde{\mu}_i^{(b)} - i\},$$

while the contribution from the m-th row and below is given by $d_P(\boldsymbol{\lambda}, \boldsymbol{\mu})$. Since the contribution from the two pieces must equal the overall change in power of t, we see that

$$\begin{aligned} d_P(\boldsymbol{\lambda}, \boldsymbol{\mu}) &= d_P(\boldsymbol{\lambda}, \mathbf{0}) - d_P(\widetilde{\boldsymbol{\mu}}, \mathbf{0}) \\ &= \sum_{a<b} \#\{i, j \mid \widetilde{\mu}_j^{(a)} - j > \widetilde{\mu}_i^{(b)} - i\} - \sum_{a<b} \#\{i, j \mid \lambda_j^{(a)} - j > \lambda_i^{(b)} - i\} \\ &= \sum_{a<b} \#\{i, j \mid \mu_j^{(a)} - j > \mu_i^{(b)} - i\} - \sum_{a<b} \#\{i, j \mid \lambda_j^{(a)} - j > \lambda_i^{(b)} - i\} \end{aligned}$$

as desired. ∎

Lemma 6.6. *Let $\boldsymbol{\lambda}$, $\boldsymbol{\mu}$, m, l_1, l_2 be as in Lemma 6.4. Then*

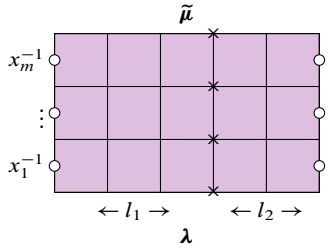

$$= (x_1 \dots x_m)^{k(l_1+l_2)} t^{d_P(\boldsymbol{\lambda},\boldsymbol{\mu})} \mathcal{L}^P_{\boldsymbol{\lambda}^c/\tilde{\boldsymbol{\mu}}^c}(X_m^{-1};t).$$

Proof. We start with Lemma 6.4. To change from purple faces to pink faces, for each $i \in [m]$, we take $x_i \mapsto \frac{1}{x_i}$ and multiply every face in the i-th row by x_i^k. This gives the desired equation. ∎

Lemma 6.7. *Let $\boldsymbol{\lambda}$, $\boldsymbol{\mu}$, m, l_1, l_2 be as in the previous lemma, except now consider $\boldsymbol{\mu}$ as an element of $P^{(k)}_{l_1+m,l_2}$ (i.e., add m more parts equal to 0). Then*

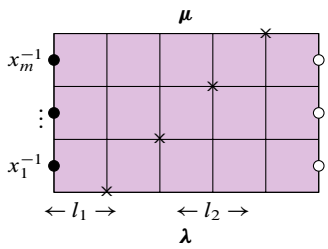

$$= (x_1 \dots x_m)^{k(l_1+l_2+1)} t^{d_P(\boldsymbol{\lambda},\boldsymbol{\mu})} \mathcal{L}^P_{\boldsymbol{\lambda}^c/\tilde{\boldsymbol{\mu}}^c}(X_m^{-1};t).$$

Proof. Starting with the lattice from the previous lemma, we add a path of each color on the left edge of each row. The paths entering from the left must end packed to the left at the top. This, along with the shift to the right by m of the zero content line, means that the top boundary is now given by $\boldsymbol{\mu}$. Adding the paths entering from the left changes the weight by the factor $(x_1 \dots x_m)^k$. ∎

Finally, we must relate the LLT polynomial of a skew partition with that of its complement.

Lemma 6.8. *Let $\boldsymbol{\lambda} \in P^{(k)}_{l_1,l_2}$ and $\boldsymbol{\mu} \in P^{(k)}_{l_1,l_2-m}$. Let $\tilde{\boldsymbol{\mu}} \in P^{(k)}_{l_1,l_2}$ be the tuple of partitions one gets by adding m to every part of every partition in $\boldsymbol{\mu}$. We have*

$$\mathcal{L}^P_{\boldsymbol{\lambda}/\boldsymbol{\mu}}(X_m;t) = (x_1 \dots x_m)^{kl_1} \mathcal{L}^P_{\boldsymbol{\lambda}^c/\tilde{\boldsymbol{\mu}}^c}(X_m^{-1};t).$$

Proof. We construct a bijection $\mathrm{SSYT}(\boldsymbol{\lambda}/\boldsymbol{\mu}) \to \mathrm{SSYT}(\boldsymbol{\lambda}^c/\tilde{\boldsymbol{\mu}}^c)$ as follows. For each skew partition in $\boldsymbol{\lambda}/\boldsymbol{\mu}$, draw it inside an $l_1 \times l_2$ box. Given any SSYT of the skew shape, go from left to right, row-by-row, and fill the cells of the box with the largest available integer not already used in that row. After rotating by 180 degrees, the newly filled cells of the box are a SSYT of the corresponding skew partition in $\boldsymbol{\lambda}^c/\tilde{\boldsymbol{\mu}}^c$. For

example, let $\lambda = (3,3,1,0)$, $\mu = (1,0,0,0)$, $l_1 = m = 4$, $l_2 = 6$. Then we have $\lambda^c = (6,5,3,3)$ and $\widetilde{\mu}^c = (2,2,2,1)$. Consider the filling

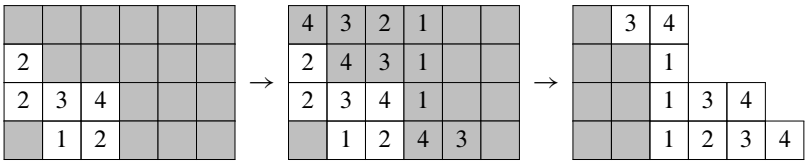

Note that under this map the x weights transform as $x^T \mapsto (x_1 \dots x_m)^{kl_1}(x^T)^{-1}$. We are left to determine what happens to the powers of t. It is easy to check that, in terms of lattice paths, flipping a corner of color a up (down) on one side of the bijection corresponds to flipping a corner of color $k-a+1$ down (up) on the other side. As the space of configurations on both sides is connected under corner flips, a corner flipping argument shows the difference in the powers of t does not depend on the configuration. Thus there is some overall power of t difference, call it $\widetilde{d}_P(\boldsymbol{\lambda}, \boldsymbol{\mu})$, so that

$$\mathcal{L}^P_{\boldsymbol{\lambda}/\boldsymbol{\mu}}(X_m;t) = (x_1 \dots x_m)^{kl_1} t^{\widetilde{d}_P(\boldsymbol{\lambda},\boldsymbol{\mu})} \mathcal{L}^P_{\boldsymbol{\lambda}^c/\widetilde{\boldsymbol{\mu}}^c}(X_m^{-1};t).$$

We need only to compute the difference in the power of t for a specific choice of configurations to compute $\widetilde{d}_P(\boldsymbol{\lambda}, \boldsymbol{\mu})$. A similar argument to the one used in the proof of Lemma 6.5 shows $\widetilde{d}_P(\boldsymbol{\lambda}, \boldsymbol{\mu}) = 0$. ∎

Combining all the above lemmas leads to the following proposition.

Proposition 6.9. *We have*

$$(\mathcal{L}^P)^*_{\boldsymbol{\lambda}/\boldsymbol{\mu}}(X_m;t) = (x_1 \dots x_m)^{k(l_2+1)} t^{d_P(\boldsymbol{\lambda},\boldsymbol{\mu})} \mathcal{L}^P_{\boldsymbol{\lambda}/\boldsymbol{\mu}}(X_m;t),$$

where the whole thing is independent of l_1, and $d_P(\boldsymbol{\lambda}, \boldsymbol{\mu})$ and $\mathcal{L}^P_{\boldsymbol{\lambda}/\boldsymbol{\mu}}$ are also independent of l_2.

6.3. Cauchy identities

Using the above, we will now prove several Cauchy identities for $\mathcal{L}$ and $\mathcal{L}^P$.

Proposition 6.10. *Let $\boldsymbol{\mu}$ and $\boldsymbol{\nu}$ be tuples of partitions, each with infinitely many parts only a finitely many of which are non-zero. Then*

$$\sum_{\boldsymbol{\lambda}} t^{d(\boldsymbol{\mu},\boldsymbol{\lambda})} \mathcal{L}_{\boldsymbol{\mu}/\boldsymbol{\lambda}}(Y_m;t) \mathcal{L}^P_{\boldsymbol{\nu}/\boldsymbol{\lambda}}(X_n;t)$$
$$= \left(\prod_{i,j} \prod_{l=0}^{k-1} (1 + x_i y_j t^l)^{-1} \right) \sum_{\boldsymbol{\lambda}} t^{d(\boldsymbol{\lambda},\boldsymbol{\nu})} \mathcal{L}^P_{\boldsymbol{\lambda}/\boldsymbol{\mu}}(X_n;t) \mathcal{L}_{\boldsymbol{\lambda}/\boldsymbol{\nu}}(Y_m;t).$$

Proof. Given $\boldsymbol{\mu}$ and $\boldsymbol{\nu}$, choose positive integers l_1 and l_2 such that maximum number of non-zero parts of a partition in $\boldsymbol{\nu}$ is less than $l_1 - m$ and the largest part of any partition in $\boldsymbol{\nu}$ is less than $l_2 + m$. Note that this ensures that l_1 is greater than the maximum number of non-zero parts of a partition in $\boldsymbol{\mu}$ and that l_2 is greater than the largest part of any partition in $\boldsymbol{\mu}$. Truncate the partitions so that $\boldsymbol{\mu} \in P^{(k)}_{l_1,l_2}$ and $\boldsymbol{\nu} \in P^{(k)}_{l_1-m,l_2+m}$. Consider the following partition function:

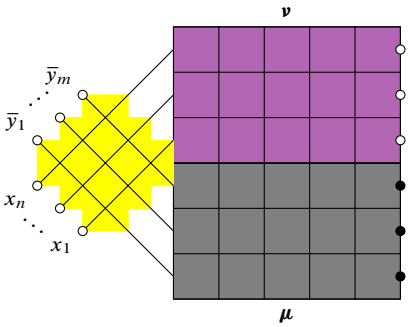

This can be split into three pieces as follows:

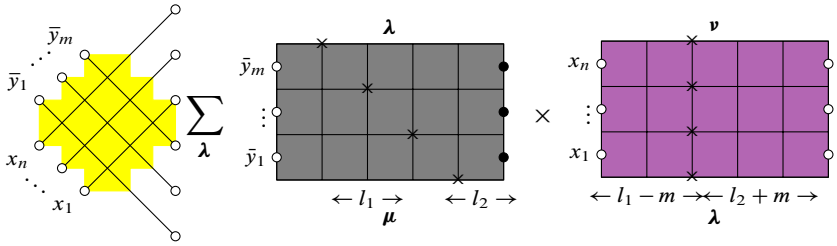

From the previous subsection, in particular Proposition 6.2, every piece is independent of l_2, so we may take $l_2 \to \infty$. Here the crosses have weight one. Using the YBE to move the crosses to the other side gives

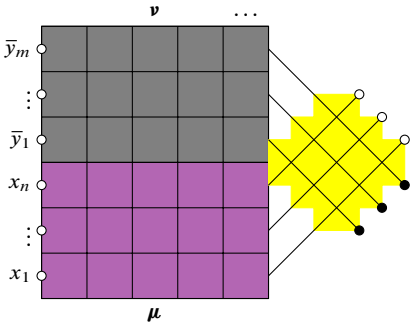

Since we have taken $l_2 \to \infty$ and paths cannot travel horizontally across a purple face, we know that the paths originating from the bottom boundary must exit from the gray

faces at the right boundary. Splitting this into parts, we get

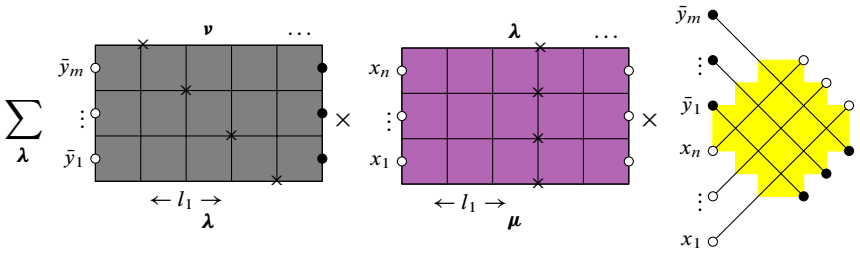

Equating the two sums results in

$$\sum_{\boldsymbol{\lambda}} \mathcal{L}^*_{\boldsymbol{\mu}/\boldsymbol{\lambda}}(Y_m;t)\mathcal{L}^P_{\boldsymbol{\nu}/\boldsymbol{\lambda}}(X_n;t)$$
$$= \left(\prod_{i,j}\prod_{l=0}^{k-1}(1+x_i y_j t^l)^{-1}\right)\sum_{\boldsymbol{\lambda}} \mathcal{L}^P_{\boldsymbol{\lambda}/\boldsymbol{\mu}}(X_n;t)\mathcal{L}^*_{\boldsymbol{\lambda}/\boldsymbol{\nu}}(Y_m;t),$$

where the prefactor on the right-hand side comes from the crosses. Using Proposition 6.2, we get

$$\sum_{\boldsymbol{\lambda}}(y_1\dots y_m)^{(l_1-m)k}(y^{\rho_m})^k t^{m(2l_1-m-1)\binom{k}{2}} t^{d(\boldsymbol{\mu},\boldsymbol{\lambda})}\mathcal{L}_{\boldsymbol{\mu}/\boldsymbol{\lambda}}(Y_m;t)\mathcal{L}^P_{\boldsymbol{\nu}/\boldsymbol{\lambda}}(X_n;t)$$
$$= \left(\prod_{i,j}\prod_{l=0}^{k-1}(1+x_i y_j t^l)^{-1}\right)\sum_{\boldsymbol{\lambda}}(y_1\cdots y_m)^{(l_1-m)k}(y^{\rho_m})^k$$
$$\times t^{m(2l_1-m-1)\binom{k}{2}} t^{d(\boldsymbol{\lambda},\boldsymbol{\nu})}\mathcal{L}^P_{\boldsymbol{\lambda}/\boldsymbol{\mu}}(X_n;t)\mathcal{L}_{\boldsymbol{\lambda}/\boldsymbol{\nu}}(Y_m;t).$$

Many terms (in particular, all the terms involving l_1) cancel, and we can then take $l_1 \to \infty$, giving the proposition. ∎

An analogous proof, using white boxes in place of purple boxes and white crosses in place of yellow crosses, gives the following proposition.

Proposition 6.11. *Let $\boldsymbol{\mu}$ and $\boldsymbol{\nu}$ be tuples of partitions, each with infinitely many parts only finitely many of which are non-zero. Then*

$$\sum_{\boldsymbol{\lambda}} t^{d(\boldsymbol{\mu},\boldsymbol{\lambda})}\mathcal{L}_{\boldsymbol{\nu}/\boldsymbol{\lambda}}(X_n;t)\mathcal{L}_{\boldsymbol{\mu}/\boldsymbol{\lambda}}(Y_m;t)$$
$$= \prod_{i,j}\prod_{l=0}^{k-1}(1-x_i y_j t^l)\sum_{\boldsymbol{\lambda}} t^{d(\boldsymbol{\lambda},\boldsymbol{\nu})}\mathcal{L}_{\boldsymbol{\lambda}/\boldsymbol{\mu}}(X_n;t)\mathcal{L}_{\boldsymbol{\lambda}/\boldsymbol{\nu}}(Y_m;t).$$

This is a slight generalization of [13, Proposition 6.12] (which we can recover by taking $\boldsymbol{\nu} = \mathbf{0}$, setting $m = n$, and swapping X and Y).

Using the white faces and the pink faces, we have the following.

Proposition 6.12. *Let $\boldsymbol{\mu}$ and $\boldsymbol{\nu}$ be tuples of partitions, each with infinitely many parts only finitely many of which are non-zero. Then*

$$\left(\prod_{i,j}\prod_{l=0}^{k-1}(1+x_i y_j t^l)^{-1}\right)\sum_{\boldsymbol{\lambda}} t^{d_P(\boldsymbol{\lambda},\boldsymbol{\nu})}\mathcal{L}_{\boldsymbol{\lambda}/\boldsymbol{\mu}}(Y_m;t)\mathcal{L}^P_{\boldsymbol{\lambda}/\boldsymbol{\nu}}(X_n;t) = \sum_{\boldsymbol{\lambda}} t^{d_P(\boldsymbol{\mu},\boldsymbol{\lambda})}\mathcal{L}^P_{\boldsymbol{\mu}/\boldsymbol{\lambda}}(X_n;t)\mathcal{L}_{\boldsymbol{\nu}/\boldsymbol{\lambda}}(Y_m;t).$$

Proof. Given $\boldsymbol{\mu}$ and $\boldsymbol{\nu}$, choose positive integers l_1, l_2 such that l_1 is greater than or equal to the number of non-zero parts in $\boldsymbol{\mu}$ and $\boldsymbol{\nu}$, l_2 is greater than or equal to the largest part in $\boldsymbol{\mu}$, and $l_2 - n$ is greater than or equal to the largest part in $\boldsymbol{\nu}$. Consider the following partition function:

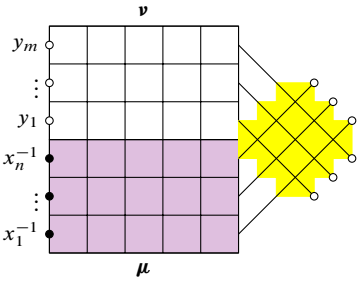

This can be split as

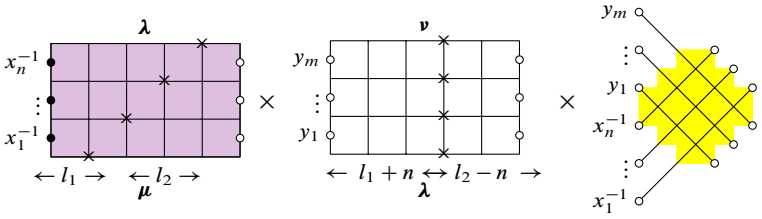

From the previous subsection, in particular Proposition 6.9, every piece is independent of l_1, so we may take $l_1 \to \infty$. We can use the YBE to move the crosses to the other side to get

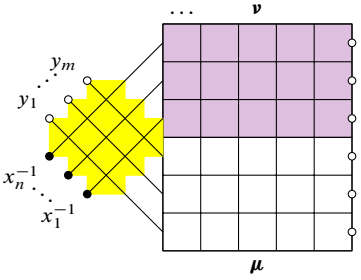

which we split into

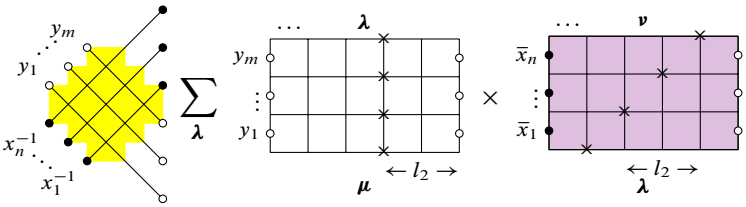

(Sufficiently far to the left in the white faces, every column is dense with vertical paths, so the paths from the cross must enter in the pink faces.) Setting this equal to the other sum gives

$$\left(\prod_{i,j}\prod_{l=0}^{k-1}(1+x_i y_j t^l)^{-1}\right)\sum_{\boldsymbol{\lambda}}\mathcal{L}_{\boldsymbol{\lambda}/\boldsymbol{\mu}}(Y_m;t)(\mathcal{L}^P)^*_{\boldsymbol{\lambda}/\boldsymbol{\nu}}(X_n;t)$$
$$=\sum_{\boldsymbol{\lambda}}(\mathcal{L}^P)^*_{\boldsymbol{\mu}/\boldsymbol{\lambda}}(X_n;t)\mathcal{L}_{\boldsymbol{\nu}/\boldsymbol{\lambda}}(Y_m;t),$$

where the prefactor on the left-hand side comes from the crosses. Using Proposition 6.9, we have

$$\left(\prod_{i,j}\prod_{l=0}^{k-1}(1+x_i y_j t^l)^{-1}\right)\sum_{\boldsymbol{\lambda}}(x_1\cdots x_n)^{k(l_2+1)}t^{d_P(\boldsymbol{\lambda},\boldsymbol{\nu})}\mathcal{L}_{\boldsymbol{\lambda}/\boldsymbol{\mu}}(Y_m;t)\mathcal{L}^P_{\boldsymbol{\lambda}/\boldsymbol{\nu}}(X_n;t)$$
$$=\sum_{\boldsymbol{\lambda}}(x_1\cdots x_n)^{k(l_2+1)}t^{d_P(\boldsymbol{\mu},\boldsymbol{\lambda})}\mathcal{L}^P_{\boldsymbol{\mu}/\boldsymbol{\lambda}}(X_n;t)\mathcal{L}_{\boldsymbol{\nu}/\boldsymbol{\lambda}}(Y_m;t).$$

Canceling the terms involving l_2 gives the proposition. ∎

Changing the white faces to purple faces, a similar computation to the above leads to the following assertion.

Proposition 6.13. *Let $\boldsymbol{\mu}$ and $\boldsymbol{\nu}$ be tuples of partitions, each with infinitely many parts only finitely many of which are non-zero. Then*

$$\left(\prod_{i,j}\prod_{l=0}^{k-1}(1-x_i y_j t^l)\right)\sum_{\boldsymbol{\lambda}}t^{d_P(\boldsymbol{\lambda},\boldsymbol{\nu})}\mathcal{L}^P_{\boldsymbol{\lambda}/\boldsymbol{\mu}}(Y_m;t)\mathcal{L}^P_{\boldsymbol{\lambda}/\boldsymbol{\nu}}(X_n;t)$$
$$=\sum_{\boldsymbol{\lambda}}t^{d_P(\boldsymbol{\mu},\boldsymbol{\lambda})}\mathcal{L}^P_{\boldsymbol{\mu}/\boldsymbol{\lambda}}(X_n;t)\mathcal{L}^P_{\boldsymbol{\nu}/\boldsymbol{\lambda}}(Y_m;t).$$

(One must be careful to only consider terms with finite degrees in y; this forces the paths to only travel from the south-west to the south-east on the cross.)

Combining these identities, we now come to the main result of this section: a Cauchy identity for the supersymmetric LLT polynomials.

Theorem 6.14. *Let $\boldsymbol{\mu}$ and $\boldsymbol{\nu}$ be tuples of partitions, each with infinitely many parts only finitely many of which are non-zero. Fix positive integers n, m, p, q. Then*

$$\sum_{\boldsymbol{\lambda}} t^{d(\boldsymbol{\mu},\boldsymbol{\lambda})} \mathcal{L}^{S}_{\boldsymbol{\nu}/\boldsymbol{\lambda}}(X_n, Y_m; t)\mathcal{L}^{S}_{\boldsymbol{\mu}/\boldsymbol{\lambda}}(W_p, Z_q; t)$$
$$= \prod_{l=0}^{k-1} \prod_{i,i'=1}^{n} \prod_{j,j'=1}^{m} \prod_{\alpha,\alpha'=1}^{p} \prod_{\beta,\beta'=1}^{q} \frac{(1 - x_i w_\alpha t^l)(1 - y_{j'} z_{\beta'} t^l)}{(1 + y_j w_{\alpha'} t^l)(1 + x_{i'} z_\beta t^l)}$$
$$\times \sum_{\boldsymbol{\lambda}} t^{d(\boldsymbol{\lambda},\boldsymbol{\nu})} \mathcal{L}^{S}_{\boldsymbol{\lambda}/\boldsymbol{\mu}}(X_n, Y_m; t)\mathcal{L}^{S}_{\boldsymbol{\lambda}/\boldsymbol{\nu}}(W_p, Z_q; t).$$

Proof. We can rewrite the left-hand side as

$$\text{l.h.s.} = \sum_{\boldsymbol{\lambda},\boldsymbol{\sigma},\boldsymbol{\rho}} \mathcal{L}^{P}_{\boldsymbol{\nu}/\boldsymbol{\rho}}(Y_m; t)\mathcal{L}_{\boldsymbol{\rho}/\boldsymbol{\lambda}}(X_n; t) t^{d_P(\boldsymbol{\mu},\boldsymbol{\sigma})} \mathcal{L}^{P}_{\boldsymbol{\mu}/\boldsymbol{\sigma}}(Z_q; t) t^{d(\boldsymbol{\sigma},\boldsymbol{\lambda})} \mathcal{L}_{\boldsymbol{\sigma}/\boldsymbol{\lambda}}(W_p; t),$$

where we use the fact that

$$d(\boldsymbol{\mu}, \boldsymbol{\lambda}) = d_P(\boldsymbol{\mu}, \boldsymbol{\sigma}) + d(\boldsymbol{\sigma}, \boldsymbol{\lambda}).$$

Applying Proposition 6.11 to the sum over $\boldsymbol{\lambda}$ with the second and fourth LLT polynomials gives

$$\text{l.h.s.} = \prod_{l=0}^{k-1} \prod_{i=1}^{n} \prod_{\alpha=1}^{p} (1 - x_i w_\alpha t^l)$$
$$\times \sum_{\boldsymbol{\lambda},\boldsymbol{\sigma},\boldsymbol{\rho}} \mathcal{L}^{P}_{\boldsymbol{\nu}/\boldsymbol{\rho}}(Y_m; t)\mathcal{L}_{\boldsymbol{\lambda}/\boldsymbol{\sigma}}(X_n; t) t^{d_P(\boldsymbol{\mu},\boldsymbol{\sigma})} \mathcal{L}^{P}_{\boldsymbol{\mu}/\boldsymbol{\sigma}}(Z_q; t) t^{d(\boldsymbol{\lambda},\boldsymbol{\rho})} \mathcal{L}_{\boldsymbol{\lambda}/\boldsymbol{\rho}}(W_p; t).$$

Applying Proposition 6.10 on the sum over $\boldsymbol{\rho}$ with the first and fourth LLT polynomials results in

$$\text{l.h.s.} = \prod_{l=0}^{k-1} \prod_{i=1}^{n} \prod_{j=1}^{m} \prod_{\alpha,\alpha'=1}^{p} \frac{1 - x_i w_\alpha t^l}{1 + y_j w_{\alpha'} t^l}$$
$$\times \sum_{\boldsymbol{\lambda},\boldsymbol{\sigma},\boldsymbol{\rho}} \mathcal{L}^{P}_{\boldsymbol{\rho}/\boldsymbol{\lambda}}(Y_m; t)\mathcal{L}_{\boldsymbol{\lambda}/\boldsymbol{\sigma}}(X_n; t) t^{d_P(\boldsymbol{\mu},\boldsymbol{\sigma})} \mathcal{L}^{P}_{\boldsymbol{\mu}/\boldsymbol{\sigma}}(Z_q; t) t^{d(\boldsymbol{\rho},\boldsymbol{\nu})} \mathcal{L}_{\boldsymbol{\rho}/\boldsymbol{\nu}}(W_p; t).$$

Applying Proposition 6.12 on the sum over $\boldsymbol{\sigma}$ with the second and third LLT polynomials gives

$$\text{l.h.s.} = \prod_{l=0}^{k-1} \prod_{i,i'=1}^{n} \prod_{j=1}^{m} \prod_{\alpha,\alpha'=1}^{p} \prod_{\beta=1}^{q} \frac{1 - x_i w_\alpha t^l}{(1 + y_j w_{\alpha'} t^l)(1 + x_{i'} z_\beta t^l)}$$
$$\times \sum_{\boldsymbol{\lambda},\boldsymbol{\sigma},\boldsymbol{\rho}} \mathcal{L}^{P}_{\boldsymbol{\rho}/\boldsymbol{\lambda}}(Y_m; t)\mathcal{L}_{\boldsymbol{\sigma}/\boldsymbol{\mu}}(X_n; t) t^{d_P(\boldsymbol{\sigma},\boldsymbol{\lambda})} \mathcal{L}^{P}_{\boldsymbol{\sigma}/\boldsymbol{\lambda}}(Z_q; t) t^{d(\boldsymbol{\rho},\boldsymbol{\nu})} \mathcal{L}_{\boldsymbol{\rho}/\boldsymbol{\nu}}(W_p; t).$$

Finally, applying Proposition 6.13 on the sum over $\boldsymbol{\lambda}$ with the first and third LLT polynomials leads to

$$\text{l.h.s.} = \prod_{l=0}^{k-1} \prod_{i,i'=1}^{n} \prod_{j,j'=1}^{m} \prod_{\alpha,\alpha'=1}^{p} \prod_{\beta,\beta'=1}^{q} \frac{(1 - x_i w_\alpha t^l)(1 - y_{j'} z_{\beta'} t^l)}{(1 + y_j w_{\alpha'} t^l)(1 + x_{i'} z_\beta t^l)} \times \sum_{\boldsymbol{\lambda},\boldsymbol{\sigma},\boldsymbol{\rho}} \mathcal{L}^P_{\boldsymbol{\lambda}/\boldsymbol{\sigma}}(Y_m; t) \mathcal{L}_{\boldsymbol{\sigma}/\boldsymbol{\mu}}(X_n; t) t^{d_P(\boldsymbol{\lambda},\boldsymbol{\rho})} \mathcal{L}^P_{\boldsymbol{\lambda}/\boldsymbol{\rho}}(Z_q; t) t^{d(\boldsymbol{\rho},\boldsymbol{\nu})} \mathcal{L}_{\boldsymbol{\rho}/\boldsymbol{\nu}}(W_p; t)$$

which can be combined into

$$\text{l.h.s.} = \prod_{l=0}^{k-1} \prod_{i,i'=1}^{n} \prod_{j,j'=1}^{m} \prod_{\alpha,\alpha'=1}^{p} \prod_{\beta,\beta'=1}^{q} \frac{(1 - x_i w_\alpha t^l)(1 - y_{j'} z_{\beta'} t^l)}{(1 + y_j w_{\alpha'} t^l)(1 + x_{i'} z_\beta t^l)} \times \sum_{\boldsymbol{\lambda}} t^{d(\boldsymbol{\lambda},\boldsymbol{\nu})} \mathcal{L}^S_{\boldsymbol{\lambda}/\boldsymbol{\mu}}(X_n, Y_m; t) \mathcal{L}^S_{\boldsymbol{\lambda}/\boldsymbol{\nu}}(W_p, Z_q; t) = \text{r.h.s.},$$

where we again use the fact that

$$d(\boldsymbol{\lambda}, \boldsymbol{\nu}) = d_P(\boldsymbol{\lambda}, \boldsymbol{\rho}) + d(\boldsymbol{\rho}, \boldsymbol{\nu}).$$

■

Appendices

A. Proof of Lemma 2.16

Throughout this section, whenever we consider a skew shape α/β, we assume α and β have the same number of parts $\ell(\alpha/\beta)$. Moreover, using Remark 2.6, we can take the Maya diagrams of α and β to have the same length. Also let $f_k(\alpha/\beta)$ denote the k-quotient of α/β.

Let λ/μ be a skew shape, and let $\boldsymbol{\lambda}/\boldsymbol{\mu} = (\lambda^{(0)}/\mu^{(0)}, \ldots, \lambda^{(k-1)}/\mu^{(k-1)})$ be its k-quotient. Let

$$T \in \mathrm{SSRT}_k(\lambda/\mu) \leftrightarrow \boldsymbol{T} = (T^{(0)}, \ldots, T^{(k-1)}) \in \mathrm{SSSYT}_k(\boldsymbol{\lambda}/\boldsymbol{\mu})$$

via the Littlewood k-quotient map. We want to prove the following two claims:

(1) A ribbon in T labeled i corresponds to a cell labeled i in $\boldsymbol{T}$, so the number of ribbons in T labeled i equals the number of cells labeled i in $\boldsymbol{T}$.

(2) Two ribbons R, R' in T whose tails u, u' have the same content modulo k correspond to two cells v, v' of the same shape in $\boldsymbol{T}$. Moreover, in this case,

$$\frac{c(u) - c(u')}{k} = c(v) - c(v').$$

We begin by discussing Maya diagrams and content lines. Let α/β be a skew shape, and let $(a_0, \dots, a_{s-1})$, $(b_0, \dots, b_{s-1})$ be the Maya diagrams of α, β, respectively. Given a cell u in α/β, we define its *adjusted content* to be

$$ac(u) := c(u) + \ell(\alpha/\beta) - 1,$$

where $c(u)$ is its content. The following facts are straightforward:

(A) The skew shape α/β consists of a single cell u if and only if $a_i = b_{i+1} = E$, $a_{i+1} = b_i = S$, and $a_j = b_j$ for $j \neq i, i+1$ for some i. In this case, if u is the single cell in α/β, we have $ac(u) = i$.

(B) The skew shape α/β consists of a single ribbon if and only if $a_i = b_{i+k} = E$, $a_{i+k} = b_i = S$, and $a_j = b_j$ for $j \neq i, i+k$ for some i. In this case, if u is the tail of the single ribbon in α/β, we have $ac(u) = i$.

The claims will follow from the next lemma.

Lemma A.1. *If λ/μ is a k-ribbon, then $\boldsymbol{\lambda}/\boldsymbol{\mu}$ consists of a single cell, i.e., $|\boldsymbol{\lambda}/\boldsymbol{\mu}| = 1$. Let u be the tail of the ribbon in λ/μ, and let v be the cell in $\boldsymbol{\lambda}/\boldsymbol{\mu}$. Write $ac(u) = qk + r$, where $0 \leq r < k$. Then v appears in $\lambda^{(r)}/\mu^{(r)}$ and has adjusted content $ac(v) = q$.*

Proof of Lemma A.1. Let u be the tail of the ribbon λ/μ. Let $(a_0, \dots, a_{s-1})$ and $(b_0, \dots, b_{s-1})$ be the Maya diagrams of λ and μ, respectively. By Remark 2.6, we may assume that $t = s/k$ is an integer. By fact (B), for some i, we have

$$ac(u) = i, \quad a_i = b_{i+k} = E, \quad a_{i+k} = b_i = S, \quad a_j = b_j \quad \text{for } j \neq i, i+k.$$

Let $(a_0^{(j)}, \dots, a_{t-1}^{(j)})$, $(b_0^{(j)}, \dots, b_{t-1}^{(j)})$ be the Maya diagrams of $\lambda^{(j)}$, $\mu^{(j)}$, respectively, for each j. By the definition of the k-quotient map, we have

$$a_l^{(j)} = a_{lk+j} \quad \text{and} \quad b_l^{(j)} = b_{lk+j}$$

for each j and l. Since $a_j = b_j$ for $j \neq i, i+k$,

$$(a_0^{(j)}, \dots, a_{t-1}^{(j)}) = (b_0^{(j)}, \dots, b_{t-1}^{(j)}) \quad \text{for } j \neq r,$$

and thus $\lambda^{(j)} = \mu^{(j)}$ for $j \neq r$. Since $a_i = b_{i+k} = E$, $a_{i+k} = b_i = S$, and $a_j = b_j$ for $j \neq i, i+k$,

$$a_q^{(r)} = b_{q+1}^{(r)} = E, \quad a_{q+1}^{(r)} = b_q^{(r)} = S, \quad \text{and} \quad a_j^{(r)} = b_j^{(r)} \quad \text{for } j \neq q, q+1.$$

Therefore, by fact (A), $\lambda^{(r)}/\mu^{(r)}$ consists of a single cell v with adjusted content $ac(v) = q$. ∎

We now prove claim (1) using Lemma A.1. Suppose that there are m ribbons $R_1, \ldots, R_m$ labeled i in T. Then we can construct a series of partitions

$$\alpha^{(0)} = \lambda_{\leq i-1}, \quad \ldots, \quad \alpha^{(m)} = \lambda_{\leq i}$$

such that $\alpha^{(j)}/\alpha^{(j-1)} = R_j$ for each $j \in [m]$. Using the lemma,

$$\begin{aligned} |f_k(\lambda_{\leq i}/\lambda_{\leq i-1})| &= |f_k(\alpha^{(m)}/\alpha^{(0)})| \\ &= \sum_{j=1}^{m} |f_k(\alpha^{(j)}/\alpha^{(j-1)})| = \sum_{j=1}^{m} |f_k(R_j)| = \sum_{j=1}^{m} 1 = m. \end{aligned}$$

However, by the definition of the Littlewood k-quotient map, $f_k(\lambda_{\leq i}/\lambda_{\leq i-1})$ (lying inside $\boldsymbol{\lambda}/\boldsymbol{\mu}$) consists of exactly the cells labeled i in $\boldsymbol{T}$, so there are m cells labeled i in $\boldsymbol{T}$.

We now prove claim (2) again using Lemma A.1. Write $ac(u) = qk + r$ and $ac(u') = q'k + r'$, where $0 \leq r, r' < k$. Since u and u' have the same content modulo k, they have the same adjusted content modulo k, hence $r = r'$. Thus, by the lemma, both v and v' appear in the same shape in $\boldsymbol{T}$, namely $T^{(r)} = T^{(r')}$. Moreover, again using the lemma, we obtain

$$\begin{aligned} \frac{c(u) - c(u')}{k} &= \frac{ac(u) - ac(u')}{k} = q - q' \\ &= ac(v) - ac(v') = c(v) - c(v'). \end{aligned}$$

B. Other formulations of LLT polynomials

We describe the relationship between coinversion LLT polynomials (Definition 2.3) and other formulations of LLT polynomials that appear in the literature.

Remark B.1. The inversion LLT polynomial, as in [17], is given by

$$\mathcal{L}^{\mathrm{HHL}}_{\boldsymbol{\lambda}/\boldsymbol{\mu}}(X;t) = \sum_{T \in \mathrm{SSYT}(\boldsymbol{\lambda}/\boldsymbol{\mu})} t^{\mathrm{inv}(T)} x^T.$$

We have the relationship

$$\mathcal{L}_{\boldsymbol{\lambda}/\boldsymbol{\mu}}(X;t) = t^m \mathcal{L}^{\mathrm{HHL}}_{\boldsymbol{\lambda}/\boldsymbol{\mu}}(X;t^{-1}),$$

where

$$\begin{aligned} m = \#\text{ triples in } \boldsymbol{\lambda}/\boldsymbol{\mu} &= \max_{U \in \mathrm{SSYT}(\boldsymbol{\lambda}/\boldsymbol{\mu})} \mathrm{coinv}(U) + \min_{U \in \mathrm{SSYT}(\boldsymbol{\lambda}/\boldsymbol{\mu})} \mathrm{inv}(U) \\ &= \min_{U \in \mathrm{SSYT}(\boldsymbol{\lambda}/\boldsymbol{\mu})} \mathrm{coinv}(U) + \max_{T \in \mathrm{SSYT}(\boldsymbol{\lambda}/\boldsymbol{\mu})} \mathrm{inv}(U). \end{aligned}$$

More explicit formulae for m are given in [13, Section 5].

Remark B.2. Define the sp LLT polynomial by

$$\mathcal{L}^{\mathrm{sp}}_{\lambda/\mu}(X;t) = \sum_{T\in \mathrm{SSRT}_k(\lambda/\mu)} t^{\mathrm{sp}(T)} x^T,$$

where

$$\mathrm{sp}(T) = \frac{\mathrm{spin}(T)}{2} - \min_{U\in \mathrm{SSRT}_k(\lambda/\mu)} \frac{\mathrm{spin}(U)}{2}.$$

If $\boldsymbol{\lambda/\mu}$ is the k-quotient of λ/μ, then

$$\mathcal{L}_{\boldsymbol{\lambda/\mu}}(X;t) = t^{m-e}\mathcal{L}^{sp}_{\lambda/\mu}(X;t),$$

where

$$e = \max_{U\in \mathrm{SSYT}(\boldsymbol{\lambda/\mu})} \mathrm{inv}(U), \quad m-e = \min_{U\in \mathrm{SSYT}(\boldsymbol{\lambda/\mu})} \mathrm{coinv}(U).$$

Remark B.3. The spin LLT polynomial, as in [9, 15, 21], is given by

$$\mathcal{L}^{\mathrm{Lam}}_{\lambda/\mu}(X;t) = \sum_{T\in \mathrm{SSRT}_k(\lambda/\mu)} t^{\mathrm{spin}(T)} x^T.$$

If $\boldsymbol{\lambda/\mu}$ is the k-quotient of λ/μ, then

$$\mathcal{L}_{\boldsymbol{\lambda/\mu}}(X;t) = t^{m-e-*}\mathcal{L}^{\mathrm{Lam}}_{\lambda/\mu}(X;t^{1/2}),$$

where

$$* = \min_{U\in \mathrm{SSRT}_k(\lambda/\mu)} \frac{\mathrm{spin}(U)}{2}.$$

It is clear from the definitions that

$$\mathcal{L}^{\mathrm{Lam}}_{\lambda/\mu}(X;t) = \mathcal{G}^{(k)}_{\lambda/\mu}(X;\cdot;t).$$

Remark B.4. Define the cosp LLT polynomial by

$$\mathcal{L}^{\mathrm{LLT}}_{\lambda/\mu}(X;t) = \sum_{T\in \mathrm{SSRT}_k(\lambda/\mu)} t^{\mathrm{cosp}(T)} x^T,$$

where

$$\mathrm{cosp}(T) = \max_{U\in \mathrm{SSRT}_k(\lambda/\mu)} \frac{\mathrm{spin}(U)}{2} - \frac{\mathrm{spin}(T)}{2}.$$

Historically, this was the original formulation of LLT polynomials [22]. If $\boldsymbol{\lambda/\mu}$ is the k-quotient of λ/μ, then

$$\mathcal{L}_{\boldsymbol{\lambda/\mu}}(X;t) = t^{m-e+\dagger-*}\mathcal{L}^{\mathrm{LLT}}_{\lambda/\mu}(X;t^{-1}),$$

where

$$\dagger = \max_{U\in \mathrm{SSRT}_k(\lambda/\mu)} \frac{\mathrm{spin}(U)}{2}.$$

C. Proofs of Propositions 3.3 and 3.4

We adopt the notation of [1] throughout this section, except we use t in place of q. In particular, we let $W_z(\mathbf{A}, \mathbf{B}; \mathbf{C}, \mathbf{D} \mid r, s)$ be the vertex weights from [1, Definition 5.1.1] with t in place of q.

The proofs of Propositions 3.3 and 3.4 utilize [1, Proposition 5.1.4], which states

$$\begin{aligned}
&\sum_{\boldsymbol{I}_2,\boldsymbol{J}_2,\boldsymbol{K}_2} W_{\chi/\gamma}(\boldsymbol{I}_1,\boldsymbol{J}_1;\boldsymbol{I}_2,\boldsymbol{J}_2 \mid r,s) W_{\chi/z}(\boldsymbol{K}_1,\boldsymbol{J}_2;\boldsymbol{K}_2,\boldsymbol{J}_3 \mid r,t) \\
&\quad \times W_{\gamma/z}(\boldsymbol{K}_2,\boldsymbol{I}_2;\boldsymbol{K}_3,\boldsymbol{I}_3 \mid s,t) \\
&\quad = \sum_{\boldsymbol{I}_2,\boldsymbol{J}_2,\boldsymbol{K}_2} W_{\gamma/z}(\boldsymbol{K}_1,\boldsymbol{I}_1;\boldsymbol{K}_2,\boldsymbol{I}_2 \mid s,t) W_{\chi/z}(\boldsymbol{K}_2,\boldsymbol{J}_1;\boldsymbol{K}_3,\boldsymbol{J}_2 \mid r,t) \\
&\qquad \times W_{\chi/\gamma}(\boldsymbol{I}_2,\boldsymbol{J}_2;\boldsymbol{I}_3,\boldsymbol{J}_3 \mid r,s)
\end{aligned} \tag{C.1}$$

for all $\chi, \gamma, z, r, s, t \in \mathbb{C}$ for any choice of boundary conditions $\boldsymbol{I}_1, \boldsymbol{J}_1, \boldsymbol{K}_1, \boldsymbol{I}_3, \boldsymbol{J}_3, \boldsymbol{K}_3 \in \{0,1\}^k$.

Proof of Proposition 3.3. Fix $S, Y, x, y \in \mathbb{C}$ and let $\alpha = -S^2$ and $\beta = SY^{1/2}$. Substituting $\chi = x$, $\gamma = \alpha$, $z = \alpha$, $r = (x/\alpha)^{1/2}$, $s = Sy^{-1/2}$, and $t = SY^{1/2}$ into (C.1) gives

$$\begin{aligned}
&\sum_{\boldsymbol{I}_2,\boldsymbol{J}_2,\boldsymbol{K}_2} W_{x/\alpha}(\boldsymbol{I}_1,\boldsymbol{J}_1;\boldsymbol{I}_2,\boldsymbol{J}_2 \mid (x/\alpha)^{1/2}, Sy^{-1/2}) \\
&\quad \times W_{x/\alpha}(\boldsymbol{K}_1,\boldsymbol{J}_2;\boldsymbol{K}_2,\boldsymbol{J}_3 \mid (x/\alpha)^{1/2}, SY^{-1/2}) \\
&\quad \times W_1(\boldsymbol{K}_2,\boldsymbol{I}_2;\boldsymbol{K}_3,\boldsymbol{I}_3 \mid Sy^{-1/2}, SY^{1/2}) \\
&\quad = \sum_{\boldsymbol{I}_2,\boldsymbol{J}_2,\boldsymbol{K}_2} W_1(\boldsymbol{K}_1,\boldsymbol{I}_1;\boldsymbol{K}_2,\boldsymbol{I}_2 \mid Sy^{-1/2}, SY^{1/2}) \\
&\qquad \times W_{x/\alpha}(\boldsymbol{K}_2,\boldsymbol{J}_1;\boldsymbol{K}_3,\boldsymbol{J}_2 \mid (x/\alpha)^{1/2}, SY^{1/2}) \\
&\qquad \times W_{x/\alpha}(\boldsymbol{I}_2,\boldsymbol{J}_2;\boldsymbol{I}_3,\boldsymbol{J}_3 \mid (x/\alpha)^{1/2}, Sy^{-1/2}).
\end{aligned}$$

Multiplying both sides by $(-\alpha)^{|\boldsymbol{J}_3|}(SY^{1/2})^{-2|\boldsymbol{J}_3|}Y^{-|\boldsymbol{I}_3|}$ leads to

$$\begin{aligned}
&\sum_{\boldsymbol{I}_2,\boldsymbol{J}_2,\boldsymbol{K}_2} W_{x/\alpha}(\boldsymbol{I}_1,\boldsymbol{J}_1;\boldsymbol{I}_2,\boldsymbol{J}_2 \mid (x/\alpha)^{1/2}, Sy^{-1/2})(-\alpha)^{|\boldsymbol{J}_3|}(SY^{1/2})^{-2|\boldsymbol{J}_3|} \\
&\quad \times W_{x/\alpha}(\boldsymbol{K}_1,\boldsymbol{J}_2;\boldsymbol{K}_2,\boldsymbol{J}_3 \mid (x/\alpha)^{1/2}, SY^{-1/2}) \\
&\quad \times Y^{-|\boldsymbol{I}_3|} W_1(\boldsymbol{K}_2,\boldsymbol{I}_2;\boldsymbol{K}_3,\boldsymbol{I}_3 \mid Sy^{-1/2}, SY^{1/2}) \\
&\quad = \sum_{\boldsymbol{I}_2,\boldsymbol{J}_2,\boldsymbol{K}_2} Y^{-|\boldsymbol{I}_2|} W_1(\boldsymbol{K}_1,\boldsymbol{I}_1;\boldsymbol{K}_2,\boldsymbol{I}_2 \mid Sy^{-1/2}, SY^{1/2})(-\alpha)^{|\boldsymbol{J}_2|}(SY^{1/2})^{-2|\boldsymbol{J}_2|} \\
&\qquad \times W_{x/\alpha}(\boldsymbol{K}_2,\boldsymbol{J}_1;\boldsymbol{K}_3,\boldsymbol{J}_2 \mid (x/\alpha)^{1/2}, SY^{1/2})(-\alpha)^{|\boldsymbol{J}_3|-|\boldsymbol{J}_2|} S^{-2|\boldsymbol{J}_3|+2|\boldsymbol{J}_2|} \\
&\qquad \times W_{x/\alpha}(\boldsymbol{I}_2,\boldsymbol{J}_2;\boldsymbol{I}_3,\boldsymbol{J}_3 \mid (x/\alpha)^{1/2}, Sy^{-1/2}),
\end{aligned}$$

where we have used $|\boldsymbol{I}_2| + |\boldsymbol{J}_2| = |\boldsymbol{I}_3| + |\boldsymbol{J}_3|$ by path conservation on the right-hand side. Substituting $\alpha = -S^2$ and $\beta = SY^{1/2}$ gives

$$\begin{aligned}
&\sum_{\boldsymbol{I}_2,\boldsymbol{J}_2,\boldsymbol{K}_2} W_{x/\alpha}(\boldsymbol{I}_1,\boldsymbol{J}_1;\boldsymbol{I}_2,\boldsymbol{J}_2 \mid (x/\alpha)^{1/2},(-y/\alpha)^{-1/2})(-\alpha)^{|\boldsymbol{J}_3|}\beta^{-2|\boldsymbol{J}_3|} \\
&\quad\times W_{x/\alpha}(\boldsymbol{K}_1,\boldsymbol{J}_2;\boldsymbol{K}_2,\boldsymbol{J}_3 \mid (x/\alpha)^{1/2},\beta)Y^{-|\boldsymbol{I}_3|} \\
&\quad\times W_1(\boldsymbol{K}_2,\boldsymbol{I}_2;\boldsymbol{K}_3,\boldsymbol{I}_3 \mid Sy^{-1/2},SY^{1/2}) \\
&\quad= \sum_{\boldsymbol{I}_2,\boldsymbol{J}_2,\boldsymbol{K}_2} Y^{-|\boldsymbol{I}_2|}W_1(\boldsymbol{K}_1,\boldsymbol{I}_1;\boldsymbol{K}_2,\boldsymbol{I}_2 \mid Sy^{-1/2},SY^{1/2})(-\alpha)^{|\boldsymbol{J}_2|}\beta^{-2|\boldsymbol{J}_2|} \\
&\qquad\times W_{x/\alpha}(\boldsymbol{K}_2,\boldsymbol{J}_1;\boldsymbol{K}_3,\boldsymbol{J}_2 \mid (x/\alpha)^{1/2},\beta) \\
&\qquad\times W_{x/\alpha}(\boldsymbol{I}_2,\boldsymbol{J}_2;\boldsymbol{I}_3,\boldsymbol{J}_3 \mid (x/\alpha)^{1/2},(-y/\alpha)^{-1/2}).
\end{aligned}$$

Taking $S \to 0$ and $Y \to 0$ (hence also $\alpha = -S^2 \to 0$ and $\beta = SY^{1/2} \to 0$) and then applying Lemma 3.1 leads to the desired YBE

$$\begin{aligned}
&\sum_{\boldsymbol{I}_2,\boldsymbol{J}_2,\boldsymbol{K}_2} R'_{y/x}(\boldsymbol{I}_1,\boldsymbol{J}_1;\boldsymbol{I}_2,\boldsymbol{J}_2)\widetilde{L}_x(\boldsymbol{K}_1,\boldsymbol{J}_2;\boldsymbol{K}_2,\boldsymbol{J}_3)\widetilde{L}'_y(\boldsymbol{K}_2,\boldsymbol{I}_2;\boldsymbol{K}_3,\boldsymbol{I}_3) \\
&\quad= \sum_{\boldsymbol{I}_2,\boldsymbol{J}_2,\boldsymbol{K}_2} L'_y(\boldsymbol{K}_1,\boldsymbol{I}_1;\boldsymbol{K}_2,\boldsymbol{I}_2)L_x(\boldsymbol{K}_2,\boldsymbol{J}_1;\boldsymbol{K}_3,\boldsymbol{J}_2)R'_{y/x}(\boldsymbol{I}_2,\boldsymbol{J}_2;\boldsymbol{I}_3,\boldsymbol{J}_3). \qquad \blacksquare
\end{aligned}$$

Proof of Proposition 3.4. Fix $S, Y, x, y \in \mathbb{C}$ and let $\alpha = -S^2$ and $\beta = SY^{1/2}$. Substituting $\chi = 1$, $\gamma = 1$, $z = 1$, $r = Sx^{-1/2}$, $s = Sy^{-1/2}$, and $t = SY^{-1/2}$ into (C.1) gives

$$\begin{aligned}
&\sum_{\boldsymbol{I}_2,\boldsymbol{J}_2,\boldsymbol{K}_2} W_1(\boldsymbol{I}_1,\boldsymbol{J}_1;\boldsymbol{I}_2,\boldsymbol{J}_2 \mid Sx^{-1/2},Sy^{-1/2})W_1(\boldsymbol{K}_1,\boldsymbol{J}_2;\boldsymbol{K}_2,\boldsymbol{J}_3 \mid Sx^{-1/2},SY^{-1/2}) \\
&\quad\times W_1(\boldsymbol{K}_2,\boldsymbol{I}_2;\boldsymbol{K}_3,\boldsymbol{I}_3 \mid Sy^{-1/2},SY^{1/2}) \\
&\quad= \sum_{\boldsymbol{I}_2,\boldsymbol{J}_2,\boldsymbol{K}_2} W_1(\boldsymbol{K}_1,\boldsymbol{I}_1;\boldsymbol{K}_2,\boldsymbol{I}_2 \mid Sy^{-1/2},SY^{1/2}) \\
&\qquad\times W_1(\boldsymbol{K}_2,\boldsymbol{J}_1;\boldsymbol{K}_3,\boldsymbol{J}_2 \mid Sx^{-1/2},SY^{1/2})W_1(\boldsymbol{I}_2,\boldsymbol{J}_2;\boldsymbol{I}_3,\boldsymbol{J}_3 \mid Sx^{-1/2},Sy^{-1/2}).
\end{aligned}$$

Multiplying both sides by $Y^{-|\boldsymbol{I}_3|-|\boldsymbol{J}_3|}$ results in

$$\begin{aligned}
&\sum_{\boldsymbol{I}_2,\boldsymbol{J}_2,\boldsymbol{K}_2} W_1(\boldsymbol{I}_1,\boldsymbol{J}_1;\boldsymbol{I}_2,\boldsymbol{J}_2 \mid Sx^{-1/2},Sy^{-1/2})Y^{-|\boldsymbol{J}_3|} \\
&\quad\times W_1(\boldsymbol{K}_1,\boldsymbol{J}_2;\boldsymbol{K}_2,\boldsymbol{J}_3 \mid Sx^{-1/2},SY^{-1/2})Y^{-|\boldsymbol{I}_3|} \\
&\quad\times W_1(\boldsymbol{K}_2,\boldsymbol{I}_2;\boldsymbol{K}_3,\boldsymbol{I}_3 \mid Sy^{-1/2},SY^{1/2}) \\
&\quad= \sum_{\boldsymbol{I}_2,\boldsymbol{J}_2,\boldsymbol{K}_2} Y^{-|\boldsymbol{I}_2|}W_1(\boldsymbol{K}_1,\boldsymbol{I}_1;\boldsymbol{K}_2,\boldsymbol{I}_2 \mid Sy^{-1/2},SY^{1/2})Y^{-|\boldsymbol{J}_2|} \\
&\qquad\times W_1(\boldsymbol{K}_2,\boldsymbol{J}_1;\boldsymbol{K}_3,\boldsymbol{J}_2 \mid Sx^{-1/2},SY^{1/2})W_1(\boldsymbol{I}_2,\boldsymbol{J}_2;\boldsymbol{I}_3,\boldsymbol{J}_3 \mid Sx^{-1/2},Sy^{-1/2}),
\end{aligned}$$

where we have used $|\boldsymbol{I}_2| + |\boldsymbol{J}_2| = |\boldsymbol{I}_3| + |\boldsymbol{J}_3|$ by path conservation on the right-hand side. Taking $S \to 0$ and $Y \to 0$ and then applying Lemma 3.1 gives the desired YBE

$$\sum_{\boldsymbol{I}_2,\boldsymbol{J}_2,\boldsymbol{K}_2} R''_{x/y}(\boldsymbol{I}_1,\boldsymbol{J}_1;\boldsymbol{I}_2,\boldsymbol{J}_2)L'_x(\boldsymbol{K}_1,\boldsymbol{J}_2;\boldsymbol{K}_2,\boldsymbol{J}_3)L'_y(\boldsymbol{K}_2,\boldsymbol{I}_2;\boldsymbol{K}_3,\boldsymbol{I}_3)$$
$$= \sum_{\boldsymbol{I}_2,\boldsymbol{J}_2,\boldsymbol{K}_2} L'_y(\boldsymbol{K}_1,\boldsymbol{I}_1;\boldsymbol{K}_2,\boldsymbol{I}_2)L'_x(\boldsymbol{K}_2,\boldsymbol{J}_1;\boldsymbol{K}_3,\boldsymbol{J}_2)R''_{x/y}(\boldsymbol{I}_2,\boldsymbol{J}_2;\boldsymbol{I}_3,\boldsymbol{J}_3). \quad \blacksquare$$

D. Example computations of $\mathcal{L}^S$ and $\mathcal{G}$

D.1. Example 1

The 2-quotient of $\lambda = (4,2)$ is $\boldsymbol{\lambda} = ((1),(2))$,

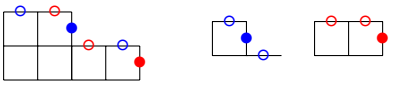

Therefore, by Proposition 5.9, we must have

$$\mathcal{L}^S_{\boldsymbol{\lambda}}(x_1;y_1;t) = t^{\square}\mathcal{G}^{(2)}_{\lambda}(x_1;y_1;t^{1/2})$$

for some half-integer $\square \in \frac{1}{2}\mathbb{Z}$. To compute $\mathcal{L}^S_{\boldsymbol{\lambda}}(x_1;y_1;t)$, we note that there are 4 configurations of the lattice $S_{1,1}(\boldsymbol{\lambda})$,

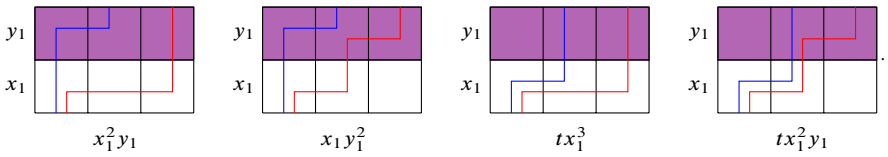

Therefore,

$$\mathcal{L}^S_{\boldsymbol{\lambda}}(x_1;y_1;t) = x_1^2y_1 + x_1y_1^2 + tx_1^3 + tx_1^2y_1.$$

To compute $\mathcal{G}^{(2)}_{\lambda}(x_1;y_1;t^{1/2})$, we note that there are 4 super 2-ribbon tableaux of shape λ in the alphabet $\{1 < 1'\}$,

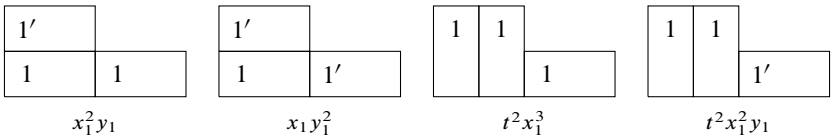

Therefore, $\mathcal{G}^{(2)}_{\lambda}(x_1;y_1;t^{1/2}) = x_1^2y_1 + x_1y_1^2 + t^2x_1^3 + t^2x_1^2y_1$. (The way we have ordered the lattice configurations and the super ribbon tableaux agrees with the bijection θ from Section 5, so that the i-th lattice configuration corresponds to the i-th super ribbon tableaux via θ.) We see that

$$\mathcal{L}^S_{\boldsymbol{\lambda}}(x_1;y_1;t) = \mathcal{G}^{(2)}_{\lambda}(x_1;y_1;t^{1/2}),$$

so in fact $\square = 0$ in this case. This agrees with the fact that the quantity

$$\square = \frac{1}{2}\sum_{a<b}\Big(\#\,\Big) + \frac{1}{2}\sum_{a<b}\Big(\#\,\Big)$$

is equal to 0 in each of these 4 configurations.

D.2. Example 2

The 3-quotient of $\lambda = (8,7,3)$ is $\boldsymbol{\lambda} = ((1),(3),(2))$,

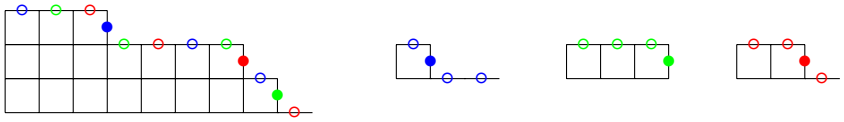

Therefore, by Proposition 5.9, we must have

$$\mathcal{L}^S_{\boldsymbol{\lambda}}(x_1;y_1;t) = t^{\square}\mathcal{G}^{(3)}_{\lambda}(x_1;y_1;t^{1/2})$$

for some half-integer $\square \in \frac{1}{2}\mathbb{Z}$. We can thus compute $\mathcal{G}^{(3)}_{\lambda}(x_1;y_1;t^{1/2})$ by computing $\mathcal{L}^S_{\boldsymbol{\lambda}}(x_1;y_1;t)$ and $\square$. To compute $\mathcal{L}^S_{\boldsymbol{\lambda}}(x_1;y_1;t)$, we note that there are 8 configurations of the lattice $S_{1,1}(\boldsymbol{\lambda})$,

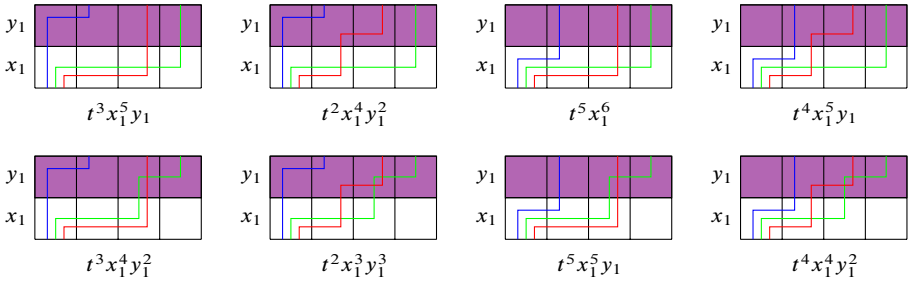

Therefore,

$$\mathcal{L}^S_{\boldsymbol{\lambda}}(x_1;y_1;t) = t^3x_1^5y_1 + t^2x_1^4y_1^2 + t^5x_1^6 + t^4x_1^5y_1 + t^3x_1^4y_1^2 + t^2x_1^3y_1^3 + t^5x_1^5y_1 + t^4x_1^4y_1^2.$$

We can also observe that the quantity

$$\square = \frac{1}{2}\sum_{a<b}\Big(\#\,\Big) + \frac{1}{2}\sum_{a<b}\Big(\#\,\Big)$$

is equal to $\frac{1}{2}$ in each of these 8 configurations, so $\square = \frac{1}{2}$. We can now compute

$$\mathscr{G}^{(3)}_{\lambda}(x_1; y_1; t) = t^{-2\square}\mathscr{L}^{S}_{\boldsymbol{\lambda}}(x_1; y_1; t^2) = t^5x_1^5y_1 + t^3x_1^4y_1^2 + t^9x_1^6 + t^7x_1^5y_1 + t^5x_1^4y_1^2 + t^3x_1^3y_1^3 + t^9x_1^5y_1 + t^7x_1^4y_1^2.$$

We see this agrees with the result obtained from explicitly computing all the super 3-ribbon tableaux of shape λ in the alphabet $\{1 < 1'\}$,

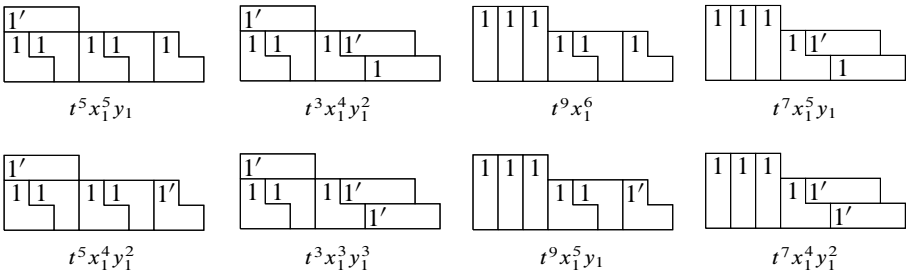

(Again, the way we have ordered the lattice configurations and the super ribbon tableaux agrees with the bijection θ from Section 5.)

Acknowledgments. The authors would like to thank Sylvie Corteel for many helpful discussions during the course of this work.

Funding. The authors were partially supported by the National Science Foundation, Grants DMS-1600447 and DMS-2054482.

References

[1] A. Aggarwal, A. Borodin, and M. Wheeler, Colored fermionic vertex models and symmetric functions. *Comm. Amer. Math. Soc.* **3** (2023), 400–630 Zbl 07751005 MR 4628347

[2] A. Ayyer, O. Mandelshtam, and J. Martin, Multispecies TAZRP and modified Macdonald polynomials. *Sém. Lothar. Combin.* **85B** (2021), article no. 56 Zbl 1505.05125 MR 4311937

[3] R. J. Baxter, *Exactly solved models in statistical mechanics*. Academic Press, London, 1982 Zbl 0538.60093 MR 690578

[4] V. V. Bazhanov and A. G. Shadrikov, Trigonometric solutions of triangle equations. Simple Lie superalgebras. *Theoret. and Math. Phys.* **73** (1987), no. 3, 1302–1312 Zbl 0659.58021 MR 939786

[5] A. Berele and A. Regev, Hook Young diagrams with applications to combinatorics and to representations of Lie superalgebras. *Adv. Math.* **64** (1987), no. 2, 118–175 Zbl 0617.17002 MR 884183

[6] A. Borodin and M. Wheeler, Colored stochastic vertex models and their spectral theory. *Astérisque* **437** (2022), ix+225 pp. Zbl 07649036 MR 4518478

[7] A. Borodin and M. Wheeler, Nonsymmetric Macdonald polynomials via integrable vertex models. *Trans. Amer. Math. Soc.* **375** (2022), no. 12, 8353–8397 Zbl 1506.05209 MR 4504641

[8] B. Brubaker, V. Buciumas, D. Bump, and H. P. A. Gustafsson, Colored vertex models and Iwahori Whittaker functions. 2020, arXiv:1906.04140

[9] B. Brubaker, V. Buciumas, D. Bump, and H. P. A. Gustafsson, Vertex operators, solvable lattice models and metaplectic Whittaker functions. *Comm. Math. Phys.* **380** (2020), no. 2, 535–579 Zbl 1456.82097 MR 4170287

[10] B. Brubaker, V. Buciumas, D. Bump, and H. P. A. Gustafsson, Colored five-vertex models and Demazure atoms. *J. Combin. Theory Ser. A* **178** (2021), article no. 105354 Zbl 1458.05257 MR 4165627

[11] B. Brubaker, D. Bump, and S. Friedberg, Schur polynomials and the Yang–Baxter equation. *Comm. Math. Phys.* **308** (2011), no. 2, 281–301 Zbl 1232.05234 MR 2851143

[12] V. Buciumas, T. Scrimshaw, and K. Weber, Colored five-vertex models and Lascoux polynomials and atoms. *J. Lond. Math. Soc. (2)* **102** (2020), no. 3, 1047–1066 Zbl 1462.05348 MR 4186121

[13] S. Corteel, A. Gitlin, D. Keating, and J. Meza, A vertex model for LLT polynomials. *Int. Math. Res. Not. IMRN* **2022** (2022), no. 20, 15869–15931 Zbl 1502.05238 MR 4498167

[14] S. Corteel, O. Mandelshtam, and L. Williams, From multiline queues to Macdonald polynomials via the exclusion process. *Sém. Lothar. Combin.* **82B** (2020), article no. 97 Zbl 1435.05204 MR 4098318

[15] M. J. Curran, C. Frechette, C. Yost-Wolff, S. W. Zhang, and V. Zhang, A lattice model for super LLT polynomials. 2022, arXiv:2110.07597

[16] A. Garbali and M. Wheeler, Modified Macdonald polynomials and integrability. *Comm. Math. Phys.* **374** (2020), no. 3, 1809–1876 Zbl 1436.82006 MR 4076089

[17] J. Haglund, M. Haiman, and N. Loehr, A combinatorial formula for Macdonald polynomials. *J. Amer. Math. Soc.* **18** (2005), no. 3, 735–761 Zbl 1061.05101 MR 2138143

[18] J. Haglund, M. Haiman, N. Loehr, J. B. Remmel, and A. Ulyanov, A combinatorial formula for the character of the diagonal coinvariants. *Duke Math. J.* **126** (2005), no. 2, 195–232 Zbl 1069.05077 MR 2115257

[19] K. Iijima, A q-multinomial expansion of LLT coefficients and plethysm multiplicities. *European J. Combin.* **34** (2013), no. 6, 968–986 Zbl 1285.05173 MR 3037982

[20] P. P. Kulish, N. Yu. Reshetikhin, and E. K. Sklyanin, Yang–Baxter equations and representation theory: I. *Lett. Math. Phys.* **5** (1981), no. 5, 393–403 Zbl 0502.35074 MR 649704

[21] T. Lam, Ribbon tableaux and the Heisenberg algebra. *Math. Z.* **250** (2005), no. 3, 685–710 Zbl 1066.05145 MR 2179617

[22] A. Lascoux, B. Leclerc, and J.-Y. Thibon, Ribbon tableaux, Hall–Littlewood functions, quantum affine algebras, and unipotent varieties. *J. Math. Phys.* **38** (1997), no. 2, 1041–1068 Zbl 0869.05068 MR 1434225

[23] D. E. Littlewood, Modular representations of symmetric groups. *Proc. Roy. Soc. London Ser. A* **209** (1951), 333–353 Zbl 0044.25702 MR 49896

[24] I. G. Macdonald, *Symmetric functions and Hall polynomials*. Oxf. Math. Monogr., The Clarendon Press, Oxford University Press, New York, 1998 Zbl 0899.05068 MR 553598

[25] E. Moens, *Supersymmetric Schur functions and Lie superalgebra representations*. Ph.D. thesis, 2007, Ghent University

[26] S. Pfannerer, A refinement of the Murnaghan–Nakayama rule by descents for border strip tableaux. *Sém. Lothar. Combin.* **85B** (2021), no. 2, article no. 37 Zbl 1505.05148 MR 4311918

[27] N. Reshetikhin, Lectures on the integrability of the six-vertex model. In *Exact methods in low-dimensional statistical physics and quantum computing*, pp. 197–266, Oxford University Press, Oxford, 2010 Zbl 1202.82022 MR 2668647

[28] D. W. Stanton and D. E. White, A Schensted algorithm for rim hook tableaux. *J. Comb. Theory Ser. A* **40** (1985), no. 2, 211–247 Zbl 0577.05001 MR 814412

[29] N. V. Tsilevich, Quantum inverse scattering method for the q-boson model and symmetric functions. *Funct. Anal. Appl.* **40** (2006), no. 3, 53–65 Zbl 1118.81041 MR 2265685

[30] M. Wheeler and P. Zinn-Justin, Refined Cauchy/Littlewood identities and six-vertex model partition functions: III. Deformed bosons. *Adv. Math.* **299** (2016), 543–600 Zbl 1341.05249 MR 3519476

Communicated by Adrian Tanasă

Received 25 October 2021; revised 23 June 2022.

Andrew Gitlin
Department of Mathematics, University of California, Berkeley, 970 Evans Hall, Berkeley, CA 94720-3840, USA; andrew_gitlin@berkeley.edu

David Keating
Department of Mathematics, University of Wisconsin-Madison, 480 Lincoln Drive, 213 Van Vleck Hall, Madison, WI 53706, USA; dkeating3@wisc.edu